

**The Development of Synergistic Heat Stabilizers for PVC  
from Zinc Borate – Zinc Phosphate**

**By  
C.Aykut ERDOĞDU**

**A Dissertation Submitted to the  
Graduate School in Partial Fulfillment of the  
Requirement for the Degree of**

**MASTER OF SCIENCE**

**Department: Chemical Engineering  
Major: Chemical Engineering**

**İzmir Institute of Technology  
İzmir, Turkey**

**August, 2004**

We approve the thesis of **C.Aykut ERDOĞDU**

**Date of Signature**

.....  
**Prof. Dr. Devrim BALKÖSE**  
Supervisor  
Department of Chemical Engineering

**30.08.2004**

.....  
**Prof. Dr. Semra ÜLKÜ**  
Co-Supervisor  
Department of Chemical Engineering

**30.08.2004**

.....  
**Prof.Dr. Tamerkan ÖZGEN**  
Department of Chemistry

**30.08.2004**

.....  
**Assist.Prof.Dr.Funda TIHMINLIOĞLU**  
Department of Chemical Engineering

**30.08.2004**

.....  
**Assist.Prof. Dr. Fikret İNAL**  
Department of Chemical Engineering

**30.08.2004**

.....  
**Prof. Dr. Devrim BALKÖSE**  
Head of Chemical Engineering Department

**30.08.2004**

## ACKNOWLEDGEMENT

The financial support of this project by 2003-IYTE-39 is gratefully acknowledged. I would like to express my sincere gratitude to my advisors Prof. Devrim BALKÖSE and Prof. Semra ÜLKÜ for their support, guidance and encouragement during this study and the preparation of the thesis.

I am very grateful to Sevdije ATAKUL, Mehmet GÖNEN, Öniz BİRSOY and Yarkin ÖZGARİP for their help, encouragement and friendship throughout this project. I want to express my thanks to Gökhan ERDOĞAN for his help for SEM and EDX analyses, Burcu ALP for TGA analyses and Özlem Çağlar DUVARCI and Filiz ÖZMIHÇI for FTIR analysis.

I also present my deepest thanks to my officemate, Emre ELTEPE and my managers in Pigment Sanayi A.Ş. Kadri ELTEPE and A.Kemal YALNIZ and all other friends for their friendship, encouragement and understandings during this study.

Finally, my thanks go to my family for their help and encouragement during the preparation of the thesis.

## TABLE OF CONTENTS

	<b>Page</b>
ABSTRACT	i
ÖZ	iii
LIST OF FIGURES	v
LIST OF TABLES	viii
CHAPTER 1. INTRODUCTION	1
CHAPTER 2. THE THERMAL DEGRADATION OF PVC	4
CHAPTER 3. THERMAL STABILIZATION AND STABILIZERS	10
3.1 Thermal Stabilization	10
3.2 Heat Stabilizers	10
3.2.1 Lead Compounds	10
3.2.2 Organotin Compounds	11
3.2.3 Compounds of Other Metals	11
3.2.4 Organic Stabilizers	11
3.3 Flame Retardants	12
3.4 Flame Retardants For PVC	14
3.4.1 Antimony Oxide	14
3.4.2 Molybdenum Oxide	15
3.4.3 Zinc Stannates	15
3.4.4 Aluminium Trihydrate	15
CHAPTER 4. ZINC BORATE AND ZINC PHOSPHATE	16
4.1 Zinc Borate	16
4.1.1 Production	17

4.1.2 Boron Mechanism	18
4.1.3 Flame Retardant Effect of ZB	19
4.2 Zinc Phosphate	28
4.2.1 Synergism in Nickel Oxide and Zinc Phosphate	28
4.2.2 IR Spectroscopic Study of Phosphate Minerals	29
CHAPTER 5. EXPERIMENTAL	32
5.1 Materials Used	32
5.2 Methods	34
5.2.1 Film Preparation	34
5.2.2 Film Characterization	35
5.2.2.1 Scanning Electron Microscope	35
5.2.2.2 Energy Dispersive X-Ray	35
5.2.3 Thermal Stability Tests	36
5.2.3.1 Static Oven Tests	36
5.2.3.2 PVC Thermomat	36
5.2.3.3 TGA Analyses	38
5.2.4 Fourier Transform Infrared Analyses	39
5.2.5 Fourier Transform Infrared Analyses by ATR Method	39
5.2.6 Colour Measurement	39
CHAPTER 6. RESULTS AND DISCUSSION	40
6.1 Characterization of Zinc Borate and Zinc Phosphate	40
6.2 Kinetic Study of Dehydrochlorination of PVC Plastigels	44
6.2.1 Kinetic Theory of Degradation PVC Plastigels	44
6.2.2 Kinetic Study of PVC Plastigels	47

6.2.3 Activation Energies of Dehydrochlorination Reactions	55
6.2.4 Preexponential Factors of Dehydrochlorination Reactions	56
6.3 Characterization of PVC Plastisols and PVC Plastigels	59
6.3.1 Thermogravimetric Study of PVC Films	59
6.4 Colour Tests of PVC Plastigels	65
6.4.1 Static Oven Test	65
6.5 Colour Measurement	67
6.6 Spectroscopy Analyses of Films	70
6.6.1 Fourier Transmission Infrared (FT-IR) Spectra Tests	70
6.6.2 Attenuated Total Reflection (ATR) Spectra Tests	76
6.7 Morphology of PVC Plastigels	82
6.8 Elemental Analyses of PVC Plastigels	87
CHAPTER 7 CONCLUSIONS	91
APPENDIX	93
REFERENCES	100

## ABSTRACT

Poly(vinyl chloride) (PVC), releases smoke and toxic gases (hydrogen chloride, HCl) during heating at temperatures above 140°C with the result of dehydrochlorination reaction. Obtaining flame retardant and smoke suppressed PVC compositions are getting more and more important. PVC is widely applied as a covering insulation for electrical and communication cables and in domestic uses such as window frames, doors, profiles, sidings and gutters because of its high level of combustion resistance. For this reason, many additives are studied to achieve better compositions than the present ones.

In this study, the synergistic effects of zinc borate (ZB) – zinc phosphate (ZP) on thermal stability of plastigels obtained from PVC and dioctylphthalate (DOP) plastisols were investigated using spectroscopic and thermal techniques.

Plastigels having a total of 2.5 parts (w/w) of zinc borate and zinc phosphate, 80 parts (w/w) of DOP and 100 parts (w/w) of PVC were gelled at 140°C for 15 minutes in a vacuum oven. The plastigel films having different compositions of ZB and ZP were investigated after heating at 140°C and 160°C from 15 minutes to 90 minutes by using Fourier Transform Infrared (FT-IR) spectroscopy, Scanning Electron Microscope (SEM), Energy Dispersive X-ray (EDX). The kinetic studies were made by PVC Thermomat 763 instrument. HCl gas released due to heating of the plastigel films at both 140°C and 160°C in PVC Thermomat instrument under nitrogen gas increases the conductivity of deionized water in measuring vessels of this instrument. By measuring the conductivity change in water caused by the absorption of HCl released, the thermal degradation of PVC plastigel films were studied by means of reaction rates, rate constants and activation energies. Compositions having only ZB or ZP have retarded dehydrochlorination of PVC compared with the control sample. However, the compositions with both ZB and ZP have a superior synergistic effect on char formation of PVC. Since induction times of the compositions having both ZB and ZP were higher than that of the control samples having only ZB or only ZP, the synergistic effect was observed.

The compositions greatly promote the char formation of PVC. The thermal stability of plastigels was also studied by their yellowness index (YI). The elemental

compositions of these films were investigated in atomic scale using EDX and SEM and their compositions were calculated both for particles and matrix.



## ÖZ

Poli(vinil klorür) (PVC), 140°C' nin üstünde ısıtıldığında dehidroklorinasyon reaksiyonundan dolayı duman ve zehirli gazları (hidrojen klorür, HCl) ortama salar. Alev geciktirici ve duman önleyici katkı maddelerine sahip PVC birleşimlerinin eldesi gittikçe daha önem kazanmaktadır. PVC elektrik ve haberleşme kablolarında izolasyon malzemesi ve evlerimizde kapı ve pencere çerçevelerinde, profillerde yanmaya karşı yüksek rezistansından dolayı gittikçe daha çok kullanılmaktadır. Bu nedenle, mevcutlardan daha iyi bir birleşim elde etmek için birçok katkı malzemesi araştırılmaktadır.

Bu çalışmada, çinko borat (ZB), çinko fosfat (ZP), PVC ve dioktilfitalat (DOP) plastisollerinden elde edilen plastijellerin termal kararlılığı üzerindeki sinerjistik etkileri spektroskopik ve termal teknikler kullanılarak incelenmiştir.

Toplam 2.5 kısım (ağırlıkça) çinko borat ve çinko fosfat, 80 kısım (ağırlıkça) DOP ve 100 kısım (ağırlıkça) PVC karışımına sahip olan plastijeller havayla dolaşımı sağlanan bir vakum fırınında 140°C altında jelleştirilmiştir. Çeşitli çinko borat ve çinko fosfat oranlarına sahip olan plastijeller 140°C ve 160°C altında 15 dakikadan 90 dakikaya kadar 15 dakikalık aralıklarla ısıtılmış ve bu numuneler üzerinde FT-IR spektroskopisi, elektron taramalı mikroskop, EDX analizleri yapılmıştır. Kinetik çalışmalar 763 PVC Thermomat cihazıyla yapılmıştır. Plastijellerin 140°C ve 160°C altında ısıtılmalarından dolayı açığa çıkan HCl gazı azot gazı yardımıyla bu cihazın ölçüm hücrelerine taşınarak deionize suyun içerisindeki iletkenlik değerlerini arttırmıştır. Açığa çıkan HCl gazının deionize suyun içine absorplanarak suyun iletkenlik değerlerini değiştirmesi ve bu değerlerin ölçülmesinden PVC plastijel filmlerinin ısı kararlılığı reaksiyon hızları, reaksiyon sabitleri ve aktivasyon enerjileri cinsinden çalışılmıştır. Sadece çinko borat ya da sadece çinko fosfat içeren birleşimlerin PVC'nin dehidroklorinasyonunu, kontrol örneğine göre geciktirdiği görülmüştür. Aynı zamanda hem çinko borat hem de çinko fosfat içeren birleşimler PVC'nin kömürleşmesinde daha iyi sinerjistik etkiye sahiptir. Çinko borat ve çinko fosfat içeren birleşimlerin indüksiyon zamanları kontrol numunesine göre daha yüksek olduğundan dolayı sinerjistik etkinin olduğu gözlenmiştir.

Birleşimler kömürleşmeyi de hızlandırmıştır. Isıl kararlılıkları ayrıca sarılık indeksleri yönünden de incelenmiştir. Filmlerin elemental içerikleri atomik ölçüde EDX ve taramalı elektron mikroskobu yardımıyla incelenmiş ve kompozisyonları hesaplanmıştır.

## LIST OF FIGURES

	Page
<b>Figure 1.1</b> PVC molecule	1
<b>Figure 2.1</b> The general mechanism of degradation of PVC	5
<b>Figure 3.1</b> A comparison of the effect of antimony oxide and ZB on the oxygen index of flexible PVC containing from 20 to 50 phr DOP	15
<b>Figure 4.1</b> Scanning-type electron microphotograph of Zinc Borate	18
<b>Figure 4.2</b> a) Effects of ATH, ZB and ZB – ATH contents on LOI of PVC. b) Effects of ATH, ZB, and ZB – ATH contents of smoke density of PVC	21
<b>Figure 4.3</b> a) TGA curves of PVC and PVC/ZB – ATH, b) Effects of ATH, ZB, and ZB – ATH contents on char residue of PVC	22
<b>Figure 4.4</b> Effects of ZB and ZB – ATH content on the LOI of PVC	23
<b>Figure 4.5</b> Effects of the ZB and ZB – ATH content on the impact strength of PVC	24
<b>Figure 4.6</b> Effects of ZB and ZB – ATH content on the yield strength of PVC	24
<b>Figure 4.7</b> LOI Values (%) of the compositions	25
<b>Figure 4.8</b> Changes of dynamic FTIR spectra obtained from the thermo-oxidative degradation of LLDPE/10% EG/20% ZB blends in the condensed phase with different pyrolysis times. (a): 300°C, b):400°C	26
<b>Figure.4.9</b> Infrared spectroscopic results for parahopeite	31
<b>Figure 5.1</b> Dioctyl Phthalate Molecule	33
<b>Figure 5.2</b> Blade of Film Applicator and Film Applicator	35
<b>Figure 5.3</b> PVC Thermomat Instrument	37
<b>Figure 5.4</b> Top view of PVC Thermomat instrument	38
<b>Figure 5.5</b> The measuring blocks of 763 PVC Thermomat instrument	39
<b>Figure 6.1</b> TGA curve of ZB powder	41
<b>Figure 6.2</b> TGA curve of ZP powder	42
<b>Figure 6.3</b> FT-IR spectra of ZB powder sample	43
<b>Figure 6.4</b> FT-IR spectra of ZP powder sample	43
<b>Figure 6.5</b> The Scanning electron micrographs of the ZB and ZP powders a.) ZB, 2 $\mu\text{m}$ , b.) ZB, 10 $\mu\text{m}$ , c.) ZP, 10 $\mu\text{m}$ .,d.) ZP, 20 $\mu\text{m}$	44
<b>Figure 6.6</b> A representative curve for PVC Thermomat results	48
<b>Figure 6.7</b> PVC Thermomat Results of PVC films heated at 140°C	49

<b>Figure 6.8</b> PVC Thermomat Results of PVC films heated at 160°C	50
<b>Figure 6.9</b> The bar graph of evaluated induction time for zinc borate at 140°C	54
<b>Figure 6.10</b> The bar graph of visual induction time for zinc borate at 140°C	54
<b>Figure 6.11</b> The bar graph of evaluated induction time for zinc borate at 160°C	55
<b>Figure 6.12</b> The bar graph of visual induction time for zinc borate at 160°C	55
<b>Figure 6.13</b> Kinetic compensation effect curve for the samples having different compositions	59
<b>Figure 6.14</b> (a) TGA curves of Sample Nos.1 – 4	62
<b>Figure 6.14</b> (b) TGA curves of Sample Nos.5 – 8	62
<b>Figure 6.15</b> The onset temperature bar graph of the samples	65
<b>Figure 6.16</b> The change of yellowness index tendency of the PVC plastigel films with time at 140°C	70
<b>Figure 6.17</b> The change of yellowness index tendency of the PVC plastigel films with time at 160°C	70
<b>Figure 6.18</b> FT-IR spectra of PVC control sample at 140°C and 160°C.	72
<b>Figure 6.19</b> FT-IR spectra of sample having 1.36% ZP at 140°C and 160°C.	73
<b>Figure 6.20</b> FT-IR spectra of sample having 0.27% ZB and 1.29% ZP at 140°C and 160°C	73
<b>Figure 6.21</b> FT-IR spectra of sample having 0.54% ZB and 0.81% ZP at 140°C and 160°C	74
<b>Figure 6.22</b> FT-IR spectra of sample having 0.68% ZB and 0.68% ZP at 140°C and 160°C	74
<b>Figure 6.23</b> FT-IR spectra of sample having 0.81% ZB and 0.54% ZP at 140°C and 160°C	75
<b>Figure 6.24</b> FT-IR spectra of sample having 1.29% ZB and 0.27% ZP at 140°C and 160°C	75
<b>Figure 6.25</b> FT-IR spectra of sample having 1.36% ZB at 140°C and 160°C.	76
<b>Figure 6.26</b> Absorbance versus ZB wt% at 1580cm <sup>-1</sup> at 140 and 160°C.	76
<b>Figure 6.27</b> Absorbance versus ZB wt% at 3227cm <sup>-1</sup> at 140 and 160°C.	77
<b>Figure 6.28</b> FT-IR spectra of PVC Control sample at 140°C and 160°C.	78
<b>Figure 6.29</b> FT-IR spectra of sSample having 0.00% ZB and 1.36% ZP at 140°C and 160°C.	79
<b>Figure 6.30</b> FT-IR spectra of sample having 0.27% ZB and 1.29% ZP at 140°C and 160°C.	79

<b>Figure 6.31</b> FT-IR spectra of sample having 0.54% ZB and 0.81% ZP at 140°C and 160°C.	80
<b>Figure 6.32</b> FT-IR spectra of sample having 0.68% ZB and 0.68% ZP at 140°C and 160°C.	80
<b>Figure 6.33</b> FT-IR spectra of sample having 0.81% ZB and 0.54% ZP at 140°C and 160°C.	81
<b>Figure 6.34</b> FT-IR spectra of sample having 1.29% ZB and 0.27% ZP at 140°C and 160°C.	81
<b>Figure 6.35</b> FT-IR spectra of sample No.8 having 1.36% ZB and 0.00% ZP at 140°C and 160°C.	82
<b>Figure 6.36</b> Absorbance versus ZB wt% at 1540cm <sup>-1</sup> at 140 and 160°C.	82
<b>Figure 6.37</b> Absorbance versus ZB wt% at 3227cm <sup>-1</sup> at 140 and 160°C.	83
<b>Figure 6.38</b> SEM microphotographs of PVC control samples	
a) Heated at 140°C for 15 min. b) Heated at 160°C for 90 min	84
<b>Figure 6.39</b> SEM microphotographs of sample having 1.36% ZP only.	
a) Heated at 140°C for 15 min. b) Heated at 160°C for 90 min	84
<b>Figure 6.40</b> SEM microphotographs of sample having 0.27% ZB and 1.29% ZP.	
a) Heated at 140°C for 15 min. b) Heated at 160°C for 90 min	85
<b>Figure 6.41</b> SEM microphotographs of sample having 0.54% ZB and 0.81% ZP.	
a) Heated at 140°C for 15 min. b) Heated at 160°C for 90 min	85
<b>Figure 6.42</b> SEM microphotographs of sample having 0.68% ZB and 0.68% ZP.	
a) Heated at 140°C for 15 min. b) Heated at 160°C for 90 min	86
<b>Figure 6.43</b> SEM microphotographs of sample having 0.81% ZB and 0.54% ZP.	
a) Heated at 140°C for 15 min. b) Heated at 160°C for 90 min	86
<b>Figure 6.44</b> SEM microphotographs of sample having 1.29% ZB and 0.27% ZP.	
a) Heated at 140°C for 15 min. b) Heated at 160°C for 90 min	87
<b>Figure 6.45</b> SEM microphotographs of sample having 1.36% ZB only.	
a) Heated at 140°C for 15 min. b) Heated at 160°C for 90 min	87
<b>Figure 6.46</b> a) EDX analysis of elements of PVC plastigel having 1.36% ZP only.	
b) SEM micrograph of PVC plastigel having 1.36% ZP only.	
c) EDX analysis of elements of PVC plastigel having 0.27% ZB + 1.29% ZP.	
d) SEM micrograph of PVC plastigel having 0.27% ZB + 1.29% ZP	89

## LIST OF TABLES

	<b>Page</b>
<b>Table 1.1</b> Principal groups of fire retardants and their market in 2003	2
<b>Table 3.1</b> Effect of flame retardancy of molybdenum oxide and antimony oxide	16
<b>Table 4.1</b> Manufacturers and Trade Names of some ZB Flame Retardants	19
<b>Table 4.2</b> Composition of flame-retardant coatings	25
<b>Table 4.3</b> The Composition in US.Patent No.5,886,072	28
<b>Table 4.4</b> The compositions of US.Patent No.5,338,791	28
<b>Table 4.5</b> The results of US.Patent No.5,338,791	28
<b>Table 4.6</b> Test results and compositions of US.Patent No.3,965,068	29
<b>Table 5.1</b> The general product specifications of Viscobyk 5025	33
<b>Table 5.2</b> The general product specifications of STORFLAM ZB 2335	34
<b>Table 5.3</b> The general product specifications of ZP – 46	34
<b>Table 5.4</b> The compositions used in the experiments	36
<b>Table 6.1</b> Elemental composition of the ZB and ZP powder	44
<b>Table 6.2</b> PVC Thermomat Results at 140°C of PVC plastigels	52
<b>Table 6.3</b> PVC Thermomat Results at 160°C of PVC plastigels	53
<b>Table 6.4</b> Activation energies of PVC plastigels heated at 140° and 160°C	57
<b>Table 6.5</b> Preexponential factors of PVC plastigels heated at 140° and 160°C	58
<b>Table 6.6</b> Mass loss of PVC plastigel films at 225°C	63
<b>Table 6.7</b> Mass loss of PVC plastigel films at 400°C	63
<b>Table 6.8</b> Mass loss of PVC plastigel films at 600°C	64
<b>Table 6.9</b> Onset temperatures of PVC plastigel films	64
<b>Table 6.10</b> The appearance of the film samples heated at 140°C for different time periods	67

<b>Table 6.11</b> The appearance of the film samples heated at 160°C for different time periods	67
<b>Table 6.12</b> Yellowness Index values of the PVC Films heated at 140°C	68
<b>Table 6.13</b> Yellowness Index values of the PVC Films heated at 160°C	68
<b>Table 6.14</b> The theoretical compositions of components	89
<b>Table 6.15</b> Elemental analyses of particles at 140°C for 15 minutes (Average values)	90
<b>Table 6.16</b> Elemental analyses of polymer phase at 140°C for 15 minutes (Average values)	90
<b>Table 6.17</b> Elemental analyses of particles at 160°C for 90 minutes (Average values)	91
<b>Table 6.18</b> Elemental analyses of polymer phase at 160°C for 90 minutes (Average values)	91
<b>Table A.1</b> The EDX results of PVC control sample at 140°C for 15 minutes	94
<b>Table A.2</b> The EDX results of sample 1.36% ZP only at 140°C for 15 minutes	94
<b>Table A.3</b> The EDX results of sample 0.27% ZB + 1.29% ZP at 140°C for 15 minutes	94
<b>Table A.4</b> The EDX results of sample 0.54% ZB + 0.81% ZP at 140°C for 15 minutes	94
<b>Table A.5</b> The EDX results of sample 0.68% ZB + 0.68% ZP at 140°C for 15 minutes	95
<b>Table A.6</b> The EDX results of sample 0.81% ZB + 0.54% ZP at 140°C for 15 minutes	95
<b>Table A.7</b> The EDX results of sample 1.27% ZB + 0.29% ZP at 140°C for 15 minutes	95

<b>Table A.8</b> The EDX results of sample 1.27% ZB + 0.29% ZP at 140°C for 15 minutes	95
<b>Table A.9</b> The EDX results of PVC control sample at 160°C for 90 minutes	96
<b>Table A.10</b> The EDX results of sample 1.36% ZP only at 160°C for 90 minutes	96
<b>Table A.11</b> The EDX results of sample 0.27% ZB + 1.29% ZP at 160°C for 90 minutes	96
<b>Table A.12</b> The EDX results of sample 0.54% ZB + 0.81% ZP at 160°C for 90 minutes	97
<b>Table A.13</b> The EDX results of sample 0.68% ZB + 0.68% ZP at 160°C for 90 minutes	97
<b>Table A.14</b> The EDX results of sample 0.81% ZB + 0.54% ZP at 160°C for 90 minutes	97
<b>Table A.15</b> The EDX results of sample 1.27% ZB + 0.29% ZP at 160°C for 90 minutes	98
<b>Table A.16</b> The EDX results of sample 1.27% ZB + 0.29% ZP at 160°C for 90 minutes	98
<b>Table A.17</b> CIE XYZ and Lab* values of white paper	98
<b>Table A.18</b> CIE XYZ and Lab* values of the PVC plastigel films heated at 140°C for 15 minutes.	99
<b>Table A.19</b> CIE XYZ and Lab* values of the PVC plastigel films heated at 160°C for 90 minutes.	100



## CHAPTER 1

### INTRODUCTION

It is well known that poly (vinyl chloride) (PVC) has high chlorine content, so it is an incombustible material. The construction of buildings often requires the use of fire or flame retardant jacketing, facing materials for heating, duct insulation, electrical insulation applications, cables and domestic uses such as in gutters, doors, profiles, house sidings, and similar applications involving plies of combustible sheet material or plies of such sheet materials laminated to various substrates such as aluminium foil and fibre glass batting.

The general formula of PVC is  $-(\text{CH}_2\text{CHCl})_n-$ .

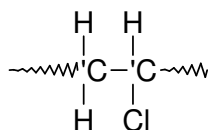


Figure 1.1 PVC molecule.

Because of its lower cost and versatility, PVC is often used to prepare such sheet materials by being blended with various additives which are designed to impart the required flame retardant characteristics. However, although PVC has a good flame retardancy because of its high chlorine content, PVC is not a safe material by means of fire hazards because it releases high levels of smoke and toxic gases like hydrogen chloride, benzene, toluene and other aromatic compounds leading to a colour change from brown and even black in the end (Pi et.al., 2002; Ning, and Guo, 2000; Baltacıoğlu and Balköse, 1999).

Additives such as compounds containing metals like antimony, zinc, copper, iron, aluminium, magnesium and molybdenum are widely used in reduced flammability and smoke suppression, the most important commercial smoke suppressants are zinc and aluminium compounds (Pi et.al., 2002; Ning and Guo, 2000). Many of these additives have been aimed at the effects of these compounds on the flame retardancy and smoke suppression of PVC as well as on the chemistry of PVC decomposition. Metal compounds are used to displace the labile chlorine atom in PVC polymer chain by more stable groups.

Nonetheless a large number of fire retardant additives are possible. The development of the field of fire retardant additives has achieved many different compounds and research has led to a diversity of additives and a thriving market. Fire retardants are now the most used plastics additives, exceeding 40% of a \$1 billion market in 1991 (Kirk-Othmer, 1994). This market is expected to increase. Table 1.1 gives the principal groups of chemicals (Tektaş, Mergen, 2003).

Table 1.1 Principal groups of fire retardants and their market in 2003 (Tektaş, Mergen, 2003).

<b>Group</b>	<b>USA, %</b>	<b>West Europe, %</b>
Al(OH) <sub>3</sub>	39	47
Brominated compounds	27	13
Phosphonated compounds	12	23
Chlorinated compounds	11	3
Antimony oxides	8	7
Mg(OH) <sub>2</sub>	1	2
Others*	2	5

\*Zinc borate and some other borate flame retardants.

85% of all of the flame retardants produced all around the world is used in plastics. As it is seen the most widely used compound is Al(OH)<sub>3</sub> and its usage is around 50%. Currently, borates have a low demand in world flame retardant market. In North America, annual demand of flame retardants is 350,000 ton and the borates have a 1% share in this market making 3,500 ton per annum. However, from 1991 onwards the share of borate compounds as flame retardants has increased and it is still increasing therefore the major producer in USA, U.S.Borax has increased its capacity. The market increase of zinc borate all around the world is expected to be 12 – 15 % (Tektaş, Mergen, 2003).

PVC plastisol is a mixture of PVC powder and plasticizer. It is transformed into the solid substance of the ultimate paste-derived product by heating at an elevated temperature, known as *gelation*. As the temperature of the plastisol rises, the plasticizer penetrates into the polymer particles which swell and merge, first loosely and then more fully, until the process culminates in complete mutual solution of polymer and

plasticizer with the formation of homogeneous plasticized PVC melt (Titow et.al., 1985).

To enhance the fire retardancy and to improve the thermal stability of PVC, the synergistic effect of the combination of Zinc Borate (ZB) and Zinc Phosphate (ZP) on the flame retardancy, char residue, thermal degradation kinetics of PVC and its mechanism were studied in this study. The study aims to find out the optimum synergistic composition of ZB and ZP in PVC thermal stabilization.

Thermal stabilization of PVC was determined by PVC Thermomat instrument. The conductivities of deionized water in which the plastigel films were placed and heated at elevated temperatures in the presence of nitrogen gas, were measured with respect to time. The time when the conductivity starts to increase is marked as *Induction Time* and the time when the conductivity reaches 50  $\mu\text{S}/\text{cm}$  is marked as *Stability Time*, which is the maximum acceptable level of degradation. The char residue of formation was investigated by TGA analyses. It was calculated by the ratios of the initial masses of PVC plastigel films to final masses after heating.

ZB and ZP were supplied from commercial products for all of the tests.

## CHAPTER 2

### THE THERMAL DEGRADATION OF PVC

PVC is commonly used as a thermoplastic because of its wide variability of properties allowing its application in rigid and soft products. However, PVC has very poor thermal, thermo oxidative light stability. The degradation of PVC and some copolymers, and the ways in which various stabilizers counteract and modify the process, have been widely studied for many years. The major chain degradation occurs by the elimination of HCl and simultaneous formation of conjugated double bond leading to a colour change (progressing with the extent of breakdown from light yellow, through reddish brown, to almost black in severe cases) and also which causes the deteriorations of physical, chemical and electrical properties. Dehydrochlorination can occur at only moderately elevated temperatures (about 100°C). It is catalyzed by the HCl evolved (autocatalysis), and can also be promoted or initiated by other strong acids (Titow et.al., 1985). Numerous stabilizers have been developed to neutralize the released HCl and prohibit further degradation by preventive reactions.

PVC polymers and copolymers are susceptible to degradation by heat (the thermal degradation is sometimes referred to as “thermolysis”) and by light (photolysis, also called photo degradation, and in some contexts photochemical degradation); in both cases degradation is rapid and more severe in the presence of oxygen. Heat stabilizers are incorporated in all PVC compositions to protect the polymer against thermal degradation at high temperatures of composition and also subsequently in service by eliminating the labile chlorine atom near the double bond.

The general mechanism of degradation of PVC is shown in Figure 2.1.

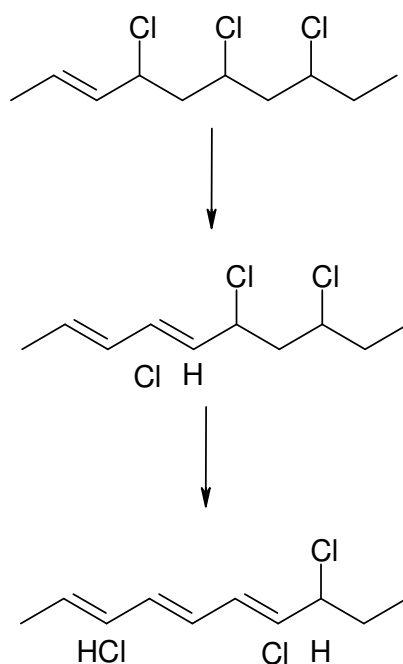
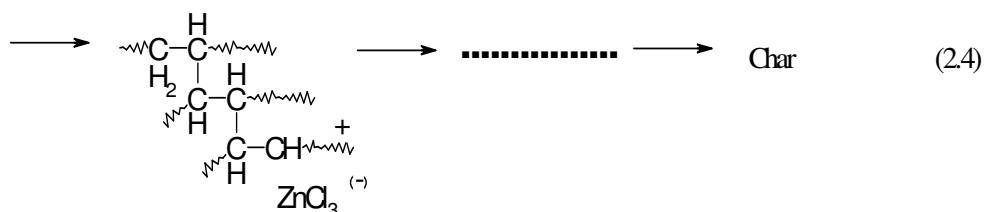
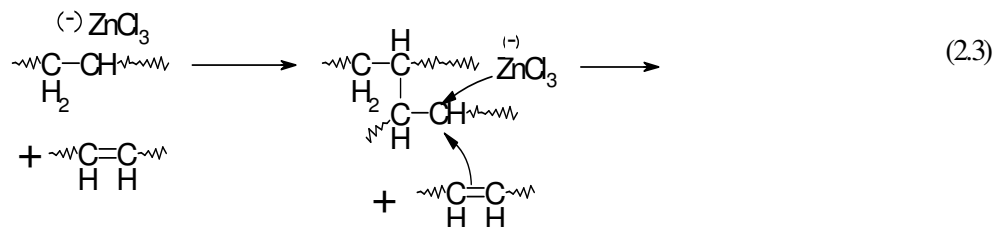
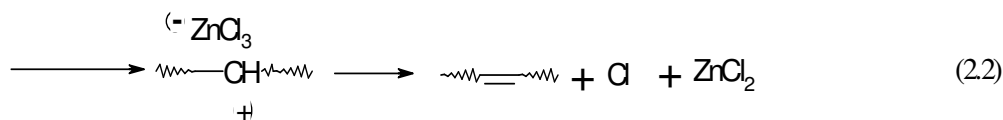
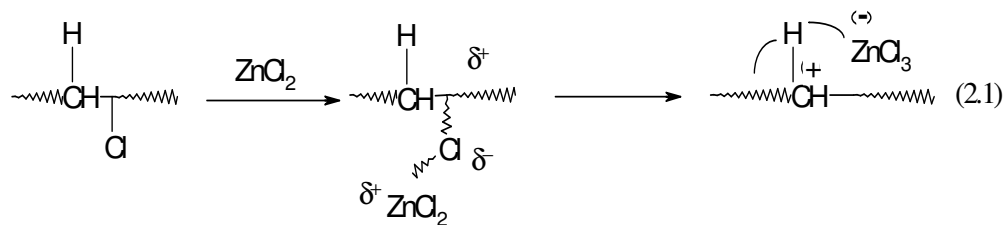


Figure 2.1. The general mechanism of degradation of PVC.

A detailed mechanism has been suggested (Ning and Guo, 2000).  $\text{ZnCl}_2$  from zinc salts of thermal stabilizers which is formed along with the thermal decomposition of PVC acts as an effective catalyst for the ionic dehydrochlorination of PVC. The dehydrochlorination of PVC with the influence of  $\text{ZnCl}_2$  is observed with the formation of trans-polyene structures which results in increased char formation and smoke formation. The said mechanism is given as follows,



(Ning and Guo,2000).

The process starts with a chlorine atom activated by an adjacent allylic bond configuration where that is already present in mid-chain; chlorine in the same position relative to an allylic end-group would also be activated.

Dehydrochlorination can occur at only moderately elevated temperatures (about 100°C). It is catalysed by the HCl evolved (autocatalysis), and can also be promoted or initiated by other strong acids.

In addition to dehydrochlorination, thermal degradation of PVC polymer in the presence of oxygen also involves oxidation, with the formation of hydroperoxide, cyclic peroxide, and keto groups, some of which can provide additional active sites for initiation of dehydrochlorination.

Chain scission and cross-linking can also take place as degradation proceeds, both in air and in an inert atmosphere.

If the thermal stability of PVC polymer or composition at a given temperature is defined in terms of time required for one of the main manifestations of degradation to

reach a stated level and if the degradation is treated as a unified process, thermally activated in the classic manner, the appropriate Arrhenius-type relationship may be written in the form below:

$$t = t_0 * \exp(-E / RT) \quad (2.5)$$

where;

t is the duration of stability;

t<sub>0</sub> is a constant;

E is the activation energy for thermal degradation of PVC polymer in the conditions (and/or composition) concerned;

R is the ideal gas constant and

T is the absolute temperature.

The activation energy for thermal degradation of an uPVC composition is quoted by Chauffoureaux, et.al.(1979) as 25.9 kcal mol<sup>-1</sup>, by Rice and Adam (1977) as 20 kcal mol<sup>-1</sup>.

Susceptibility to the thermal degradation varies with the process of manufacture of the PVC polymer and also with the source of supply. Other things being equal, the susceptibility increases (inherent stability decreases) in the sequence:

Mass polymer → suspension polymer → emulsion polymer

Higher molecular weight makes for greater resistance to degradation. The stability of PVC resin can also be adversely influenced by other constituents (e.g. antistatic agents, some colorants). The ease of stabilization and response to particular stabilizers in particular conditions also vary with the above features.

Rate of dehydrochlorination can be evaluated by measuring the conductivity change in the solution into which the evolved HCl gas is solved from the heated PVC polymer. Electrical conduction is a transport phenomenon in which electrical charge (carried by electrons or ions) moves through the system. The *electric current I* is defined as the rate of flow of charge through the conducting material:

$$I \equiv dQ/dt \quad (2.6)$$

where dQ is the charge that passes through a cross section of the conductor in time dt. The *electric current density j* is the electric current per unit cross-sectional area:

$$j \equiv I/A \quad (2.7)$$

where A is the conductor's cross-sectional area. The SI unit of current is the *ampere*, A and equals one coulomb per second.

$$1A = 1C/S \quad (2.8)$$

The *conductivity κ* of a substance is defined by

$$\kappa = j/E \quad \text{or} \quad j = \kappa E \quad (2.9)$$

where, E is the magnitude of the electric field. The higher the conductivity κ, the greater the current density j that flows for a given applied electric field. The reciprocal of the conductivity is the *resistivity ρ*:

$$\rho = 1/\kappa \quad (2.10)$$

The resistivity is measured in Ω.m and the conductivity in m<sup>-1</sup>.Ω<sup>-1</sup>. The reciprocal of Ω is *Siemens (S)*. Hence conductivity is S.m<sup>-1</sup>.

$$1 \Omega \equiv 1 \text{ V/A} = 1 \text{ kgm}^2 \text{ s}^{-1} \text{ C}^{-2} \quad (2.11)$$

The current in an electrolyte solution is the sum of the currents carried by the individual ions. The conductivity of the solution is

$$\kappa = \sum_i |z_i| F u_i c_i \quad (2.12)$$

Where,

$u_i$  is the mobility of ion i (m<sup>2</sup>/V.s),

F is the Faraday's constant (F = 96485 °C/mol),

$|z_i|$  = Total charge number,

$c_i$  = Concentration of the solution (mol/m<sup>3</sup>).

The mobility of the ions is the sum of the mobility of cations and anions.

$$\kappa = z_+ F u_+ c_+ + |z_-| F u_- c_- \quad (2.13)$$

The mobility of H<sup>+</sup> and Cl<sup>-</sup> in water at 25°C for HCl is as follows (Levine, 1995) ;



$$u_{\text{H}^+} = 36.25 \cdot 10^{-8}, \text{ m}^2/\text{V}\cdot\text{s} \quad (2.14)$$

$$u_{\text{Cl}^-} = 7.913 \cdot 10^{-8}, \text{ m}^2/\text{V}\cdot\text{s} \quad (2.15)$$

$$u_{\text{HCl}} = 44.163 \cdot 10^{-8}, \text{ m}^2/\text{V}\cdot\text{s} \quad (2.16)$$

## CHAPTER 3

### THERMAL STABILIZATION and STABILIZERS

#### 3.1 Thermal Stabilization

PVC polymers and copolymers are susceptible to degradation by heat and light: in both cases degradation is rapid and more severe in the presence of oxygen. Heat stabilizers are incorporated in all PVC compositions to protect the polymer against thermal degradation at high temperatures of processing and also subsequently in service.

The main outward manifestations of thermal degradation of PVC (at temperatures sensibly below those of pyrolytic decomposition and combustion, against which no stabilization is possible) are the evolution of HCl, development of colour (from light yellow, through reddish brown, to almost black in severe cases) and deterioration of physical, chemical and electrical properties (Titow et.al., 1985).

#### 3.2 Heat Stabilizers

All heat stabilizers and stabilizer systems in industrial use are of the “external” kind in the application sense, in that they are additives incorporated in the PVC by physical admixing. On the basis, the compounds used as heat stabilizers for PVC may be divided into the following general groups:

- I. Lead compounds;
- II. Organotin compounds;
- III. Compounds of other metals;
- IV. Organic stabilizers.

### 3.2.1 Lead Compounds

These are either lead salts or lead soaps (salts with stearic acid). The main advantage of these old-established stabilizers is cost-effective good heat-stabilizing power, and particular suitability for use in electrical insulation. However, they are not suitable for clear compositions, where their toxicity presents a hazard, as, for example, in food-contact applications (e.g. packaging films, containers), products for medical use, or children's toys (Titow et al., 1985). Some of the well known lead compounds are basic lead carbonate, tribasic lead sulphate, dibasic lead phosphate, lead silicate and lead stearate.

### 3.2.2 Organotin Compounds

Commercial organotin stabilizers are mainly compounds of the general formula below on the left, but also the one on the right is used too.

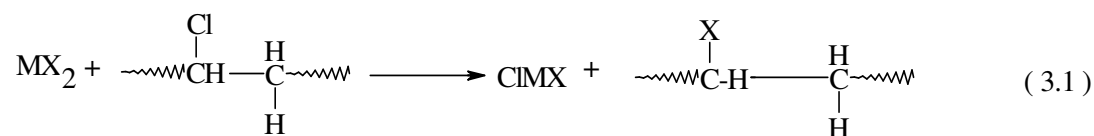


The nomenclature is largely associated with the R groups. Because their stabilizing effects in PVC are lower and their toxicity high, than those of compounds above, they are normally regarded as undesirable by-products and the production processes run so as to minimize their formation (Titow et.al., 1985).

### 3.2.3 Compounds of other metals

Apart from those of lead and tin, certain compounds are also of interest as stabilizers for PVC: stearates and laureates of zinc, calcium, aluminium, barium, antimony, lithium, magnesium, sodium, potassium and cadmium.

According to Frye-Horst mechanism, an esterification reaction takes place where the chlorine atom is bonded to the molecule between PVC and fatty acid salt of metal ion ( $M^{++}$ ).



where X: Carboxylate anion.

Further combinations of two or three of these compounds are also used stabilizers. Composite metal stabilizers are also widely used in solid (powder, flake), liquid, or paste forms. More recently concentrates of some systems in PVC polymer have also becoming important (Titow et.al., 1985).

### 3.2.4 Organic Stabilizers

The organic stabilizers are widely used because they are uniformly and intimately dispersible in PVC compositions but some have limited compatibility with plasticizers, or particular plasticizer/resin combinations in pPVC. To count some of them,

- Esters of aminocrotonic acid,
- Urea derivatives (phenyl urea, diphenyl urea),
- Epoxy compounds,
- Organic phosphates and
- Miscellaneous organic co-stabilizers (Titow et.al., 1985).

### 3.3 Flame Retardants

In order for a solid to burn it must be volatilized, because combustion is almost exclusively a gas-phase phenomenon. In the case of a polymer, this means that decomposition must occur. The decomposition produces low molecular weight chemical compounds that eventually enter the gas phase. Heat from combustion causes further decomposition and volatilization, and therefore combustion. For a compound to function as a flame retardant it must interrupt this cycle in some way.

A compound or mixture of compounds that when added to or incorporated chemically into a polymer serves to slow or hinder the ignition or growth of fire, the foregoing effect occurring primarily in the vapour phase.

Flame (or fire) retardant additives are most often used to improve fire performance of low-to-moderate cost commodity polymers. These additives may be physically blended with or chemically bonded to host polymer. They generally affect either low ignition susceptibility or once ignited, lower flammability. Ignition resistance can be improved solely from the thermal behaviour of the additive in the condensed phase. Retardants such as alumina add to the heat capacity of the product, thus increasing the enthalpy needed to bring the polymer to a temperature at which fracture of the chemical bonds occurs. The endothermic volatilization of bound water can be a significant component of the effectiveness of this family of retardants such as in zinc borates. Other additives, such as organophosphates, change polymer decomposition chemistry. These materials can induce the formation of a cross-linked, more stable solid and can also lead to the formation of a surface char layer. This layer both insulates the product from further thermal degradation and impedes the flow of potentially flammable decomposition products from the interior of the product to the gas phase where combustion would occur.

Flame retardants function in the vapour phase where the enthalpy-generating combustion reactions occur. Halogen-containing species, for instance, can be selected to vaporize at the same temperature as the polymer fragments. Coexisting in the reactive area of the flame, the halogens are effective at decreasing the concentrations of the free radicals that propagate flames, thus reducing the flame intensity, the enthalpy returned to the product, and the burning rate, in that order. They can also be self-extinguishing (Bowen, 1985; Jenkner et.al., 1982).

Compound of chlorine and bromine are the halogen compounds having commercial significance as flame-retardant chemicals. Fluorine compounds are expensive except in special cases. Iodine compounds although effective, are expensive and too unstable to be used. Halogenated flame retardants can be broken down into three classes:

- i. Brominated aliphatic,
- ii. Chlorinated aliphatic, and
- iii. Brominated aromatic which the thermal stability increases from up to down.

It is commonly thought that it is desirable for the flame retardant to decompose with the liberation of halogen at a somewhat lower temperature than the decomposition temperature of the polymer (Babrauskas, 1984 and 1987).

Useful materials incorporating fire-retardant additives are not always straightforward to produce. Loadings of 10% are common, and far higher levels of flame retardants are used in some formulations.

Nonetheless a large number of fire-retardant additives are possible.

- I. Phosphate esters,
- II. Halogenated phosphates,
- III. Chlorinated hydrocarbons,
- IV. Brominated hydrocarbons,
- V. Brominated bisphenol-A
- VI. Antimony trioxide,
- VII. Borates,
- VIII. Aluminium trihydrate,
- IX. Magnesium hydroxide.

### **3.4 Fire Retardants for PVC**

PVC is a hard, brittle polymer that is self-extinguishing. In order to make PVC useful and more pliable, plasticizers are added. More often than not the plasticizers are flammable and make the formulation less flame resistant. Flammability increases as the plasticizer is increased and the relative amount of chlorine decreased. The flame resistance of the poly (vinyl chloride) can be increased by the addition of an inorganic flame retardant synergist.

- I. Antimony oxide
- II. Molybdenum oxide
- III. Zinc stannates
- IV. Aluminum trihydrate
- V. Zinc borate

(Peacock et.al., 1991 in Kirk-Othmer, 1994).

### 3.4.1. Antimony Oxide

The effect of antimony oxide and ZB on the oxygen index of flexible poly (vinyl chloride) containing from 20 to 50 parts of plasticizer is shown in Figure 3.1.

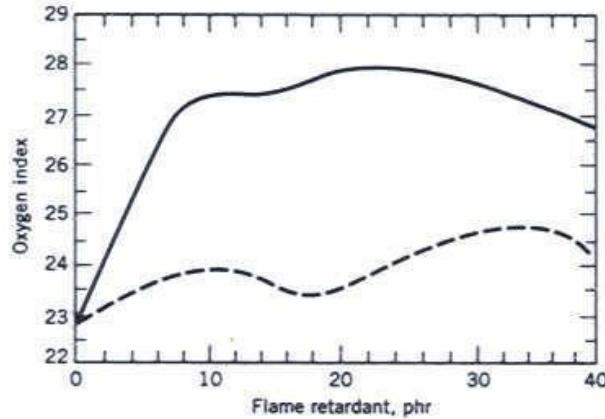


Figure 3.1 A comparison of the effect of antimony oxide (—) and ZB (----) on the oxygen index of flexible PVC containing from 20 to 50 phr DOP (Kirk-Othmer, 1994).

The flame resistance increases with the addition of antimony oxide until the oxygen index appears to reach a maximum at about 8 parts of  $Sb_2O_3$ . Further addition does not have any increased beneficial amount (Kirk-Othmer, 1994).

### 3.4.2. Molybdenum Oxide

Molybdenum compounds incorporated into flexible PVC not only increases flame resistance, but also decrease smoke evolution. In Table 3.1, the effect of molybdenum oxide on the oxygen index of flexible PVC containing 50 parts of a plasticizer is compared with antimony oxide. Antimony oxide is superior synergist for flame retardancy but has little or no effect on smoke evolution. However, combinations of molybdenum oxide and antimony trioxide may be used to reduce the total inorganic flame retardant additive package, and obtain improved flame resistance and reduce smoke (Kirk-Othmer, 1994).

Table 3.1 Effect of flame retardancy of molybdenum oxide and antimony oxide (Kirk-Othmer, 1994).

<b>Sb<sub>2</sub>O<sub>3</sub></b>	<b>MoO<sub>3</sub></b>	<b>Oxygen Index</b>	<b>Smoke</b>
-	-	24.5	10.7
2.0	-	27.5	9.2
-	2.0	26.0	6.8
2.0	2.0	29.5	6.0

### 3.4.3. Zinc Stannates

The zinc stannates are also effective synergists for flexible PVC; however, antimony oxide is more effective. If more chlorine such as in chlorinated paraffin is added, the stannates become more effective and outperform antimony oxide (Kirk-Othmer, 1994).

### 3.4.4 Aluminium Trihydrate

Aluminium trihydrate, Al<sub>2</sub>O<sub>3</sub>·3H<sub>2</sub>O, (ATH) is manufactured from either bauxite ore or recovered aluminium by either the Bayer or sinter process. It is generally used as a secondary flame retardant in flexible PVC because of the high concentration needed to be effective.

It is the least expensive and least effective of the flame retarders. It is only about one-fourth to one-half as effective as the halogens. Usually about 50 – 60% of aluminium trihydrate is needed to obtain some acceptable degree of flame retardancy. It is also limited to plastics processed higher than 220°C (Kirk-Othmer, 1994).

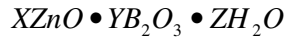


## CHAPTER 4

### ZINC BORATE AND ZINC PHOSPHATE

#### 4.1 Zinc Borate

The most widely used flame retardant is zinc borate [CAS No.1332-07-6], prepared as an insoluble double salt from water-soluble zinc and boron compounds. Compounds having varying amounts of zinc, boron, and water of hydration are available. The general molecular formula of zinc borate is



And some examples for X, Y and Z are

$$X=4, Y=1, Z=1$$

$$X=2, Y=3, Z=3.5$$

$$X=2, Y=3, Z=7.5$$

$$X=2, Y=3, Z=5$$

$$X=2, Y=3, Z=7$$

The ratio of these components affects the temperature at which the flame-inhibiting powers are activated, as well as the temperature at which they can be processed. Zinc borates can either be used alone or in combination with other halogen synergists, such as antimony trioxide. In some instances zinc borate is used with alumina trihydrate to form a glass-like substance that inhibits polymer degradation.

Zinc borate is also effective in enhancing the flame-inhibiting powers of chlorine. Although zinc borate increases flame resistance, it is not as effective as antimony oxide, as is illustrated in the Figure 3.1.

However zinc borate can be used in combination with antimony oxide to obtain equivalent and in some instances enhance effects over what can be obtained using either of the two synergists alone (Kirk-Othmer, 1970).

#### 4.1.1 Production of ZB

In general, an aqueous solution was prepared by dissolving boric acid in pure water in the stoichiometric amount which is compatible with the desired final zinc borate crystal structure. Zinc oxide and boric acid are later added to this solution and stirred and mixed together and kept on reacting at temperatures between 70 – 100°C. The temperature and time values change according to the final desired structure also. The obtained product is filtered, washed with water, dried at 105°C and ground.

For example, Zinc Borate  $2\text{ZnO}\cdot 3\text{B}_2\text{O}_3\cdot 7\text{H}_2\text{O}$  is formed when borax is added to aqueous solutions of soluble zinc salts at temperatures below about 70°C.

A different crystalline hydrate,  $2\text{ZnO}\cdot 3\text{B}_2\text{O}_3\cdot 3.5\text{H}_2\text{O}$ , equivalent to  $4\text{ZnO}\cdot 6\text{B}_2\text{O}_3\cdot 7\text{H}_2\text{O}$ , is produced when the reaction between zinc oxide and boric acid is carried out at temperatures of 90 – 100°C. This compound has the unusual property of retaining its water of hydration at temperatures up to 290°C. This thermal stability makes it attractive as a fire retardant additive for plastics and rubbers that require high processing temperatures. It is also used as an anticorrosive pigment in coatings. Some of the ZB producers are tabulated in Table 4.1.

Individual particles of ZB are independent rhombic hexahedrons, the length of a side of each particle lying in a range of 0.3 to 7 μm (Sawada H., 2002).

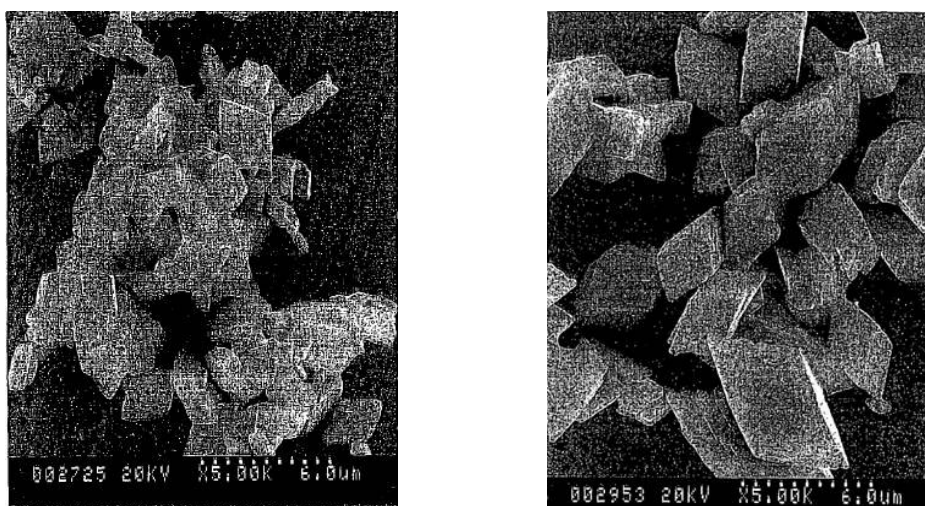


Fig.4.1 Scanning-type electron microphotograph (Mag.: x5000) of Zinc Borate(Sawada H., 2002).

### 4.1.2 Boron Mechanism

Boron functions as a flame retardant in both the condensed and vapour phases. Under flaming conditions boron and halogens form the corresponding trihalide. Because boron trihalides are effective Lewis acids, they promote cross-linking, minimizing decomposition of the polymer into volatile flammable gases. These trihalides are also volatile; thus they vaporize into the flame and release halogen which then functions as a flame inhibitor (Shen et.al., 1990).

Borons also react with hydroxyl-containing polymers such as cellulose. When exposed to a flame the boron and hydroxyl groups form a glassy ester that coats the substrate and reduces the polymer degradation. A similar type of action has been observed in the boron-alumina trihydrate system (Shen et.al., 1990; Hilado, 1974; Byrne,et.al., 1966).

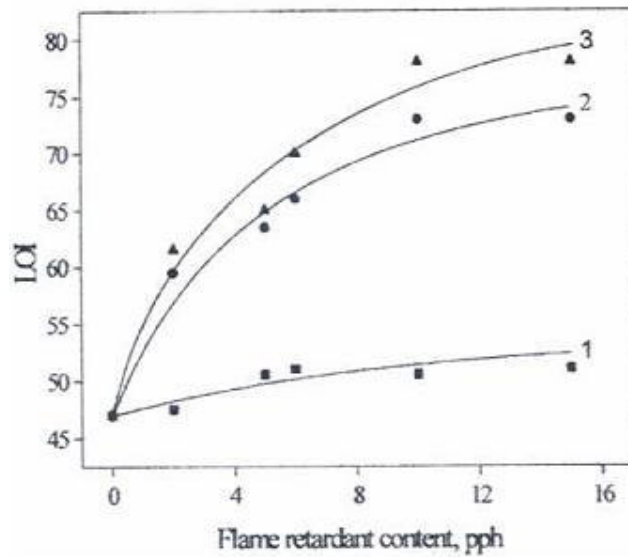
Table 4.1 Manufacturers and Trade Names of some ZB Flame Retardants (Kirk-Othmer, 1994).

Manufacturer	Trade Name	Composition	CAS No
Climax Performance Materials	ZB 467	$4\text{ZnO}\cdot 6\text{B}_2\text{O}_3\cdot 7\text{H}_2\text{O}$	[12513-27-8]
	ZB 223	$2\text{ZnO}\cdot 3\text{B}_2\text{O}_3\cdot 3\text{H}_2\text{O}$	
	ZB 113	$\text{ZnO}\cdot \text{B}_2\text{O}_3\cdot 3\text{H}_2\text{O}$	
	ZB 237	$2\text{ZnO}\cdot 3\text{B}_2\text{O}_3\cdot 7\text{H}_2\text{O}$	
	ZB 325	$3\text{ZnO}\cdot 2\text{B}_2\text{O}_3\cdot 5\text{H}_2\text{O}$	
U.S.Borax	Firebrake ZB	$2\text{ZnO}\cdot 3\text{B}_2\text{O}_3\cdot 5\text{H}_2\text{O}$	[13701-59-2]
		$\text{Zn}(\text{BO}_2)_2$	
Hebei Hongxing Chemicals Co.		$2\text{ZnO}\cdot 3\text{B}_2\text{O}_3\cdot 3.5\text{H}_2\text{O}$	[12513-27-8]
Waardals		$2\text{ZnO}\cdot 3\text{B}_2\text{O}_3\cdot 3.5\text{H}_2\text{O}$	[12351-27-8]
Heron Chemicals	Storflam	$2\text{ZnO}\cdot 3\text{B}_2\text{O}_3\cdot 3.5\text{H}_2\text{O}$	[12513-27-8]

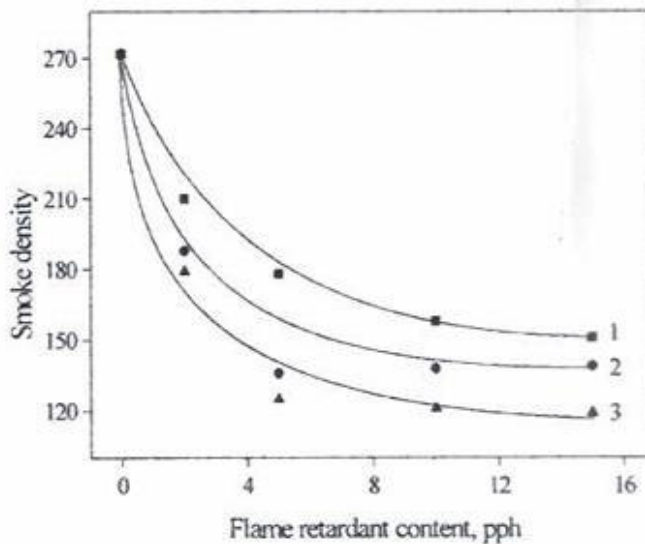
### **4.1.3 Flame Retardant Effect of ZB**

Ning and Guo [2000] have studied the effects of zinc borate and aluminium trihydrate (ATH) and their mixtures on the flame retardant and smoke suppressant properties of PVC as well as their mechanism for flame retardancy and smoke suppression through LOI, smoke density test, TGA, GC-MS, and SEM. They have found that small amounts of ZB, ATH and their mixture can greatly increase the LOI of PVC and reduce the smoke density, hazardous gases released and char formation of PVC. The mixture of ZB and ATH had a good synergistic effect on the flame retardancy and smoke suppression of PVC. TGA and GC – MS results showed that incorporation of a small amount of ZB, ATH, and their mixture greatly promoted the char formation of PVC and decreased the amount of hazardous gases such as benzene and toluene released in PVC during combustion. Their mechanism was also proposed.

As shown in the Figure 4.2 a and b, the LOI of PVC increased and smoke density decreased with increase of the amount of ZB, ATH and ZB – ATH. The LOI of PVC/ZB – ATH is much higher than that of PVC/ZB and PVC/ATH. The smoke density of PVC/ZB – ATH is much lower than that of PVC/ZB and PVC/ATH, which indicated that ZB and ATH have a good synergistic effect on the flame retardancy and smoke density of PVC.



(a)



(b)

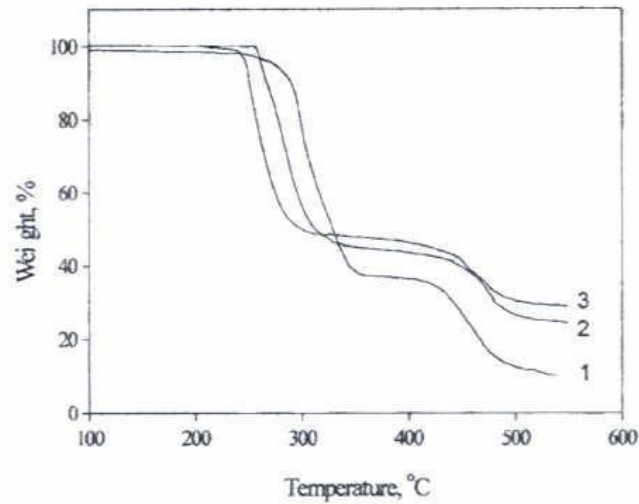
Figure 4.2 a) Effects of ATH (1), ZB (2) and ZB – ATH (3) contents on LOI of PVC.

b) Effects of ATH (1), ZB (2), and ZB – ATH (3) contents of smoke density of PVC (Ning and Guo, 2000).

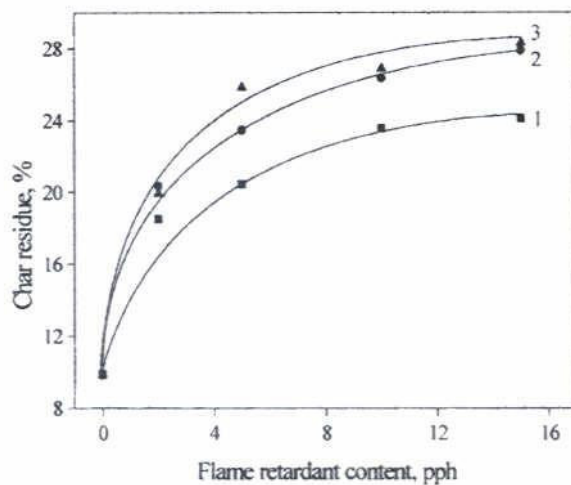
As shown in Figure 4.3 (a) and (b), the thermal decomposition of PVC was divided into two stages: The thermal decomposition in the first stage was mainly the evolution of HCl. The thermal decomposition in the second stage was mainly cyclization of conjugated polyene sequences to form aromatic compounds. The incorporation of small amount of ZB and ZB – ATH greatly decreased the weight loss of the PVC thermal

decomposition. The char residue of PVC increased about 130% after incorporation of 5 pph of ZB and ZB – ATH, respectively, also indicating that ZB and ZB – ATH are good smoke suppressants for PVC.

PVC, PVC/ZB, PVC/ATH, and PVC/ZB – ATH samples were burned in air in a spirit lamp and the char residue calculated (Fig.4.3). The char residue increased as the contents of ZB, ATH and ZB – ATH increased.



(a)



(b)

Figure 4.3 a) TGA curves of PVC and PVC/ZB – ATH,  
 b) Effects of ATH (1), ZB (2), and ZB – ATH (3) contents on char residue of PVC (Ning and Guo, 2000).

Mechanochemical modification of ZB and ATH in PVC by high-energy mechanical milling and their mechanical properties were studied by Pi et.al. (2002). The effect of mechanochemical improvement of these additives on the release of aromatic compounds during burning of PVC was characterized by ultraviolet spectroscopy (UV), Gas chromatography mass spectrometry (GC-MS), Limiting oxygen index (LOI), stress-strain behaviour, and SEM. The chemical bonding of PVC with ZB or ZB – ATH was generated during mechanical milling. The incorporation of ZB and ATH can greatly increased the LOI of PVC and suppressed the release of aromatic compounds during burning of PVC. The mechanochemical modification increased the impact and yield strengths and elongation at break of PVC/ZB and ATH and also increased the LOI.

As shown in Figure 4.4, the LOI of PVC/ZB and PVC/ZB – ATH went up with increasing ZB and ZB – ATH content. The LOI of PVC/ZB-2 and PVC/ZB – ATH-2, treated, was much higher than that of corresponding PVC/ZB-1 and PVC/ZB – ATH-1, untreated due to the decrease in the particle sizes, the increase in surface areas and the chemically bonding between PVC and ZB or ZB – ATH.

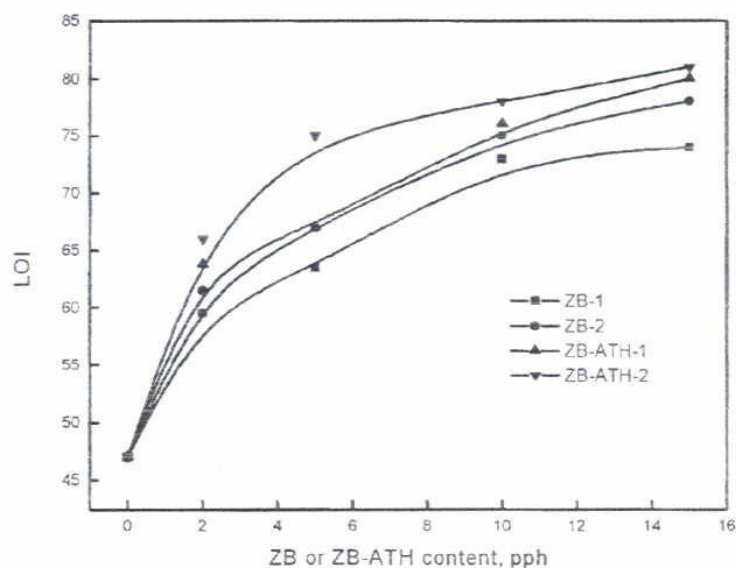


Figure 4.4 Effects of ZB and ZB – ATH content on the LOI of PVC (Ning and Guo, 2002) 1 : Untreated, 2 : Treated.

As shown in Figure 4.5, the impact strength of PVC/ZB – ATH-1 almost remained unchanged with increasing ZB – ATH-1 content, whereas the impact strength of

PVC/ZB – ATH-2 increased with rising ZB – ATH-2 content, and the impact strength of PVC/ZB – ATH-2 was higher than that of PVC/ZB – ATH-1.

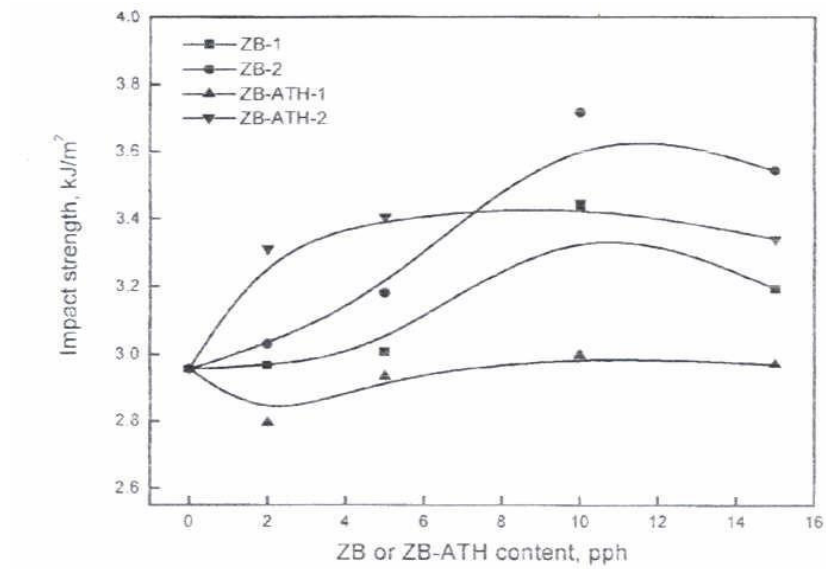


Figure 4.5 Effects of the ZB and ZB – ATH content on the impact strength of PVC (Ning and Guo, 2002) 1 : Untreated, 2 : Treated.

Figure 4.6 shows that the yield strength of PVC decreased with increasing ZB and ZB – ATH content but the treated ones have higher yield strength.

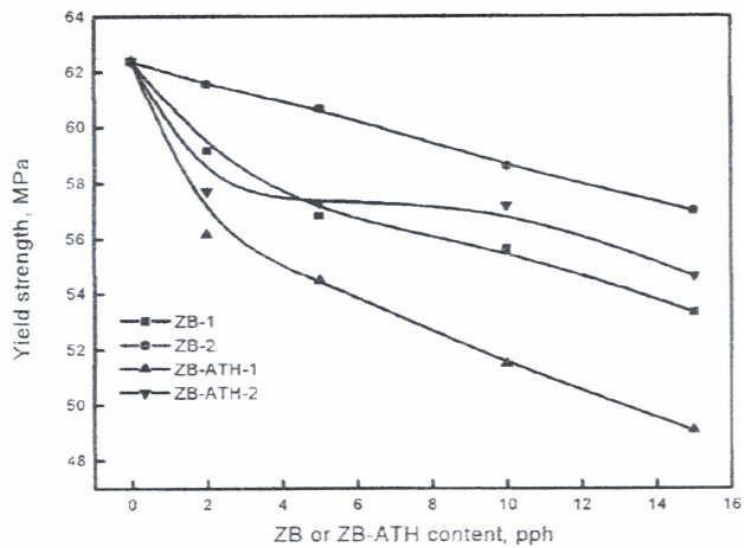


Figure 4.6 Effects of ZB and ZB – ATH content on the yield strength of PVC (Ning and Guo, 2002) 1 : Untreated, 2 : Treated.



Giudice and Benitez, [2001] discussed the influence of ZB having 3.5 H<sub>2</sub>O and 7.5 H<sub>2</sub>O. Eight different paint compositions were prepared. LOI, and flame spread index (FSI) tests were carried out to test the flame retardancy. As shown in Figure 4.7, results of LOI tests indicate that the compositions having both ZB's (No.5) and having only 7.5 H<sub>2</sub>O (No.3) with antimony trioxide have the maximum values. All sample compositions are given in Table 4.2.

Table 4.2. Composition of flame-retardant coatings, % by volume on solids<sup>a</sup> (Guidice and Benitez, 2001).

Component	1	2	3	4	5	6	7	8
Titanium dioxide	11.5	11.5	11.5	11.5	11.5	11.5	11.5	11.5
Antimony trioxide	9.0	6.0	6.0	6.0	3.0	-	-	-
Zinc borate <sup>b</sup>	-	3.0	-	1.5	3.0	4.5	9.0	-
Zinc borate <sup>c</sup>	-	-	3.0	1.5	3.0	4.5	-	9.0
Micronized talc	22.4	22.4	22.4	22.4	22.4	22.4	22.4	22.4
Chlorinated alkyd resin	52.4	52.4	52.4	52.4	52.4	52.4	52.4	52.4
Bentone (gel)	2.8	2.8	2.8	2.8	2.8	2.8	2.8	2.8
Additives	1.9	1.9	1.9	1.9	1.9	1.9	1.9	1.9

<sup>a</sup> PVC (pigment volume concentration), 42.9% <sup>b</sup> 2ZnO·3B<sub>2</sub>O<sub>3</sub>·3.5H<sub>2</sub>O,

<sup>c</sup> 2ZnO·3B<sub>2</sub>O<sub>3</sub>·7.5H<sub>2</sub>O, <sup>d</sup> 24.9% chlorine content.

Samples No.6 – 8 had the lowest LOI values with no antimony trioxide in their compositions.

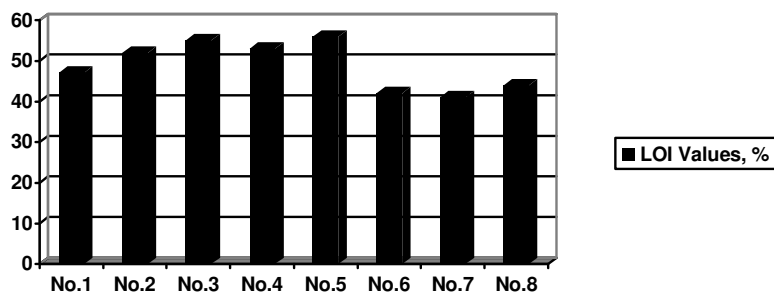


Figure 4.7 LOI Values (%) of the compositions(Guidice and Benitez, 2001).

The UL94 tests carried out also have shown that all of the compositions passed the tests in Class A.

Xie et.al., [2000] have studied the flammability characterization and the flame retarding mechanism of expandable graphite (EG) combined with other halogen-free flame retardants (HFFR) such as phosphorus-nitrogen compound, ammonium polyphosphate, red phosphorus and zinc borate, in polyolefins (PO) blends, in which the intumescent charred layers, as good heat-insulation materials, played a crucial role in increasing the thermo-oxidative temperature and decreasing the thermo-oxidation heat. Thus they have traced dynamic thermo-oxidative degradation of various LLDPE/EG/HFFR systems by real time Fourier transform infrared spectroscopy.

Figure 4.8 (a) and (b) show the dynamic FTIR spectra from the thermo-oxidative degradation of LLDPE/EG/ZB blends at 300 and 400°C, respectively. The small peak at 3227 cm<sup>-1</sup> and several peaks between 900 and 1300 cm<sup>-1</sup> are characteristics of zinc borate additive. It can be seen from Fig.4.8 that the decreases of main peak intensities at 2916, 2854, 1610, 1455 and 720 cm<sup>-1</sup> with increasing Thermo-oxidative Degradation (TOD) times indicate the breakdown of LLDPE main chains. It can be noticed that the intensities of several peaks between 900 and 1300 cm<sup>-1</sup> decrease slowly with increasing TOD times. This might be due to the dehydration or breakdown of ZB on heating in the temperature range of 300 – 400 °C and the formation of boric acid to promote the formation of surface expanded carbonaceous char structures between flame and polyolefins in the condition of fire.

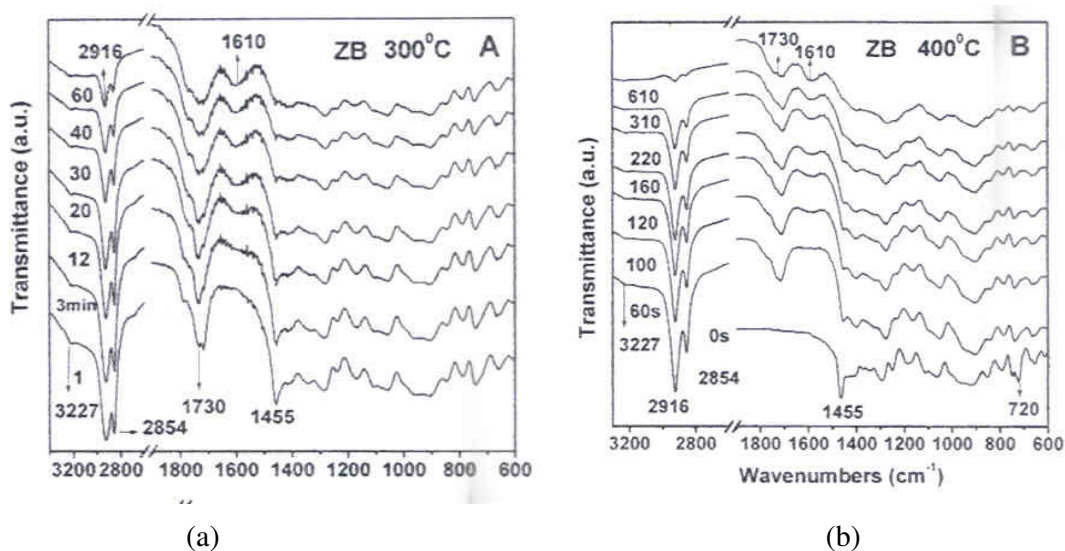


Fig.4.8 Changes of dynamic FTIR spectra obtained from the thermo-oxidative degradation of LLDPE/10% EG/20% ZB blends in the condensed phase with different pyrolysis times. (a): 300°C, (b): 400°C (Xie et.al.,2000).

In a US.Patent taken by Linsky, [1999] several flame retardant compositions for cable jacketing and wire insulation that contain ATH and ZB were studied. The compositions were tested according to oxygen index, smoke density, elongation stress, brittle point and tensile strength. The composition was prepared according to the compositions shown in Table 4.3.

This composition exhibited an oxygen index of 49 which was very high and smoke char test of 1.8% which was very low. Elongation, brittle point, tensile strength tests gave values of 225%, 0°C and 2515 lbs/in<sup>2</sup>, respectively.

In a US.Patent taken by Chaplin, [1994] relates to fire-retardant compositions. ZB and divalent metallic stannate, zinc stannate (ZS), in halogen containing compositions provides an increased fire-retardant effect, which is greater than that expected from the use of either ZB or ZS alone. The combination also suppresses smoke production.

In order to test the fire-retardant characteristics of the compositions having 10 parts per hundred (phr) of fire-retardant totally, each sample was flame tested and Concentration of Oxygen Index (COI) amounts of smoke and carbon monoxide (CO) measured. The studied compositions are tabulated in Table 4.4 and the results in Table 4.5.

The results presented in Table 4.5 show that better fire-retardant properties were obtained from the samples containing both ZB and ZS than would have been used individually. As well as resulting in a synergistic fire-retardant effect, the study also showed that the use of a decreased amount of ZB and ZS relative to the amount used when either component was used on its own was possible.

Table 4.3 The Composition in US.Patent by Linsky [1999].

<b>Ingredient</b>	<b>Amount, phr</b>
PVC resin	100
Pentaerythritol ester plasticizer	33
Calcined clay	5
Aluminium trihydrate	70
Basic lead heat stabilizer	6
Stearic acid lubricant	0.25
Antimony trioxide	5
Brominated phthalate ester	10
Isodecyl diphenyl phosphate	5
Ammonium octamolybdate	10
Zinc borate	2

Table 4.4 The compositions of US.Patent by Chaplin [1994].

<b>Amounts in phr</b>	<b>Component</b>	<b>Product Name</b>	<b>Manufacturer</b>
100	PVC	VY 110/51	Hydro Polymer
50	DOP	Reomol	Ciba Geigy
4	Stabiliser	Irgastab BC26	Ciba Geigy
0.7	Wax	Irgawax	Ciba Geigy

Table 4.5 The results of US.Patent by Chaplin [1994].

<b>Sample</b>	<b>ZB, phr</b>	<b>ZS, phr</b>	<b>COI</b>	<b>Smoke, D<sub>m</sub></b>	<b>CO, ppm</b>
1	10	-	24.7	386	548
2	8	2	26.3	374	661
3	6	4	26.6	365	720
4	4	6	28.3	378	780
5	2	8	28.5	355	820
6	-	10	28.8	391	857

## 4.2 Zinc Phosphate

The most important phosphate containing anticorrosive pigment is zinc phosphate [CAS No.7779-90-0],  $Zn_3(PO_4)_2$ , MW = 385. It can be used with a large number of binders and has a very wide range of uses. Zinc phosphate is usually produced on an industrial scale from zinc oxide and phosphoric acid, or from zinc salts and phosphates.

### 4.2.1 Synergism in Nickel Oxide and Zinc Phosphate

Dickens, [1976] calculated the smoke density of smoke retardant PVC compositions of Ni and Zinc salts in US.Patent No 3,965,068; such as Nickel oxide and Nickel carbonate with Zinc Phosphate(ZP) and Zinc Sulphate and the results were evaluated according to their smoke formation during burning in NBS Smoke Chamber. It has been clearly stated out that the compositions with NiO and ZP has reduced the smoke generation. As shown in Table 4.6, NiO – ZP synergistically produced lower maximum rate of smoke generation, maximum smoke density and smoke reduction when compared with only NiO and ZP.

Table 4.6 Test results and compositions of US.Patent No.3,965,068 (Dickens, 1976).

NiO, phr	$Zn_3(PO_4)_2$ , phr	Maximum Rate of Smoke Generation, $min^{-1}$	Maximum Smoke Density per gram sample, $D_m/g$	Smoke Reduction, %
-	-	428	54.2	-
2	-	285	50.7	6.5
-	2	240	24.7	54.4
1	1	132	21.4	60.5
5	-	198	43.0	20.7
-	5	228	27.7	48.9
4	1	124	15.9	70.7
5	-	247	48.9	28.7

#### 4.2.2 IR Spectroscopic Study of Phosphate Minerals

Frost, [2003] studied the characterization of natural zinc phosphates including hopeite and parahopeite ( $\text{Zn}_3(\text{PO}_4)_2 \cdot 4\text{H}_2\text{O}$ ), spencerite ( $\text{Zn}_2\text{PO}_4(\text{OH}) \cdot 1.5\text{H}_2\text{O}$ ), tarbuttite ( $\text{Zn}_2\text{PO}_4\text{OH}$ ), scholzite ( $\text{CaZn}_2(\text{PO}_4)_2 \cdot 3\text{H}_2\text{O}$ ) and paraschozite ( $\text{CaZn}_2(\text{PO}_4)_2 \cdot 2\text{H}_2\text{O}$ ) by the use of Raman and infrared spectroscopy. Zinc phosphates are important in the study of the phosphatisation of metals. Raman spectroscopy in combination with infrared spectroscopy has been used to characterise the zinc phosphate minerals. The minerals may be characterised by the patterns of the hydroxyl stretching vibrations in both the Raman and infrared spectra. Each mineral is identified by its own characteristic Raman spectrum. The use of Raman spectroscopy has serious implications for the study of zinc phosphate coatings, secondary mineral formation involving zinc phosphates and the use of zinc phosphates in dental applications.

For hopeite, four infrared bands are observed at 3542, 3473, 3338 and 3149  $\text{cm}^{-1}$ . In a previous study by Pawling et.al [2001], reported infrared bands at 3537, 3410, 3263 and 3181  $\text{cm}^{-1}$ .

The crystal structure of parahopeite is  $\text{Zn}_3(\text{PO}_4)_2 \cdot 4\text{H}_2\text{O}$  and four bands are observed in the infrared spectrum of parahopeite at 3451, 3311, 3143 and 3043  $\text{cm}^{-1}$  as shown in Fig.4.9. It is depicted that there are two non-equivalent water molecules in the unit cell of parahopeite. These water OH stretching vibrations will show in-phase and out-of-phase behaviour resulting in the prediction of four bands in infrared spectrum.

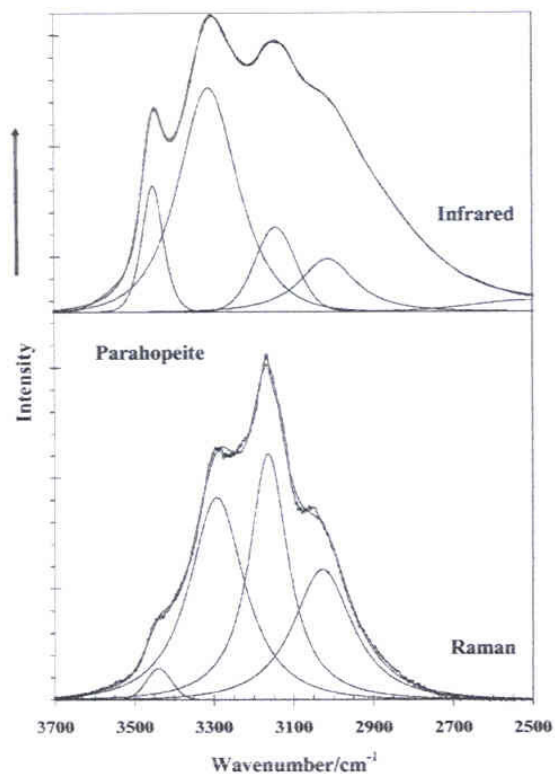


Figure.4.9. Infrared spectroscopic results for parahopeite (Frost, 2003).

Spencerite differs from hopeite and parahopeite in that phosphate has been replaced by OH units. A similar structure exists for spencerite as for parahopeite. Spencerite has one hydroxyl unit and consequently the higher wave number band at  $3520\text{ cm}^{-1}$  in the infrared spectrum is assigned to the symmetric stretching vibration.

The infrared spectrum of the hydroxyl stretching region of tarbuttite shows single intense band at  $3428\text{ cm}^{-1}$  with a tail extending to lower wave numbers.

Scholzites have apparent stacking disorders. Thus, several polytypes can exist and one of these is paraschozite. It is no doubt caused by variation in the moles of water of crystallization. Three bands were observed in the infrared spectrum of the hydroxyl stretching region at  $3425$ ,  $3310$  and  $3204\text{ cm}^{-1}$ . The Raman spectrum of scholzite in the hydroxyl stretching region shows four bands at  $3437$ ,  $3343$ ,  $3283$  and  $3185\text{ cm}^{-1}$  and three bands of infrared spectrum at  $3425$ ,  $3310$  and  $3204\text{ cm}^{-1}$ .

In the infrared spectra component bands are curve resolved at  $1137$ ,  $1096$ ,  $1059$ ,  $1019$  and  $995\text{ cm}^{-1}$  for the  $\text{PO}_4$  stretching vibrations of hopeite.

The infrared spectrum of parahopeite shows two bands of PO<sub>4</sub> stretching vibrations at 951 and 919 cm<sup>-1</sup>.

In the infrared spectrum of spencerite there are two bands of PO<sub>4</sub> stretching vibrations at 940 (ν<sub>1</sub>), 1048, 1010 and 987 cm<sup>-1</sup> (ν<sub>3</sub>). An infrared band is observed at 842 cm<sup>-1</sup> and may be attributed to water liberation mode.

The infrared spectrum of tarbuttite shows two bands at 954 and 902 cm<sup>-1</sup> and also at 1088, 1056 and 990 cm<sup>-1</sup>.

The pattern of the infrared spectrum of scholzite shows a complex profile of overlapping bands. The infrared spectrum shows bands at 1107, 1047 and 999 cm<sup>-1</sup> assigned to ν<sub>3</sub> PO<sub>4</sub> antisymmetric stretching modes and at 956 and 929 cm<sup>-1</sup> assigned to ν<sub>1</sub> PO<sub>4</sub> symmetric stretching modes.



## CHAPTER 5

### EXPERIMENTAL

#### 5.1 Materials Used

The PVC used was PVC – Petvinil P.38/74 (Emulsion type PVC) from Petkim – Aliğa, İzmir. The Dioctyl Phthalate (DOP) used as plasticizer throughout the experiments was from Merck with a molecular formula as  $C_{24}H_{38}O_4$  and MW = 390.54 with a purity of 98% min. and a density of 0.98 g/ml. Its molecular structure is given in Figure 5.1.

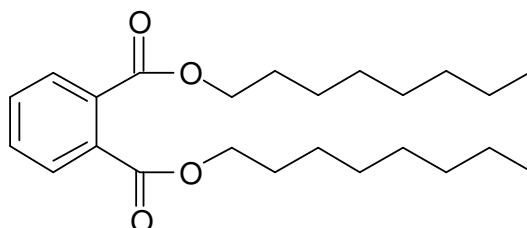


Fig.5.1 Dioctyl Phthalate Molecule

Viscobyk 5025 (carboxylic acid derivative) was used obtained from BYK Chemie as a wetting agent. The technical specs of Viscobyk 5025 is given in Table 5.1.

Table 5.1 The general product specifications of Viscobyk 5025

Density at 20°C, g/ml	0,88
Refractive Index	1,452
Flash Point, °C	170
Solidification Point, °C	-15

The zinc borate used was STORFLAM ZB 2335[CAS No.1332-07-6] having the molecular formula of  $2ZnO \cdot 3B_2O_3 \cdot 3.5H_2O$  from Heron Chemicals. The specification of the zinc borate has given in Table 5.2.

The zinc phosphate pigment used was ZP – 46 from Pigment Sanayi A.Ş., Kemalpaşa – İzmir. The general formula of the zinc phosphate [CAS No.7779-90-0], was  $Zn_3(PO_4)_2$ , MW = 385. The specification of zinc phosphate used has given in Table 5.3.

Table 5.2. The general product specifications of STORFLAM ZB 2335

Appearance	White amorphous powder
ZnO Content, % min.	37.0
B <sub>2</sub> O <sub>3</sub> Content, % min.	47.0
Water of Crystallisation, % min	16.0
Volatile Loss 1 hour at 105°C, % max.	1.5
Bulk Density, g/cm <sup>3</sup>	0.3 – 0.5
pH on Filtrate of 20% aqueous solution	7.0 – 8.0
Sieve Residue (200 mesh – 75 micron), % max.	0.2
Ignition Loss at 950°C, % max.	15.5

Table 5.3. The general product specifications of ZP – 46.

Specific Gravity	3.3
Bulk Density, g/cm <sup>3</sup>	0.3
Tamped Apparent Density, kg/cm <sup>3</sup>	0.5
Oil Absorption, g/100g	40
pH	7.0
Moisture and Volatile Matter at 105°C, % max	1.0
44µm Sieve Residue, % max.	0.5
Matter Soluble in Water, % max.	0.5

## 5.2 Methods

### 5.2.1 Film Preparation

Diethyl phthalate (DOP) plasticizer in 80 parts per hundred (phr) (43.2 wt %) was mixed by every 100 phr (54.1 wt%) PVC thoroughly with the addition of 5 phr (2.7 wt %) of wetting agent Viscobyk 5025 in a mechanical mixer (IKA Labortechnik) at room temperature for 30 minutes to prepare the *PVC resin* or *plasticols* to be used all through the experiment. At room temperature the plasticols have little or no solvating effect on the resins. The dissolving action of the plasticols progresses due to the temperature increase (Titow et.al., 1985).

Samples were prepared by adding zinc borate and zinc phosphate in proposed compositions weighed in a balance. The referred compositions are given in Table 5.4. They were then mixed thoroughly by a glass rod until obtaining completely uniform mixture by the PVC particles in DOP. Subsequent to the mixing, the resulting compositions were then poured onto gloss cardboard papers which were then passed through a film applicator (Sheen 113N) which is capable of sheeting them into forms of thin, self-supporting films. The blade of film applicator used has a thickness of 90  $\mu\text{m}$  being optimum for almost all purposes. At an intermediate temperature enough solvation occurs for the plasticols to *solidify* or to *gel* (Titow et.al., 1985). Therefore the filmed samples were heated in a vacuum oven (EV 018 by Nüve) at  $140^{\circ}\text{C} \pm 3^{\circ}\text{C}$  for 15 minutes. As the temperature increases, solvation continues until the mass becomes more or less homogeneous. The physical properties depend greatly upon the composition of plasticols.

The compositions used in this thesis are given in Table 5.4.

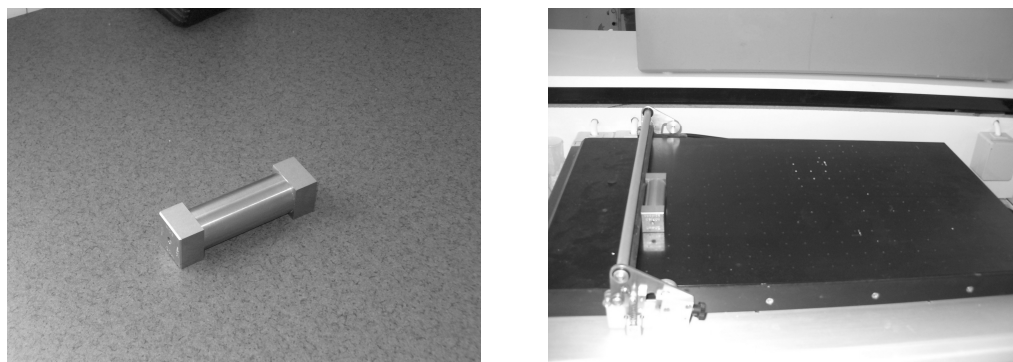


Fig.5.2 Blade of Film Applicator and Film Applicator.

Table 5.4. The compositions used in the experiments (Values in phr) (wt/wt).

Sample No.	PVC	DOP	Viscobyk 5025	ZB	ZP
No.1	100	80	5	-	-
No.2	100	80	5	-	2.5
No.3	100	80	5	0.5	2.0
No.4	100	80	5	1.0	1.5
No.5	100	80	5	1.25	1.25
No.6	100	80	5	1.5	1.0
No.7	100	80	5	2.0	0.5
No.8	100	80	5	2.5	-

### 5.2.2 Film Characterization

Films were characterized by using Scanning Electron Microscope (SEM) and Energy Dispersive X-Ray (EDX).

#### 5.2.2.1 Scanning Electron Microscope, SEM

Microstructural characterization of the filmed samples was done by X-Ray energy spectrometer (the XL-305 FEG SEM instrument by Philips).

The films of eight different compositions heated at 160°C for 90 minutes and at 140°C for 15 minutes were tested with this instrument to see the effects of heated and unheated samples. At least three different microphotographs were taken at different magnifications; 150x, 250x and 350x.

#### 5.2.2.2 Energy Dispersive X-Ray, EDX

The filmed samples were characterized by an Energy Dispersive X-ray (EDX) instrument (the XL-305 FEG SEM instrument by Philips) to investigate the effect of heating temperature and heating time on the microstructural properties of the samples. The samples were heated at 140°C for 15 minutes and at 160°C for 90 minutes. The films heated (at 160°C for 90 minutes) and unheated (at 140°C for 15 minutes) were examined and compared with this instrument. Either two or three points from particles

and polymer phases were chosen and investigated from the cross section areas of PVC films and finally average values were obtained.

### **5.2.3 Thermal Stability Tests**

The thermal stability tests were carried out to investigate the heating effects on the thermal stability of the films. To establish these tests, static oven test, PVC Thermomat tests and Thermogravimetric (TGA) tests were done.

#### **5.2.3.1 Static Oven Tests**

To investigate the effects of heating at high temperatures, each film was first of all heated at 140°C and then at 160°C up to 90 minutes in a vacuum oven (EV 018 by Nüve) and six samples were taken at 15 minute intervals from the samples to establish further tests of TGA, PVC Thermomat, FT-IR and colour tests.

The static oven tests were performed in a vacuum oven. The films were cut into 6 pieces of 5 x 1 cm. and properly labelled as 15 min., 30 min., 45 min., 60 min., 75 min. and 90 min placed onto a glass plate. These films were placed in the oven and heated at 140°C and 160°C for 90 minutes. At the end of the proposed time, each sample was taken out of the oven for further tests of physical deterioration and colour change. The colour tests were evaluated both visually and by a spectrophotometer. The heated samples were also examined by a FT-IR, TGA, PVC Thermomat, SEM, and EDX.

#### **5.2.3.2 PVC Thermomat**

The heated samples both at 140°C and at 160°C were examined in the PVC Thermomat instrument (763 PVC Thermomat, Metrohm) to propose a general mechanism of PVC degradation at high temperatures. A general view of PVC Thermomat is shown in Fig.5.3 below.



Fig.5.3. PVC Thermomat Instrument.

The 763 PVC Thermomat is a PC-controlled instrument used to study the degradation kinetics of PVC. PVC Thermomat is equipped with two heating blocks each with four measuring positions. Two sets of four samples can be heated and measured at two different temperatures at each block individually or namely, eight samples can be measured at the same temperature which can be seen in Figure 5.4 below.

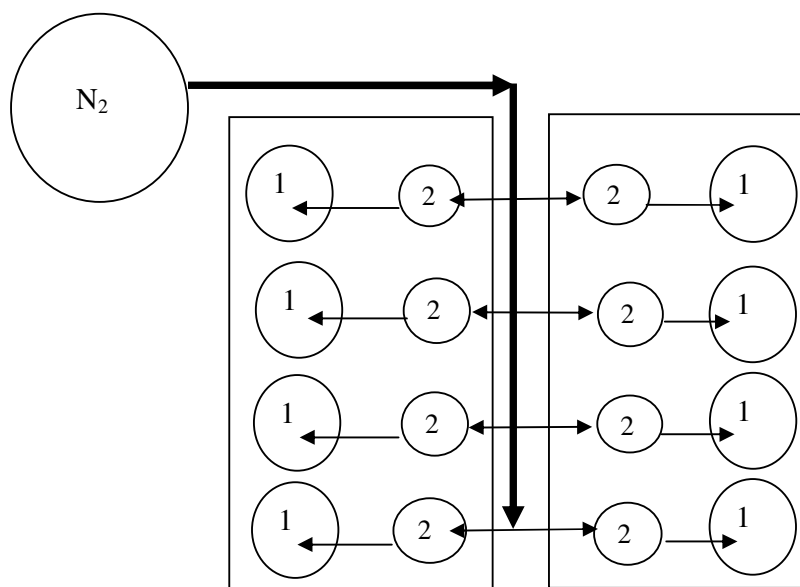


Figure 5.4 Top view of PVC Thermomat instrument 1: Measuring cells at 25°C, 2:Sample cells (heated cells).

The evaluation algorithm of program determines the point of induction and stability time where *induction time* is the time elapsed before the conductivity starts to rise sharply and *stability time* is the time required to achieve a given conductivity alteration (In this thesis 50  $\mu\text{S}$  is used).

The determination of thermal stability of PVC is based on the fact that PVC decomposes at higher temperatures with the release of HCl. The HCl formed is taken up by  $\text{N}_2$  gas stream and transferred into the measuring vessel where it is absorbed in the distilled water. The decomposition process is monitored by measuring the conductivity of the aqueous HCl solution. Both the stability and the induction time are determined. Hence the PVC decomposition mechanism is proposed.

The samples were cut into small squares of 5 mm. and having a weight of  $0.5 \text{ g} \pm 0.01$  and later they were put into the sample cells of the instrument. Into measuring

cells, distilled water was put at 25°C to be able to measure the conductivity change of water. The sample cells were heated at 140°C and 160°C. The instrument kept on running until all of the samples have reached their stability and induction times.

The measuring blocks of this instrument can be viewed in Fig. 5.5

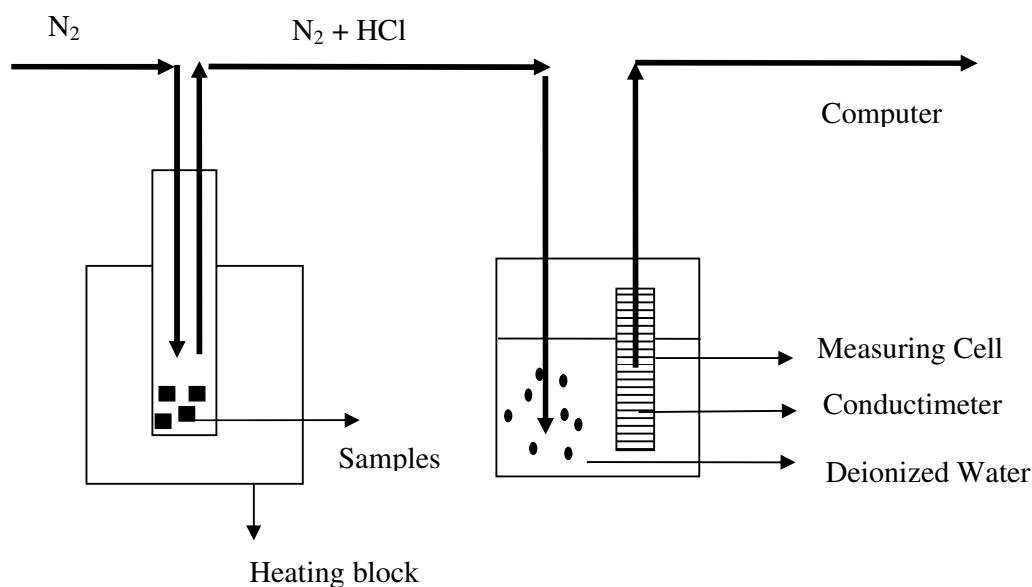


Fig.5.5. The measuring blocks of 763 PVC Thermomat instrument.

### 5.2.3.3. Thermogravimetric Analyses (TGA)

To learn the thermal behaviour of the films, TGA instrument was also used. PVC films gelled at 140°C for 15 minutes were tested in this instrument (Instrument Setaram Labsys) under N<sub>2</sub> atmosphere at a heating rate of 10°C per minute. The graphs of mass loss versus temperature were obtained to determine the char residue and the heat stability. The tests were carried out up to 600°C.

#### 5.2.4 Fourier Transform Infrared Analyses by Transmission

To determine which functional groups are present in the films, FT – IR instrument (the FT-IR 8601 by Shimadzu) was used. The heated and unheated films prepared previously were tested in this instrument. The resultant FT – IR spectra were used to determine the atomic and atomic – atomic structures. From this point, one can determine the effects of heating at high temperature on the films. KBr disc technique was used for ZB and ZP.

#### 5.2.5 Fourier Transform Infrared Analyses by ATR method

FTS 3000 MX by Digilab was used to determine the functional groups at the surface of the PVC films. Transmission IR spectrum of films gives ideas about bulk of the PVC films, but ATR spectrum gives information about the surface of the films therefore ATR attachment was used for this purpose.

#### 5.2.6 Colour Measurement

Both the heated and unheated films were investigated by a colour spectrophotometer instrument (Spectrocam, Avantes) to find out their yellowness index values. The yellowness index is a measure to have an idea on the physical deterioration of the heated films when comparing with the unheated ones. The change in colour due to high temperature will be differentiating point in this test. During the calculation of yellowness index, the tristimulus values according to illuminant C and 2° observer are used as a standard according to the formula in Eqn.5.1.

$$YI = \frac{(128X - 106Z)}{Y} \quad (5.1)$$

where X, Y and Z are tristimulus values according to 2° observer and C illuminant.

Another way of measuring the colour differences between two films is calculating  $\Delta E$  value of which its formula is given as;

$$\Delta E = \sqrt{(L_2 - L_1)^2 + (a_2 - a_1)^2 + (b_2 - b_1)^2} \quad (5.2)$$

where L is the lightness value, a is the value of green – red and b is the value of blue – yellow scales. This is a scale formed in 3-D sphere system. These values are also calculated from the X, Y and Z tristimulus values.



## CHAPTER 6

### RESULTS AND DISCUSSION

#### 6.1 Characterization of Zinc Borate and Zinc Phosphate

The Thermogravimetric analyses curves of ZB and ZP in powder forms are investigated in Fig.6.1 and Fig.6.2, respectively.

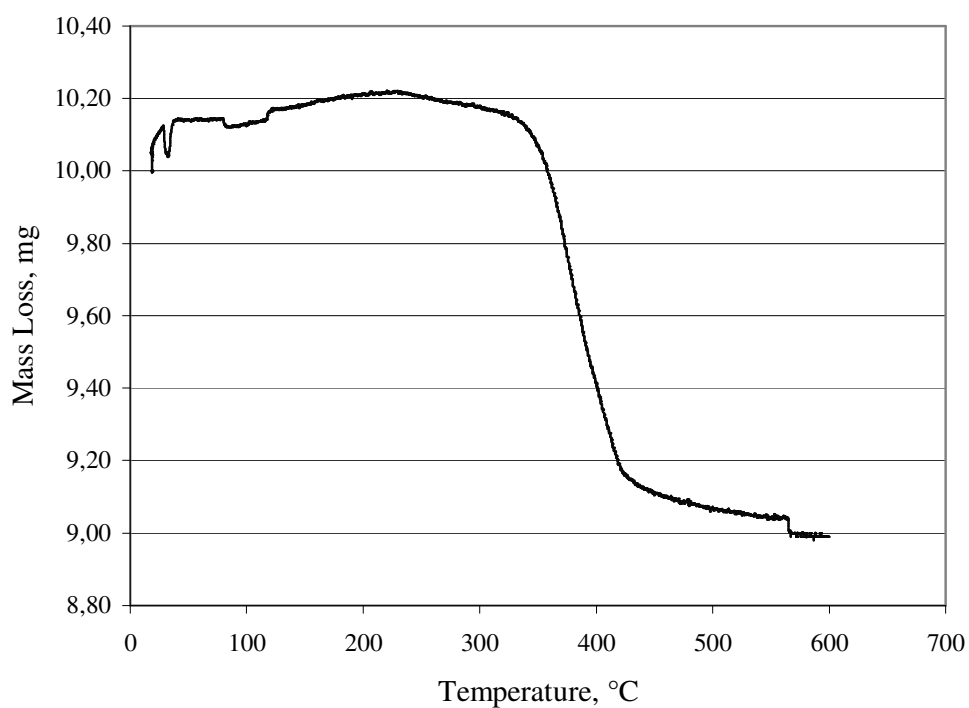


Figure 6.1 TGA curve of ZB powder.

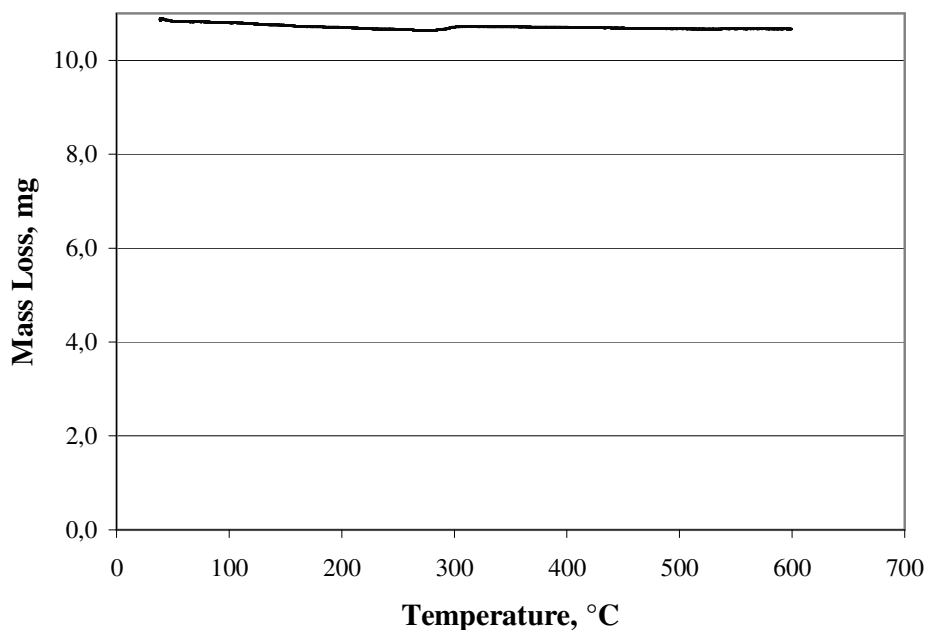


Figure 6.2 TGA curve of ZP powder.

It can be concluded that ZB starts to lose its crystal water at around 315 – 320°C. When the TGA curve of ZP is analyzed, it is clear that it does not lose much of its mass.

FTIR spectra of ZB and ZP in powder forms are given in Figures 6.3 and 6.4, respectively. The peak at 3227  $\text{cm}^{-1}$  in Fig.6.3 belongs to  $\text{ZnO}\cdot\text{B}_2\text{O}_3$ . Also there are several peaks between 900 and 1300  $\text{cm}^{-1}$  which are characteristics of ZB (Xie et.al, 2000). There is also OH stretching at 3200  $\text{cm}^{-1}$ . The peaks belonging to ZP are also clear in Fig.6.4; the peaks observed at 1080 and 890  $\text{cm}^{-1}$  are the P-O symmetric and asymmetric vibration in P-O-P chains; respectively. There is also OH stretching and water bending at 3200 and 1600  $\text{cm}^{-1}$ . These are consistent with a previous study by Xie et.al, 2000.

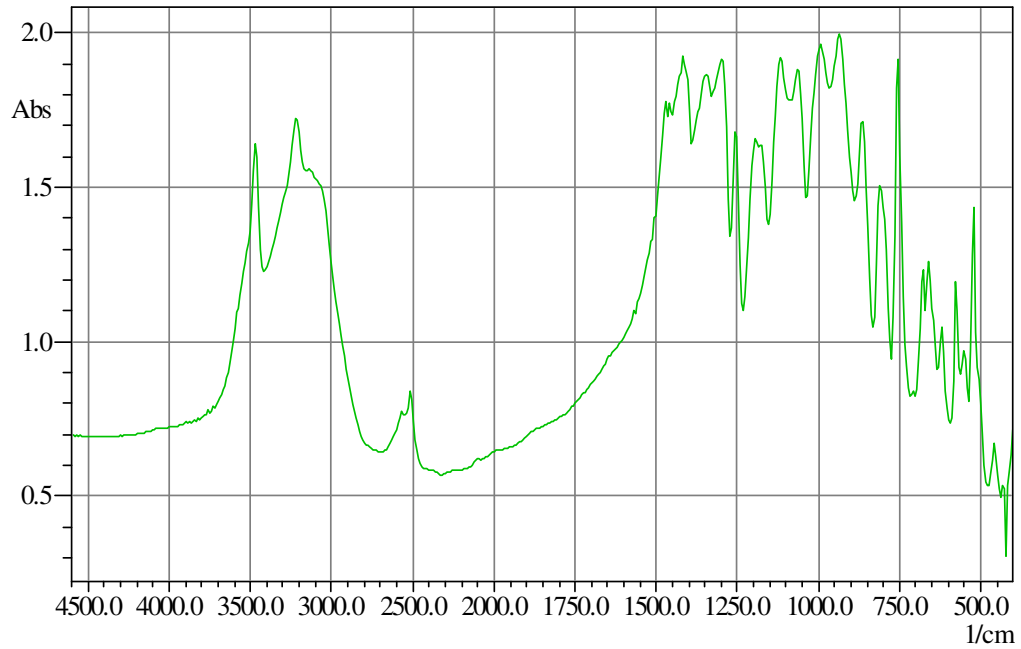


Fig.6.3 FT-IR spectra of ZB powder sample.

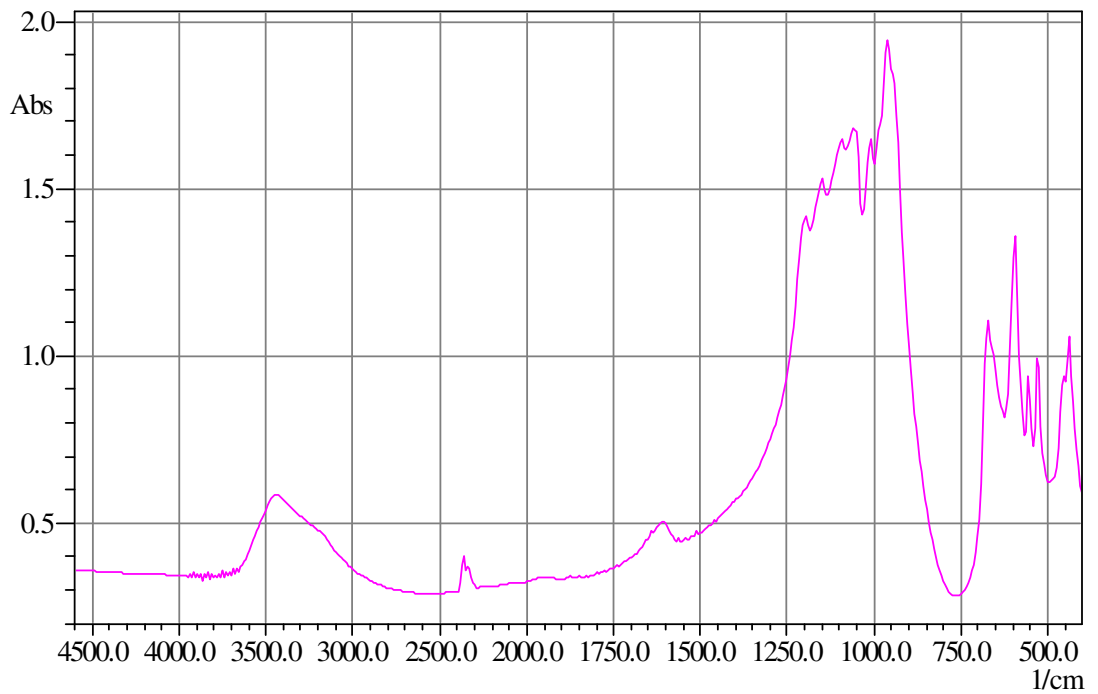


Fig.6.4 FT-IR spectra of ZP powder sample.

Scanning electron micrographs of the ZB and ZP were also taken and they are given in Figure 6.5. The average particle sizes of ZB and ZP were 3  $\mu\text{m}$  and 5  $\mu\text{m}$ , respectively.

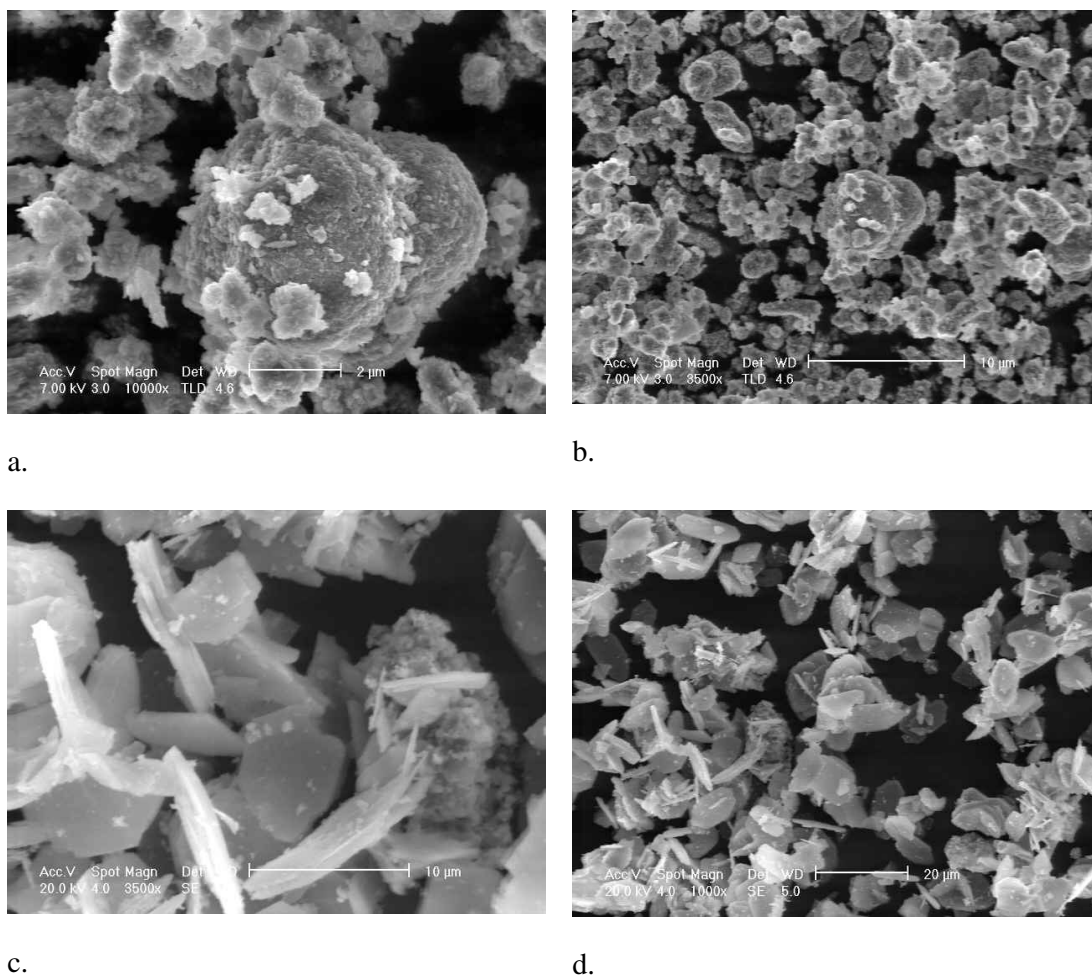


Figure 6.5 The Scanning electron micrographs of the ZB and ZP powders

a.) ZB, 10000x magnified. b.) ZB, 3500x magnified.

c.) ZP, 3500x magnified. d.) ZP, 1000x magnified.

The EDX analyses of the powder samples are tabulated in Table 6.1. The EDX analyses indicated molar Zn/B ratio was 0.34 for ZB which was very close to 0.33 of  $2\text{ZnO} \cdot 3\text{B}_2\text{O}_3$ . Similarly, molar Zn/P ratio was found to be 1.86 which was close to 1.5 of  $\text{Zn}_3(\text{PO}_4)_2$ .

Table 6.1 Elemental composition of the ZB and ZP powder.

Elements	ZB-2335	ZP-46
Zn	33.2	53.1
O	50.4	31.1
P	-	15.9
B	16.4	-

## 6.2 Kinetic Study of Dehydrochlorination of PVC Plastigels

In these tests, kinetic parameters such as activation energies, rates and rate constants and frequencies of the plastigels were evaluated in PVC Thermomat. Chopped films were put into the test tubes of Thermomat. On the other side, deionized water poured into test tubes was used to record the conductivity change. The HCl gas evolved from the heated samples were carried out by N<sub>2</sub> gas stream into the tubes filled with deionized water. In the tubes filled with deionized water, the conductivity change was recorded with respect to time according to the HCl gas evolved. This test was carried out at both 140°C and at 160°C for every composition prepared.

### 6.2.1 Kinetic Theory of degradation of PVC Plastigels

The slopes (  $\alpha$  ) of the curves showing the conductivity (  $\kappa$  ) changes with respect to time (  $t$  ) were used to calculate the reaction rate constants and reaction rates ( 6.1 ). From these figures the induction and stability time values were also obtained.

$$\alpha = \frac{d\kappa}{dt} \quad (6.1)$$

The current in an electrolyte solution is the sum of the currents carried by the individual ions. The conductivity of the solution is

$$\kappa = \sum_i |z_i| F u_i c_i \quad (6.2)$$

where

$\kappa$  is the conductivity

$u_i$  is the mobility of ion  $i$  (m<sup>2</sup>/V.s),

$F$  is the Faraday's constant ( $F = 96485$  °C/mol),

$|z_i|$  = Total charge number,

$c_i$  = Concentration of the solution (mol/m<sup>3</sup>),

The mobility of the ions is the sum of the mobility of cations and anions.

$$\kappa = z_+ Fu_+ c_+ + |z_-| Fu_- c_- \quad (6.3)$$

Hence, if the Equation 6.2 is derivated with respect to time, rate of dehydrochlorination of PVC can be calculated with respect to time.

$$slope = \frac{d}{dt}(\kappa) = \frac{d}{dt} \left( \sum_i |z_i| Fu_i C_i \right) \quad (6.4)$$

The rate of dehydrochlorination of PVC is dependent on the concentration of unreacted HCl present in the PVC.

Rate of dehydrochlorination can be written as follows

$$\frac{dC_{HCl}}{dt} = k(C_0 - C_{HCl}) \quad (6.5)$$

where  $dC_{HCl}/dt$  is the rate of dehydrochlorination ( $\mu\text{mol/g PVCs}$ ),

$k$  is the reaction rate constant ( $s^{-1}$ ),

$C_0$  is potential double bonds to be formed when 100% of HCl is eliminated per 1 g of PVC ( $\mu\text{mol/g PVC}$ ),

$C_{HCl}$  is the concentration of evolved HCl ( $\mu\text{mol/g PVC}$ ).

$C_0 = 16.5 \times 10^3 \mu\text{mol/g PVC}$  (Atakul, 2004).

At initial stage of dehydrochlorination  $C_{HCl} \ll C_0$ , we can assume that  $C_0 - C_{HCl} = 16.5 \times 10^3 \mu\text{mol/g PVC}$ .

Then the Equation 6.4 becomes as follows,

$$\frac{d}{dt}(C_{HCl}) = kC_0 \quad (6.6)$$

The rate of dehydrochlorination can be calculated from the slopes of the conductivity change versus time graphs.

$$\frac{d\kappa}{dt} = F \cdot \sum |Z_i| \cdot \frac{dC_{HCl,w}}{dt} \cdot U_{HCl} \quad (6.7)$$

where;

$C_{HCl,w}$  is the concentration of HCl in water.

Assumption; all HCl evolved from PVC was absorbed by water.

$$\frac{dC_{HCl,w}}{dt} \cdot V_w = \frac{dn_{HCl}}{dt} \quad (6.8)$$

$n_{HCl}$  = Moles of evolved HCl gas.

$V_w$  = Volume of water in measuring vessel

$$V_w = 6 \times 10^{-5} \text{ m}^3$$

$$\frac{dC_{HCl}}{dt} = \frac{dn_{HCl}}{dt} \cdot \frac{1}{m \cdot CF} \quad (6.9)$$

$m$  = Mass of plastisol in reaction vessel

$CF$  = Correction factor which is fraction of PVC in PVC plastisol

$$k = \frac{dC_{HCl}}{dt} \cdot \frac{1}{C_o} = \frac{dn_{HCl}}{dt} \cdot \frac{1}{m \cdot CF} \cdot \frac{1}{C_o} \quad (6.10)$$

(Atakul, 2004).

The dehydrochlorination curves can be separated into two parts; *initial region* and *linear region*. Therefore, two rate constants can be evaluated for each reaction. Initial rate constants are obtained from the slopes of initial region of the curves where the release of HCl gas started to release; whereas linear region rate constant are obtained from the slopes of linear region where the release of HCl gas accelerates.

In this study, two temperatures were used to evaluate the kinetic parameters; 140°C and 160°C.

## 6.2.2 Kinetic Study of PVC plastigel films

The PVC plastigel films containing zinc borate and zinc phosphate were studied in PVC Thermomat instrument to calculate the reaction rates and reaction rate constants at 140°C and at 160°C. A representative PVC Thermomat curve is given in Figure 6.6. As it is seen in the figure, the time value where the conductivity begins to increase is the *visual induction time*, the time at the intersection between the tangent line of linear region and the x-axis is the *evaluated induction time*, the time value at the 50  $\mu\text{S}$  conductivity is the *stability time*.

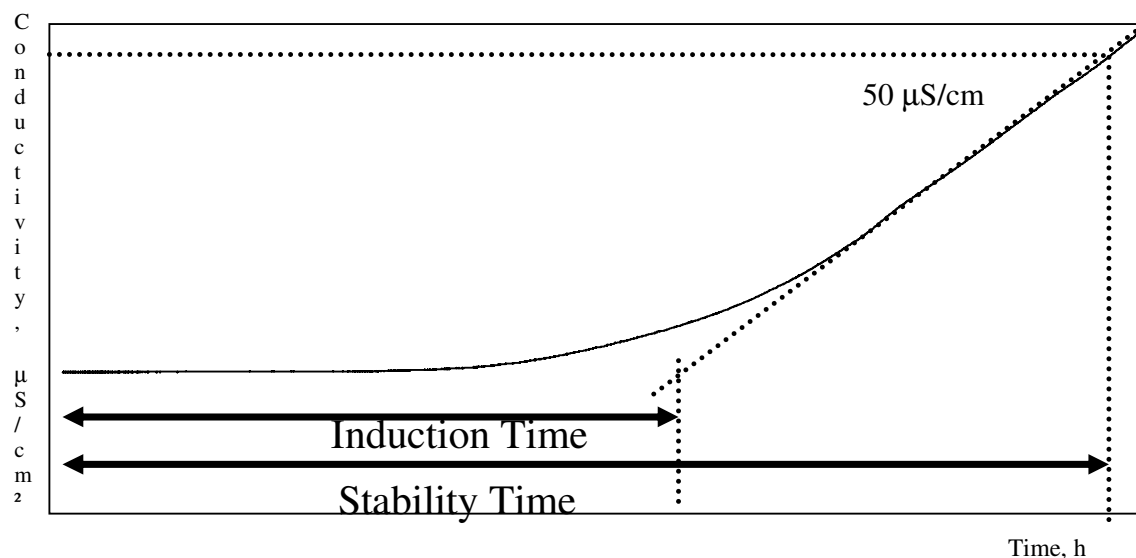
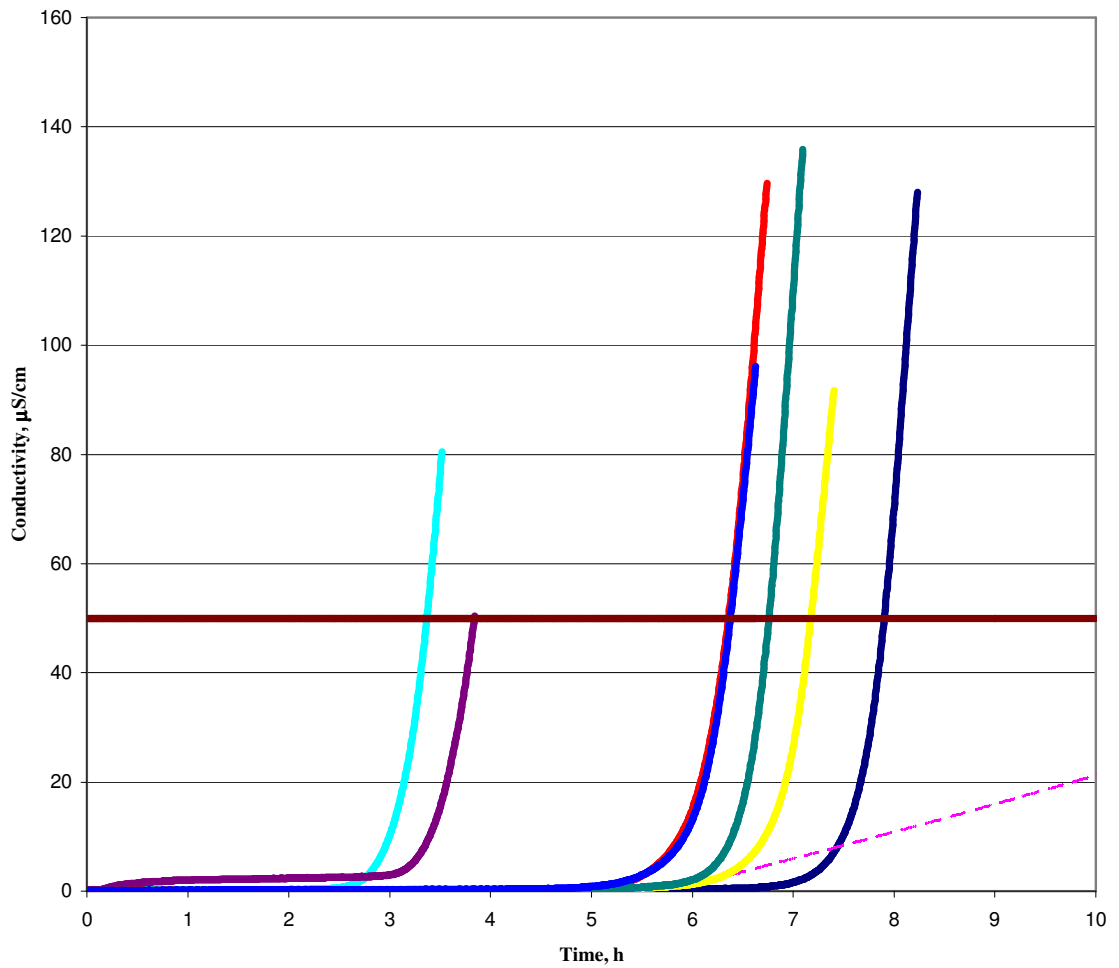


Figure 6.6 A representative curve for PVC Thermomat results.

The conductivity versus time curves of one run are represented for 140°C and 160°C, in Fig.6.7 and Fig.6.8; respectively. The calculated average rate constants and rates as well as induction and stability time are shown in Table 6.2 and 6.3.

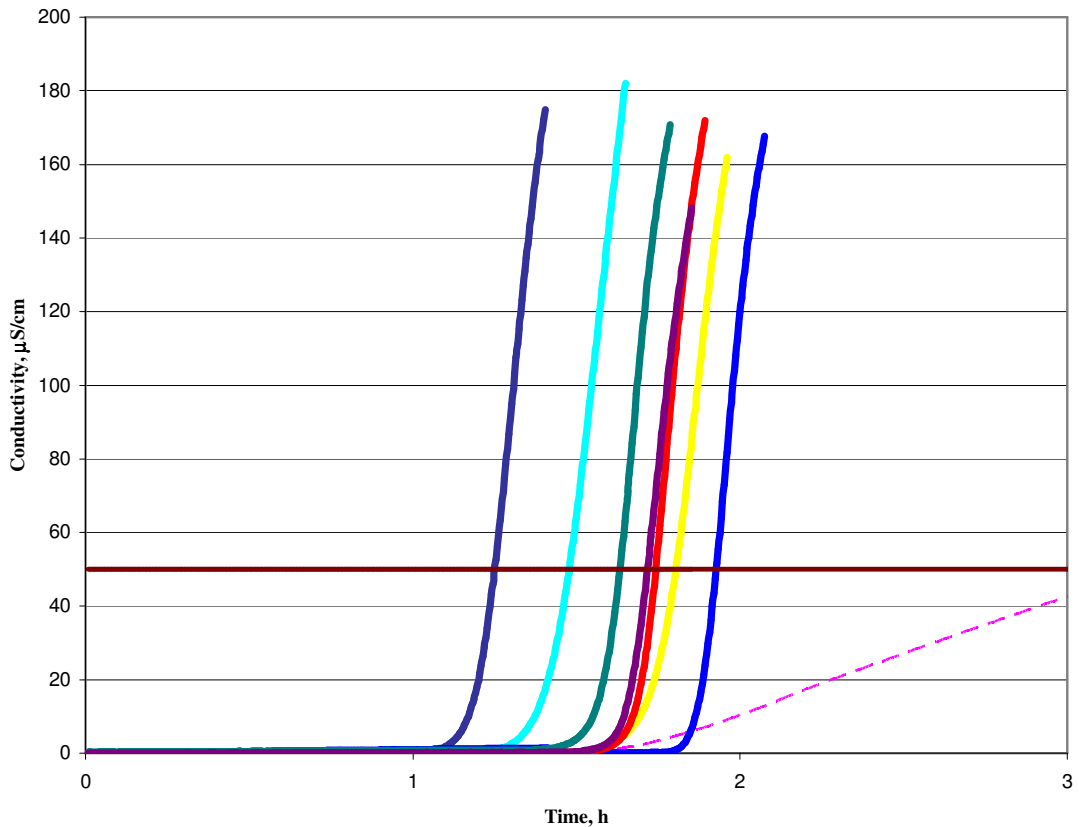




(All values below are wt%).

- PVC Control,      — 1.36 % ZB,      — 1.36% ZP,
- 0.68%ZB+ 0.68% ZP,      — 0.54% ZB+ 0.81% ZP,
- 0.81% ZB + 0.54% ZP,      — 0.27% ZB + 1.29% ZP,
- 1.29% ZB + 0.27% ZP,      — 50 µS/cm Stability Time Limit.

Figure.6.7. PVC Thermomat Results of PVC films heated at 140°C.



(All values below are wt%).

- - - PVC Control,     
 — 1.36 % ZB,     
 — 1.36% ZP,
- 0.68%ZB+ 0.68% ZP,     
 — 0.54% ZB+ 0.81% ZP,
- 0.81% ZB + 0.54% ZP,     
 — 0.27% ZB + 1.29% ZP,
- 1.29% ZB + 0.27% ZP,     
 — 50 µS/cm Stability Time Limit.

Figure.6.8. PVC Thermomat Results of PVC films heated at 160°C.

As shown in Figs.6.7 and 6.8, the kinetic curves are composed of two sections; an initial slowly increasing section followed by a rapid increasing curve. The former is called as *initial region* while the latter as *linear region*. The lesser slopes of curve of the conductivity in the initial section can be explained through the slower release of HCl gas due to the presence of additives and the higher slopes of the curve of conductivity in the linear region can be explained by the rapid release of HCl gas.

When the curves of the PVC films at seven different compositions were compared with pure PVC as a control, it is obvious that PVC control sample has the longest

stability time of 15 hours. However, if the induction times are examined, film having only 1.36% of ZB only has a higher value than the control sample but the composition having only ZP does not have. Sample having 0.54% ZB and 0.81% ZP, sample having 0.81% ZB and 0.54% ZP and sample having 0.27% ZB and 1.29% ZP had also higher values than the control sample.

If the PVC Thermomat data for 160°C are analysed first of all it is clear that the both induction and stability time values were decreased by 1:5 of their previous values. Again here PVC control sample had the highest stability time with a steep long lasting slope. However, samples having 0.54% ZB and 0.81% ZP and 0.81% ZB and 0.54% ZP and also 0.27% ZB and 1.29% ZP had the highest values, but in general all of the compositions had better results than PVC control sample.

As shown in Table 6.4, the activation energies of the initial regions have higher values than the activation energies of the linear region except in Sample No.6. This can be explained by the rapid dehydrochlorination reactions occurring in the linear region. Due to the presence of zinc borate and zinc phosphate in the initial region, the activation energies are higher which means that there must be more energy applied to the system to initiate the reaction when compared with the linear region. When linear region values are examined, lower values indicate an acceleration of the HCl release.

When the induction and stability time values at 160°C are compared with each other, the decrease in the values are clearly noticeable. Sample having 0.54% ZB and 0.81% ZP composition has especially showed synergism compared to the sample having only 1.36% ZB or 1.36% ZP only in its composition. But also samples having composition of 0.81% ZB and 0.54% ZP and 0.27% ZB and 1.29% ZP have also had higher induction times indicating synergistic results compared with the former at 140°C.

The induction time of PVC control sample at 160°C had a lower value than its counter. However all of the film compositions had shown similar results due to the release of HCl gas. Similar to the former case, again 0.54% ZB and 0.81% ZP composition has especially showed synergism compared to the sample having only 1.36% ZB or 1.36% ZP only in its composition.

According to Frye – Horst mechanism, anions exchange with labile chlorine atoms next to double bonds or carbonyl substituents. The ZB and ZP in the system react with the HCl released from the system during heating by exchanging their borate and phosphate ions, respectively.



where X: Phosphate or borate anion. The bond between C and phosphate or borate anions are more stable than C – Cl bond. At long heating times, this bond will be broken also and HCl gas will be released.

The reactions occurring in the PVC system is as follows;

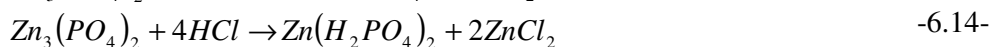
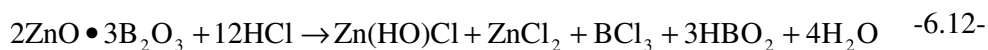


Table 6.2 PVC Thermomat Results at 140°C of PVC plastigels.

No	ZB, wt%	ZP, wt%	Induction Time, h (Evaluated)	Induction Time, h (Visual)	Stability Time, h	Initial Rate Constant $\times 10^7$ , $\text{min}^{-1}$	Linear Rate Constant $\times 10^4$ , $\text{min}^{-1}$
1	0.00	0.00	2.99	3.00	15.21	4.02	0.05
2	0.00	1.36	3.28	2.30	3.22	23.09	1.85
3	0.27	1.29	6.72	5.80	6.76	7.67	3.14
4	0.54	0.81	7.86	6.80	7.91	15.42	2.96
5	0.68	0.68	3.53	1.10	3.84	13.85	1.32
6	0.81	0.54	6.37	5.20	6.36	27.71	2.40
7	1.29	0.27	6.25	4.70	6.38	5.26	1.61
8	1.36	0.00	7.04	5.40	7.18	5.36	1.89

Table 6.3. PVC Thermomat Results at 160°C of PVC plastigels.

<i>No.</i>	<i>ZB, wt%</i>	<i>ZP, wt%</i>	<i>Induction Time, h (Evaluated)</i>	<i>Induction Time, h (Visual)</i>	<i>Stability Time, h</i>	<i>Initial Rate Constantx10<sup>6</sup>, min<sup>-1</sup></i>	<i>Linear Rate Constantx10<sup>4</sup>, min<sup>-1</sup></i>
1	0.00	0.00	1.49	0.7	3.35	4.86	0.3
2	0.00	1.36	1.22	0.95	1.25	9.24	7.31
3	0.27	1.29	1.59	1.38	1.64	2.72	8.72
4	0.54	0.81	1.87	1.80	1.93	12.15	10.28
5	0.68	0.68	1.20	1.07	1.25	12.31	9.51
6	0.81	0.54	1.69	1.55	1.75	10.26	11.08
7	1.29	0.27	1.66	1.56	1.72	5.14	8.15
8	1.36	0.00	1.77	1.60	1.81	4.62	7.48

To show the synergism with the help of induction time, Figures 6.9 to Figure 6.12 were given at seven different compositions and compared with PVC control sample at 140 and 160°C. Evaluated induction time is the induction time at the intersection point of the slopes of initial and linear regions measured by the software of PVC Thermomat instrument; while visual induction time is the induction time defined by the operator at the beginning of the increase of conductivity with time in the initial region.

As shown in these figures, the compositions show a higher induction time value meaning a synergism between them. Because not only the induction time values of the samples having only ZB or only ZP but also the induction time values of the PVC control sample are lower than the values of the compositions having both ZB and ZP.

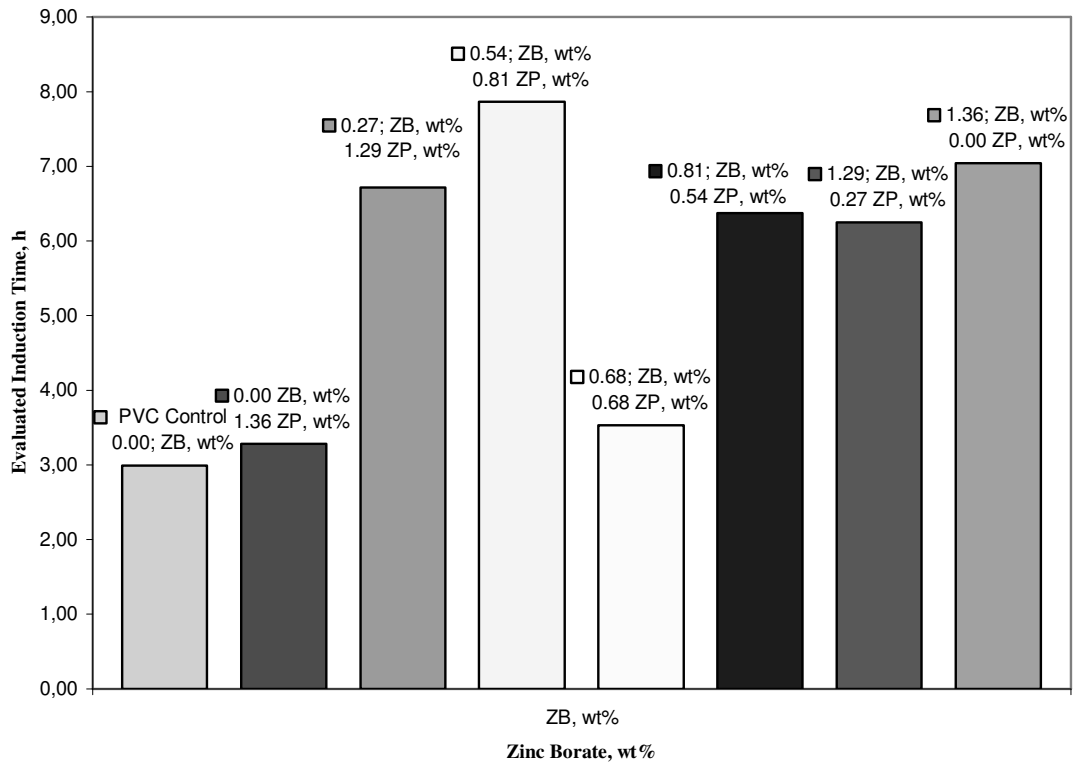


Fig.6.9 The bar graph of evaluated induction time for zinc borate at 140°C.

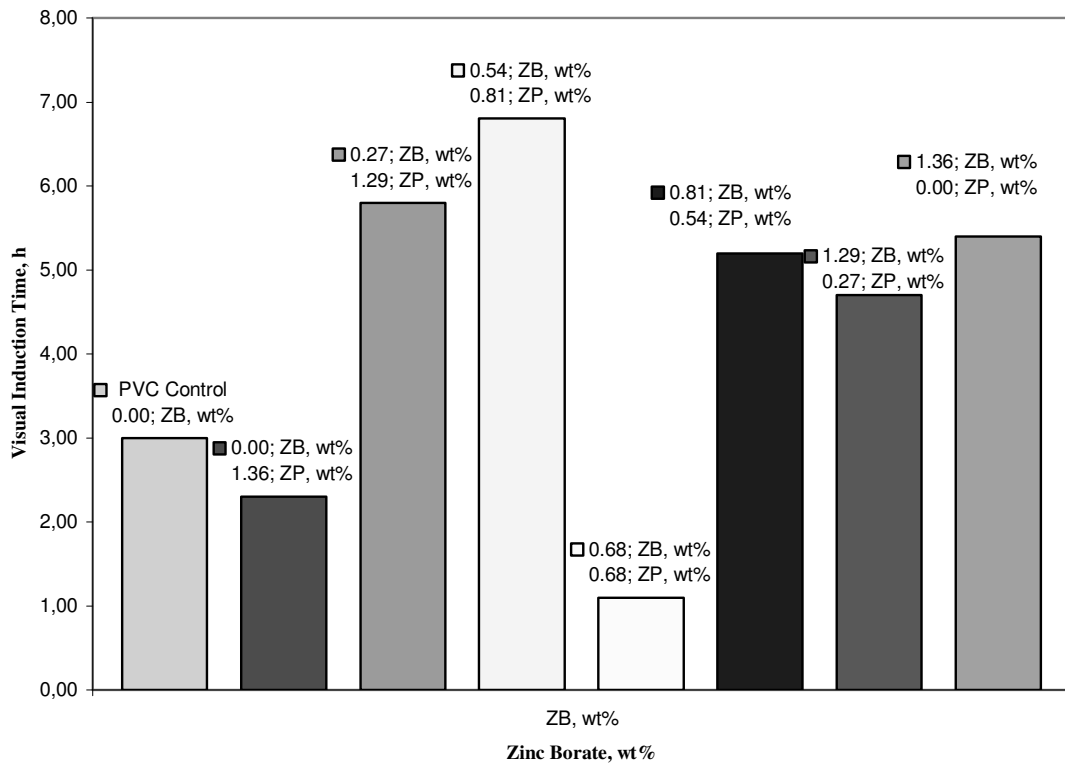


Fig.6.10 The bar graph of visual induction time for zinc borate at 140°C.

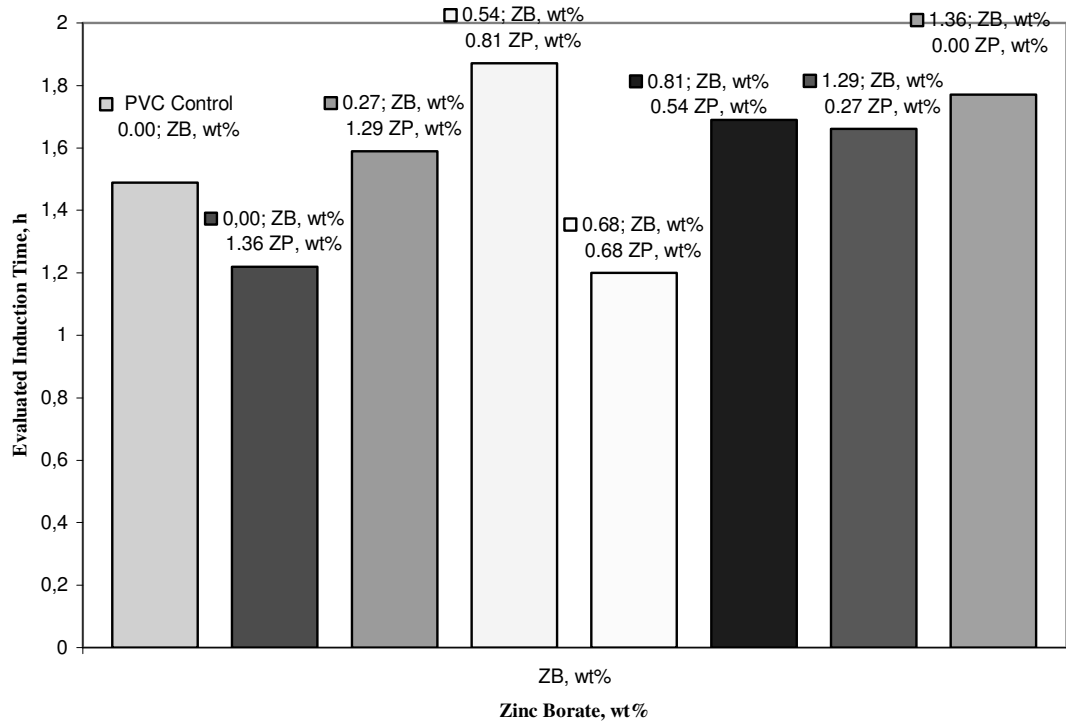


Fig.6.11 The bar graph of evaluated induction time for zinc borate at 160°C.

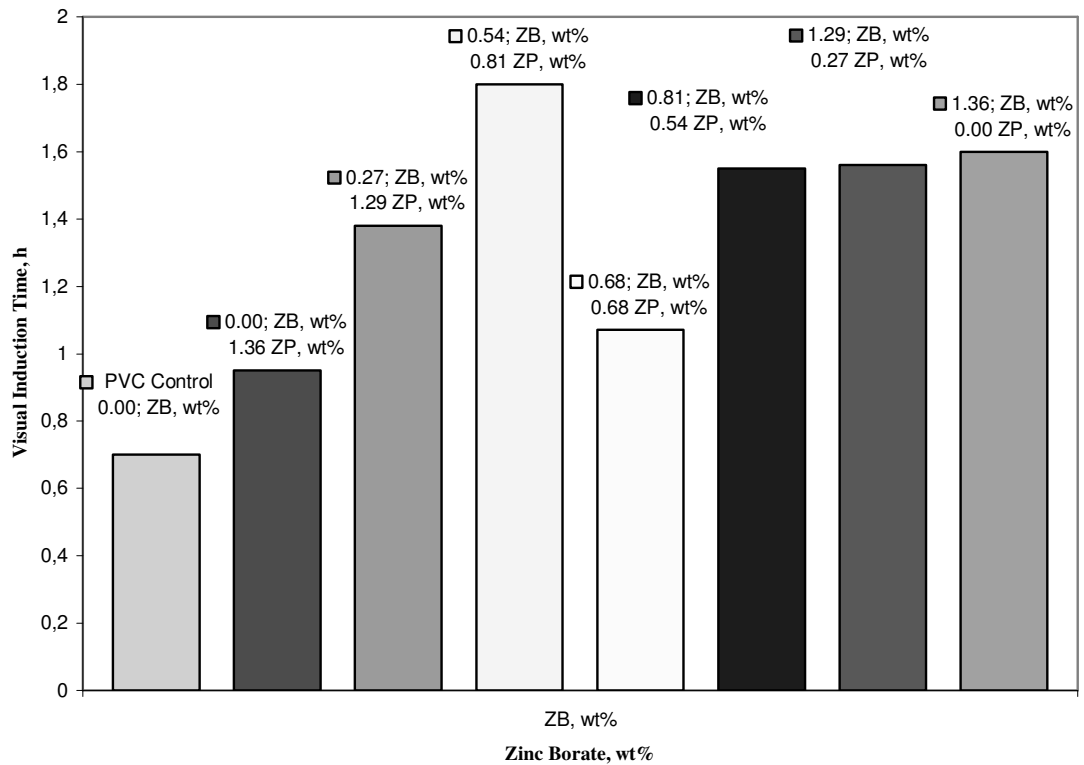


Fig.6.12 The bar graph of visual induction time for zinc borate at 160°C.

### 6.2.3 Activation Energies of Dehydrochlorination Reactions

The activation energies of dehydrochlorination reactions were calculated for the films heated at 140°C and at 160°C by use of Arrhenius equation. The preexponential factors were also evaluated from rate constant at two different temperatures.

$$k = Ae^{-E/RT} \quad (6.15)$$

where;

k = rate constant,

A = Preexponential factor or frequency.

E = Activation energy in J/mole

R = Universal gas constant (R = 8.314 J/molxK )

T = Temperature in K.

Activation energy is evaluated by the use of Arrhenius equation at two different temperatures;

$$\ln\left(\frac{k_2}{k_1}\right) = \frac{-E}{R}\left(\frac{1}{T_2} - \frac{1}{T_1}\right) \quad (6.16)$$

The activation energies of dehydrochlorination of PVC control sample with 29.7% DOP in initial and linear regions were found to be 185.3 and 135.4 kJ/mol, respectively. Atakul, 2004 has reported the degradation of PVC with 43% DOP as 129.7 and 111.3 kJ/mol.

The resultant activation energies were tabulated in Table 6.4. As can be noticed in Table 6.4, generally the values in the linear region are lower than the initial region due to the higher consumption of the additives in the initial region and therefore lack of material in the linear region. After the consumption of materials in the initial region, the effect of heating accelerates the release of HCl.

When the activation energies are compared with each other according to the sample compositions, the highest values were found in Sample having 0.81% ZB + 0.54% ZP



and Sample having 0.27% ZB + 1.29% ZP. These values are also consistent with the values in linear region. The value of the Control Sample should also be taken into account carefully. The PVC control sample has higher values than all of the compositions; and Sample having 0.27% ZB + 1.29% ZP has the lowest values indicating that it decreases the required energy for the release of HCl. But this result does not agree with induction time values. The effectiveness of the additives in the initial region causes the barrier energy to decrease leading to general lower values.

Table 6.4 Activation energies of PVC plastigels heated at 140° and 160°C.

No	ZB, wt%	ZP, wt%	Activation Energy of Initial Region, kJ/mol	Activation Energy of Linear Region, kJ/mol
1	0.00	0.00	185.3	135.4
2	0.00	1.36	103.1	102.2
3	0.27	1.29	94.0	75.9
4	0.54	0.81	153.4	92.7
5	0.68	0.68	162.4	146.8
6	0.81	0.54	97.3	113.7
7	1.29	0.27	169.3	120.5
8	1.36	0.00	160.1	102.3

#### 6.2.4 Preexponential Factors of Dehydrochlorination Reactions

Preexponential factors (A) of initial and linear regions of the kinetic curves for PVC plastigels were evaluated by using the Eq. 6.14. These values were reported in Table 6.5.

Table 6.5 Preexponential factors of PVC plastigels heated at 140° and 160°C.

No	ZB, wt%	ZP, wt%	Preexponential Factor of Initial Region, s <sup>-1</sup>	Preexponential Factor of Linear Region, s <sup>-1</sup>
1	0.00	0.00	2.15x10 <sup>-28</sup>	1.42x10 <sup>-21</sup>
3	0.00	1.36	3.41x10 <sup>-18</sup>	3.38x10 <sup>-16</sup>
7	0.27	1.29	1.23x10 <sup>-17</sup>	6.01x10 <sup>-13</sup>
5	0.54	0.81	3.78x10 <sup>-24</sup>	6.77x10 <sup>-15</sup>
4	0.68	0.68	3.15x10 <sup>-25</sup>	1.85x10 <sup>-21</sup>
6	0.81	0.54	1.86x10 <sup>-17</sup>	2.13x10 <sup>-17</sup>
8	1.29	0.27	1.92x10 <sup>-26</sup>	2.38x10 <sup>-18</sup>
2	1.36	0.00	2.22x10 <sup>-25</sup>	3.38x10 <sup>-16</sup>

As seen in Table 6.4 and 6.5, the activation energy and preexponential factor values are very different from each other. Therefore, kinetic compensation effect is to be calculated by plotting lnA vs. E curves as shown in Fig.6.13. The effect of reaction mechanisms becomes obvious by investigating these curves.

Atakul, 2004 has reported a linear relationship between lnA and E values of the samples having 33% DOP as;

$$\ln A = 0.2778E - 10.682 \text{ (initial region)}$$

$$\ln A = 0.2882E - 9.9506 \text{ (linear region),}$$

and the samples having 43% DOP, ZnSt<sub>2</sub> and zeolite as;

$$\ln A = 0.2795E - 9.6722 \text{ (initial region)}$$

$$\ln A = 0.2726E - 9.9506 \text{ (linear region),}$$

which were consistent with the literature.

A linear relationship was also observed in this study. Linear relationship of the lines both at initial and linear regions can be noticed in Figure 6.13.

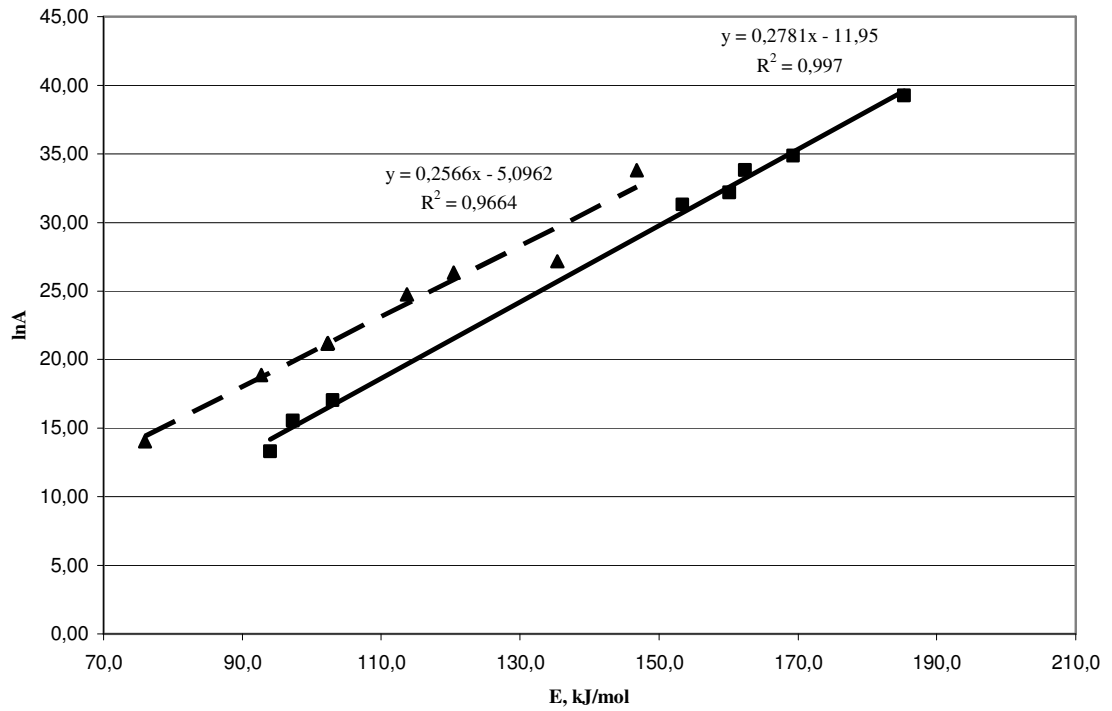


Fig.6.13. Kinetic compensation effect curve for the samples having different compositions (■: initial region, ▲: linear region).

The equations for the lines are as follows;

$$\ln A = 0.2781E - 11.95 \text{ (initial region)}$$

$$\ln A = 0.2566E - 5.0962 \text{ (linear region)}$$

While the initial region equation is consistent with the previous study, the linear region equation has nearly the same slope with initial region equation as found by Atakul [2004].

## 6.3 Characterization of PVC Plastisols and PVC Plastigels

### 6.3.1 Thermogravimetric Study of PVC Films

To have an idea about the thermal behaviour of the PVC films, TGA instrument was used to investigate by studying the mass losses of PVC due to HCl release.

As it was clearly noted in the previous study by Ning and Guo [2000], the thermal decomposition of PVC is a two-stage process; thermal decomposition in the first stage is mainly the evolution of HCl and the thermal decomposition in the second stage is mainly the cyclization of conjugated polyene sequences to form aromatic compounds. Incorporation of small amounts of ZB and ZP reduces the thermal decomposition temperature in the first stage, while it increases the thermal decomposition temperature in the second stage.

Two main kinds of mechanism of smoke suppression in PVC for metal containing compounds were proposed: One is Lewis acid mechanism and the other is reductive coupling mechanism (Starnes, et al., 1979; Lattimer and Kroenke, 1981). They are all supported by some experimental results. But the final results for these mechanisms are that all the metal compounds promote early crosslinking of PVC during decomposition to increase char formation. It is due to Lewis acid mechanism that zinc containing compounds can greatly reduce smoke formation.  $ZnCl_2$ , which formed along with the thermal decomposition of PVC, acts as an effective catalyst for the ionic dehydrochlorination of PVC due to its strong Lewis acidity. Dehydrochlorination of PVC under the influence of  $ZnCl_2$  occurs with a formation of trans-polyene structures followed by intermolecular cyclization, resulting in increased char formation and a decrease in smoke production (Ning and Guo, 2000).

Therefore by the mechanism described so far, the  $ZnCl_2$  formed decreases the smoke formation and increases char formation. When ZB and ZP is heated, small amounts of  $ZnCl_2$  are formed according to Eqn.6.12 through Eqn.6.14 by the effect of heat. The char residue values are evaluated and discussed for the samples in Tables 6.6 through 6.8 as residual mass percentage values.

Mass loss versus temperature graphs can be seen in Figure 6.14 (a) and (b). Thermal degradation behaviour of the samples was measured under  $N_2$  atmosphere at a heating rate of  $10^\circ C/minute$  and recorded from room temperature to  $600^\circ C$ . To determine the thermal degradation and stability of the films according to the two stage

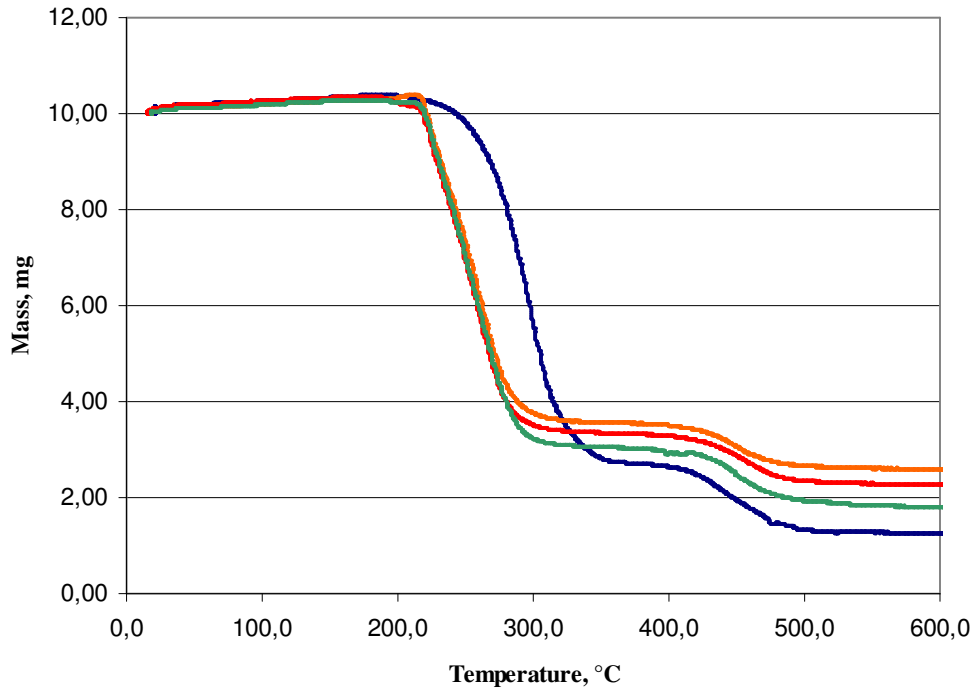
process, the curves are evaluated at 225 and 600°C. The results are evaluated in Table 6.6, 6.7 and 6.8, respectively.

These results show a beneficial interaction between ZB and ZP. It is not so clear in Table 6.6 (at 225°C) but it becomes obvious in the later two tables. The mass losses of PVC control sample and sample having 0.54% ZB + 0.81% ZP are 0% at 225°C. However, the mass losses in the rest of the samples are noticeable although they are small. When the values at 400°C are examined, the mass loss in PVC control sample had the highest value of 73.6% among other samples. Sample having 1.29% ZB + 0.271% ZP has the lowest value of 64.80%. Sample having only 1.36% ZB and the sample having only 1.36% ZP has higher values but these values are again smaller than control sample. It may be concluded that they had also lowered the degradation of PVC by themselves, however as it is clear with the results of other samples, they have lower mass loss values by the combination compositions.

When the final losses at 600°C are examined, control sample has the highest loss value of 87.5%. Sample having equivalent amounts of ZB and ZP (0.68%) comes next. At this temperature sample having 1.29% ZB + 0.27% ZP and sample having 0.54% ZB + 0.81% ZP has again the lowest value of 73.7% and 76.15%; respectively.

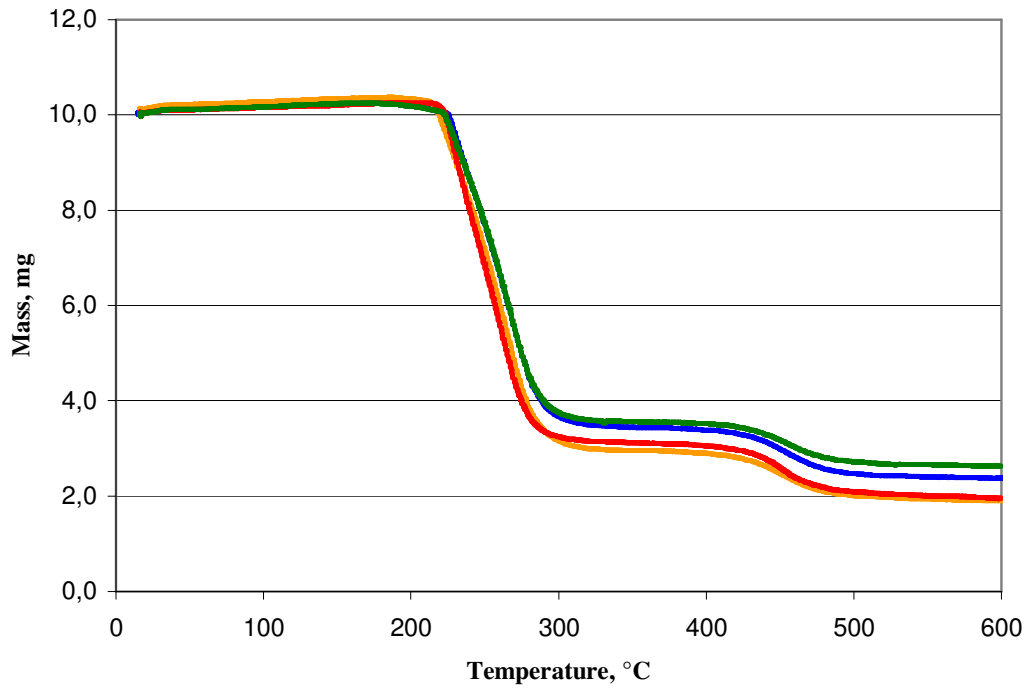
As shown in Fig.6.14 (a), PVC control sample started to lose its mass at 180°C. While sample having only 1.36% ZB has a higher onset temperature of 214°C and sample having only 1.36% ZP has a lower onset temperature of 185°C when compared with the control sample. Foregoing mass losses of these samples takes place at the same temperature value of 304°C but with different mass losses and then same temperature of 418°C. This temperature is also higher than the control sample. Of the remaining samples, the highest onset temperature is 214°C with sample having only 1.36% ZB only and 210°C with sample having 0.27% ZB and 1.29% ZP, respectively.

The char residues of the samples, which are residual mass values, are tabulated in Tables 6.6 through 6.8. The highest char residue giving samples are samples having 0.54% ZB + 0.81% ZP (26.36%), and 1.29% ZB + 0.27% ZP (23.85%). But in a general view, all of the compositions give higher char residues when compared with the control sample (12.5%). This result is consistent with the mechanism proposed in the previous section (Eqn.6.11-6.14).  $ZnCl_2$  formed suppressed the formation of smoke and catalysed the char formation which is clearly obvious in the values when compared with the PVC control.



— 1: PVC Control Sample, — 2: 1.36 wt% ZB,  
 — 3: 1.36 wt% ZP, — 4: 0.68 wt% ZB and 0.68 wt% ZP

Figure 6.14 (a) TGA curves of Sample Nos.1 – 4.



— 5: 0.54 wt% ZB and 0.81 wt% ZP, — 6: 0.81 wt% ZB and 0.54 wt% ZP,  
 — 7: 0.27 wt% ZB and 1.29 wt% ZP, — 8: 1.29 wt% ZB and 0.27 wt% ZP

Figure 6.14 (b) TGA curves of Sample Nos.5 – 8.

The onset temperatures tabulated in Table 6.9 are also graphed in Figure 6.15 according to the ZB wt %. For a comparison, PVC control sample is also added in this bar chart. As can be concluded in this bar chart, nearly all of the onset temperatures of the samples are higher than the control sample, especially the composition with 1.36% ZB only and 0.27% ZB + 1.29% ZP have got higher values compared with the control sample.

Table 6.6. Mass loss of PVC plastigel films at 225°C

No	ZB, wt%	ZP, wt%	Mass Loss, %	Residual Mass, %
1	0.00	0.00	1.44	98.56
2	0.00	1.36	9.07	90.93
3	0.27	1.29	4.00	96.00
4	0.54	0.81	0.00	100.00
5	0.68	0.68	6.91	93.09
6	0.81	0.54	8.19	91.81
7	1.29	0.27	3.70	96.30
8	1.36	0.00	7.21	92.79

Table 6.7. Mass loss of PVC plastigel films at 400°C.

No	ZB, wt%	ZP, wt%	Mass Loss, %	Residual Mass, %
1	0.00	0.00	73.60	26.64
2	0.00	1.36	67.10	32.90
3	0.27	1.29	69.50	30.5
4	0.54	0.81	66.15	33.85
5	0.68	0.68	70.65	29.35
6	0.81	0.54	71.10	28.9
7	1.29	0.27	64.80	35.20
8	1.36	0.00	65.00	35.00

Table 6.8. Mass loss of PVC plastigel films at 600°C.

<b>No</b>	<b>ZB, wt%</b>	<b>ZP, wt%</b>	<b>Mass Loss, %</b>	<b>Residual Mass, %</b>
1	0.00	0.00	87.50	12.50
2	0.00	1.36	77.20	22.80
3	0.27	1.29	80.40	19.60
4	0.54	0.81	76.15	23.85
5	0.68	0.68	81.90	18.10
6	0.81	0.54	80.90	19.10
7	1.29	0.27	73.70	26.30
8	1.36	0.00	74.20	25.80

Table 6.9 Onset temperatures of PVC plastigel films.

<b>No</b>	<b>ZB, wt%</b>	<b>ZP, wt%</b>	<b>Onset Temperatures , °C</b>
1	0.00	0.00	180
2	0.00	1.36	185
3	0.27	1.29	210
4	0.54	0.81	185
5	0.68	0.68	190
6	0.81	0.54	200
7	1.29	0.27	183
8	1.36	0.00	214



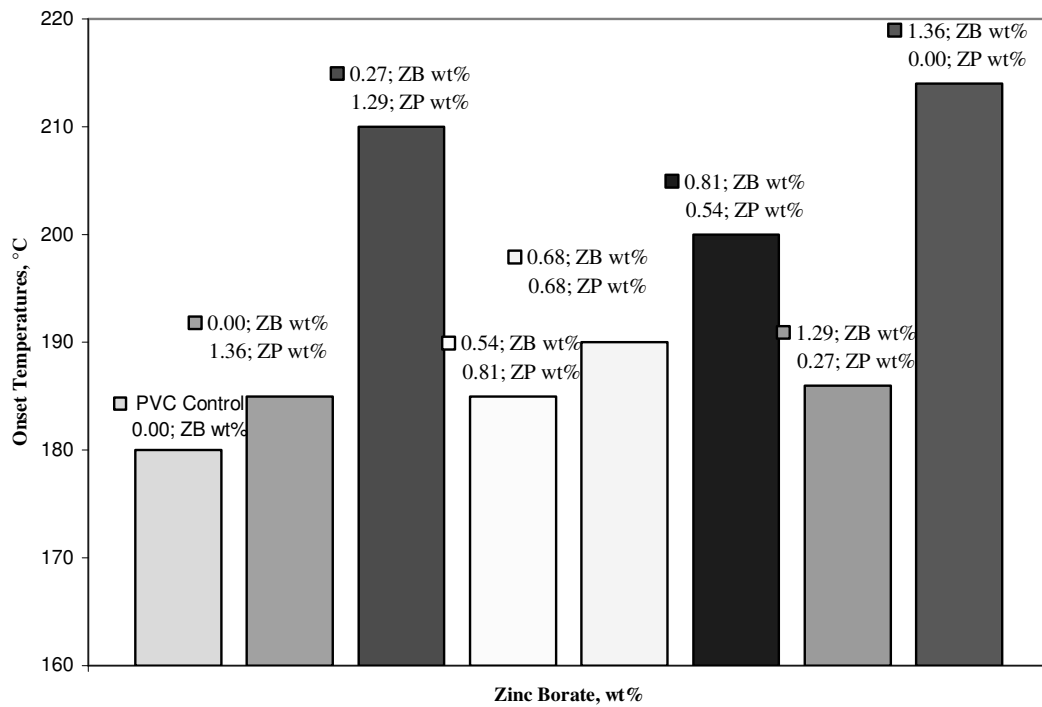


Fig.6.15. The onset temperature bar graph of the samples.

## 6.4 Colour Tests of PVC Plastigels

### 6.4.1 Static Oven Test

When PVC is heated its colour changes due to the conjugated double bonds and the polyene sequences formed. The colour varies from light brown to dark brown and even black in severe cases.

The gelled PVC films were cut into 6 pieces of 5 x 1 cm. and properly labelled as 15 min., 30 min., 45 min., 60 min., 75 min. and 90 min placed onto a glass plate. These films were then placed in a vacuum static oven and heated first of all at 140°C and then at 160°C for the time periods mentioned before. A sample film was taken out of the oven at every 15 minute interval and the appearance of the films was recorded at these intervals. All other thermal stability tests were evaluated according to these films.

The appearances of the films heated at 140°C and 160°C were tabulated in Table 6.10 and 6.11, respectively. As it is also clear in the tables, the PVC control sample at 160°C is especially degraded very easily beginning from 45 minutes with a pale brown colour and getting a brown colour at 90 minutes. But in the samples having only ZB or only ZP, although the degradation is apparent it is not as fast as in PVC control sample; especially in the composition having only ZP. The colour begins to change at 75 minutes for the sample having ZB only but the colour of the sample having ZP only does not change. The synergistic effect of ZB and ZP can be observed in the results of this test. Sample having 0.54% ZB + 0.81% ZP, sample having 0.81% ZB + 0.54% ZP and sample having 1.29% ZB + 0.27% ZP have all colours between white and yellowish meaning that they did not degrade so easily such as in the control sample and the samples having only ZB or only ZP. Their colour did not change even at 160°C at 90 minutes but the films have become opaque and slippery.

Table 6.10 The appearance of the film samples heated at 140°C for different time periods.

ZB, %	ZP, %	15 min.	30 min.	45 min.	60 min.	75 min.	90 min.
0.00	0.00	White	White	White	White	White	White
0.00	1.36	White	White	White	White	White	White
0.27	1.29	White	White	White	White	Yellowish	Yellowish
0.54	0.81	White	White	White	White	White	White
0.68	0.68	White	White	White	White	White	White
0.81	0.54	White	White	Yellowish	Yellowish	Yellowish	Yellowish
1.29	0.27	White	White	Yellowish	Yellowish	Yellowish	Yellowish
1.36	0.00	White	White	White	White	White	Light yellow

Table 6.11 The appearance of the film samples heated at 160°C for different time periods.

ZB, %	ZP, %	15 min.	30 min.	45 min.	60 min.	75 min.	90 min.
0.00	0.00	White	White	Yellowish	Light yellow	Light yellow	Light brown
0.00	1.36	White	White	White	White	White	White
0.27	1.29	White	White	White	Yellowish	Yellowish	Light brown
0.54	0.81	White	White	White	White	White	White
0.68	0.68	White	White	Light brown	Light brown	Light brown	Brown
0.81	0.54	White	White	White	White	White	White
1.29	0.27	White	White	White	White	White	White
1.36	0.00	White	White	White	White	Light brown	Light brown

## 6.5 Colour Measurement

The colour measurements were evaluated also by using a spectrometer. The X, Y and Z tristimulus values read by Avantes Spectrocam spectrophotometer were used to calculate the yellowness indexes of the films from Eqn.5.1 and the values both in L, a, b and X, Y and Z tristimulus are reported in Table A.17 to A.19 in Appendix. Yellowness index is a measure of the extent of degradation of the films as there is a colour change on the films due to heat.

Table 6.12 lists the values of yellowness index of the samples heated at 140°C while Table 6.13 lists the values of 160°C.

Table 6.12 Yellowness Index values of the PVC Films heated at 140°C.

Sample No.	ZB, %	ZP, %	15 min.	30 min.	45 min.	60 min.	75 min.	90 min.
1	0.00	0.00	6.4	11.8	10.6	8.2	9.9	7.8
2	0.00	1.36	-5.5	-2.2	-1.2	-1.4	0.1	-0.7
3	0.27	1.29	-3.5	3.7	4.3	6.9	10.3	11.6
4	0.54	0.81	-4.4	-5.2	3.1	-0.5	2.8	3.6
5	0.68	0.68	-2.5	-4.2	-4.9	-3.6	-0.7	-2.6
6	0.81	0.54	-5.0	0.2	0.7	6.6	6.9	5.7
7	1.29	0.27	-7.4	4.8	5.4	8.1	8.7	10.5
8	1.36	0.00	-6.0	-9.2	-5.9	-4.6	-5.2	41.2

Table 6.13 Yellowness Index values of the PVC Films heated at 160°C.

Sample No.	ZB, %	ZP, %	15 min.	30 min.	45 min.	60 min.	75 min.	90 min.
1	0.00	0.00	0.5	2.8	1.6	1.7	-5.1	1.6
2	0.00	1.36	-0.2	-0.1	-1.5	3.7	38.1	-5.2
3	0.27	1.29	-2.9	-4.6	-6.3	2.6	27.3	36.8
4	0.54	0.81	-2.2	0.0	2.2	0.6	3.0	-4.9
5	0.68	0.68	-1.8	-5.9	71.9	94.9	108.6	106.8
6	0.81	0.54	-3.9	-3.9	-4.7	-2.8	-1.8	-6.0
7	1.29	0.27	-3.5	-1.7	-1.0	2.4	1.1	-3.7
8	1.36	0.00	-2.3	-0.4	-3.9	0.1	20.7	82.1

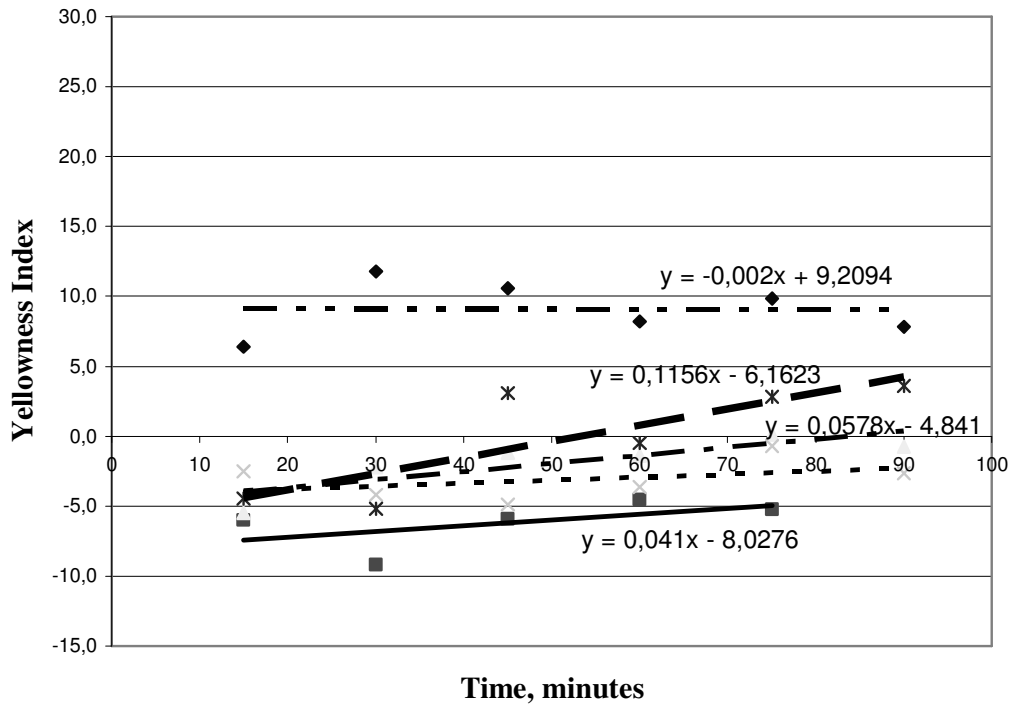
Higher or positive numbers of yellowness index indicate that the sample is degraded while negative numbers indicate that thermal stability or degradation is better.

When the results of 140°C are examined, sample having 0.68% ZB and ZP each, having equal amounts of ZB and ZP of 0.68%, had the best result but when it is heated at 160°C it has degraded very much leading to the highest number of 106.8. The sample having 0.81% ZB and 0.54% ZP has got the whitest value of -6.0 but also the sample having 0.54% ZB and 0.81% ZP has got also a whiter value of -4.9.

In general all of these numbers are consistent with the previous Tables 6.10 and 6.11 of appearances of the PVC plastigels. As a reference, a white gloss paper was put behind the films as the films were transparent. Therefore the yellowness index of the white paper was also calculated as -8.9 from its tristimulus values as 74, 77 and 95.8, respectively. The values are tabulated in Table A.17 in Appendix.

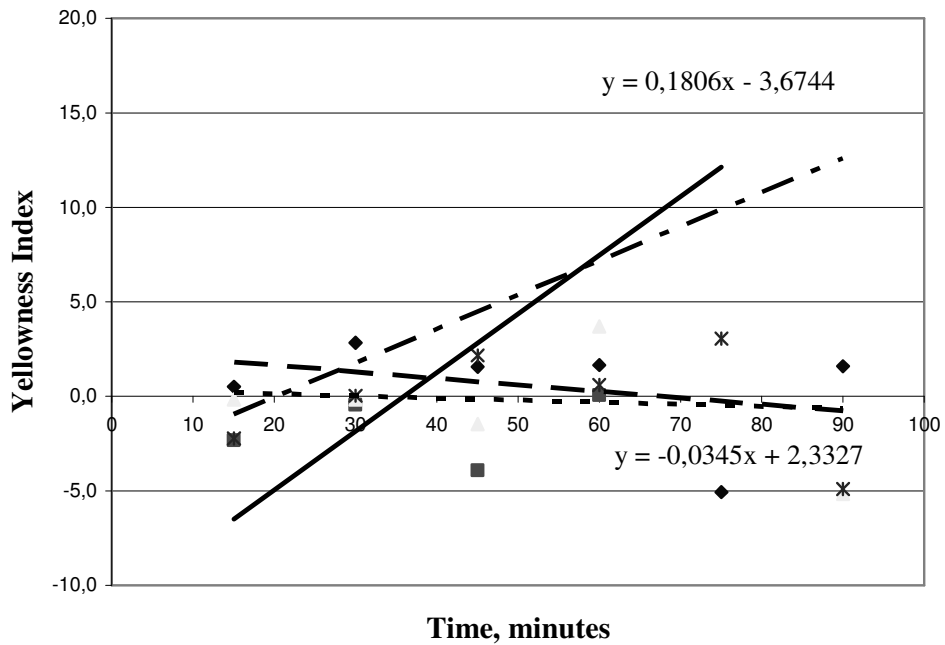
To have a better idea about the tendency of the yellowness index of the films, Figures 6.16 and 6.17 are given. These figures are specifically important due to minimizing the effect of maximum  $\Delta E$  value between two measurements. The formula for  $\Delta E$  is given in Eqn.5.2.

The instrument has an error tolerance of 0.4  $\Delta E$  between two adjacent measurements. Therefore construction of linear equations between the data points will linearize the yellowness index versus time minimizing the error between measurements. For the values at 140°C, all of them are in an increasing trend. However, at 160°C the samples having only 1.36% ZP and 0.54% ZB and 0.81% ZP have a decreasing trend leading to whiter results.



. . . PVC Control Sample, — 1.36 % ZB,  
 - - - 1.36 % ZP, - . - . 0.68 % ZB and 0.68 % ZP  
 — — — 0.54% ZB and 0.81% ZP

Fig.6.16. The change of yellowness index tendency of the PVC plastigel films with time at 140°C.



. . . PVC Control Sample, — 1.36 % ZB,  
 - - - 1.36 % ZP, - . - . 0.54% ZB and 0.81% ZP

Fig.6.17. The change of yellowness index tendency of the PVC plastigel films with time at 160°C.

## 6.6 Spectroscopic Analyses of the Films

### 6.6.1 Fourier Transmission InfraRed (FTIR) Spectra Tests

FTIR spectrum of PVC control sample is given in Figure 6.18. The IR spectrum showed bands related with CH<sub>2</sub> stretch at approximately 2910 cm<sup>-1</sup> and CH stretching vibration at 2965 cm<sup>-1</sup>, CH<sub>2</sub> bending vibration at 1425 cm<sup>-1</sup>, CH bending in CHCl vibrations at 1250 cm<sup>-1</sup> and 1333 cm<sup>-1</sup>, C-C vibration at 1098 cm<sup>-1</sup>, CH<sub>2</sub> bending(Rocking) vibration at 970 cm<sup>-1</sup>, and C-Cl stretch vibration at 690 cm<sup>-1</sup>. Between 1580 and 1600 cm<sup>-1</sup> typical peaks of aromatic rings of the plasticizer is seen. At 1715 cm<sup>-1</sup> there is C = O stretching vibration of plasticizer. These results are also consistent with previous studies (Atakul, 2004; Gökçel and Balköse, 1996).

As mentioned before, the peaks belonging to ZP are clear in Fig.6.4 and that the peaks observed at 1080 and 890 cm<sup>-1</sup> are the P-O symmetric and asymmetric vibration in P-O-P chains; respectively. But in the Figures between 6.19 and 6.25, these peaks are overlapped due to the bands of PVC which will be explained later.

FTIR spectra of the sample having 1.36% ZP only are given in Fig.6.19. In these spectra, the bands due to P-O symmetric vibration in P-O-P chain at 1080 cm<sup>-1</sup> and P-O asymmetric vibration in P-O-P chain at 890 cm<sup>-1</sup> are invisible because they are overlapped by the C-O-C stretching vibration bands of the DOP plasticizer.

FTIR spectra of the composition having 0.27% ZB + 1.29% ZP, 0.54% ZB + 0.81% ZP, 0.81% ZB + 0.54% ZP and 1.29% ZB + 0.27% ZP are given in Figures 6.20, Figure 6.21, Figure 6.23 and Figure 6.24, respectively. For all of these spectra, again the peaks at 160°C belonging to the plasticizer between 970 and 1500 cm<sup>-1</sup> gave lower absorbance values than at 140°C. This is due to the evaporation of DOP at 160°C causes the absorbance values to lower down. This becomes clearer in the control sample. As there is only PVC and DOP without any additives in the control sample, the same lower absorbance values indicate partial evaporation of DOP. This result was also reported in a previous study by Atakul, 2004.

FTIR spectra of the composition having equivalent 0.68% ZB and ZP heated at 140 and 160°C are given in Fig.6.22. Between peaks 705 cm<sup>-1</sup> and 1600 cm<sup>-1</sup> at 160°C, the absorbance values were lowered because of the high thicknesses of the films. The high thickness prevents the light pass through the films causing the absorbance values to be low.

In Fig.6.25, the FTIR spectra of the sample having 1.36% ZB only are given. At  $3227\text{ cm}^{-1}$  the peak of  $\text{ZnO}\cdot\text{B}_2\text{O}_3$  is clearly seen due to the zinc borate in its structure. The peak of ZB did not change due to heating at  $160^\circ\text{C}$  and have nearly the same absorbance value with the value at  $140^\circ\text{C}$ .

The absorbance values of the samples versus ZB percentage values in the films were graphed in Figures 6.26 and 6.27. These figures were given to have a general idea on change of amount of DOP and ZB by heating the films. Figure 6.26 is evaluated on the  $1580\text{cm}^{-1}$  which is the characteristic peak of DOP, and Figure 6.27 is evaluated on the  $3227\text{cm}^{-1}$  which is the characteristic peak of ZB. These two figures consist of the values both at  $140$  and  $160^\circ\text{C}$  to be able to make a comparison on the effects of heating. The values of  $1580\text{ cm}^{-1}$  at both  $140^\circ\text{C}$  and  $160^\circ\text{C}$  show a decreasing trend in absorbance with ZB weight percentage. Higher the absorbance value of  $1580\text{ cm}^{-1}$  band indicated higher transparency at  $160^\circ\text{C}$  heated sample. The values of  $3227\text{cm}^{-1}$  both at  $140$  and  $160^\circ\text{C}$  show an increasing trend in absorbance, having a sharper slope at  $160^\circ\text{C}$  for this band. The correlations coefficient of  $140^\circ\text{C}$  heated sample was 0.91 confirming Lambert's Beer Law was obeyed.

$$A = \epsilon \times l \times c \quad (6.17)$$

where  $A$  is absorbance,  $\epsilon$  extinction coefficient,  $l$  film thickness or path length and  $c$  is concentration of active species.

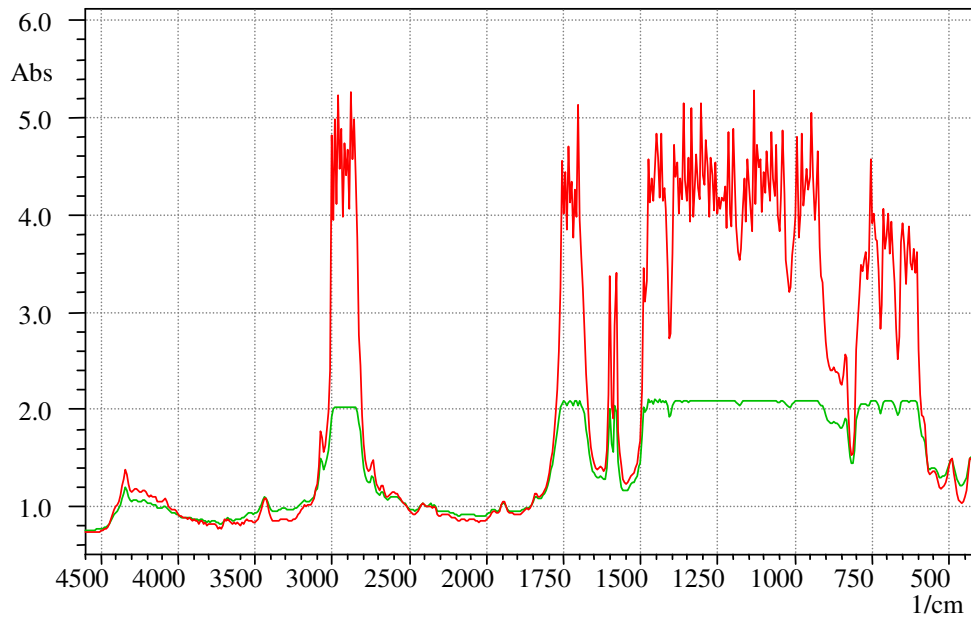


Fig.6.18 FT-IR spectra of PVC control sample at  $140^\circ\text{C}$  and  $160^\circ\text{C}$ . ( —  $140^\circ\text{C}$  at 15 min., —  $160^\circ\text{C}$  at 90 min.).



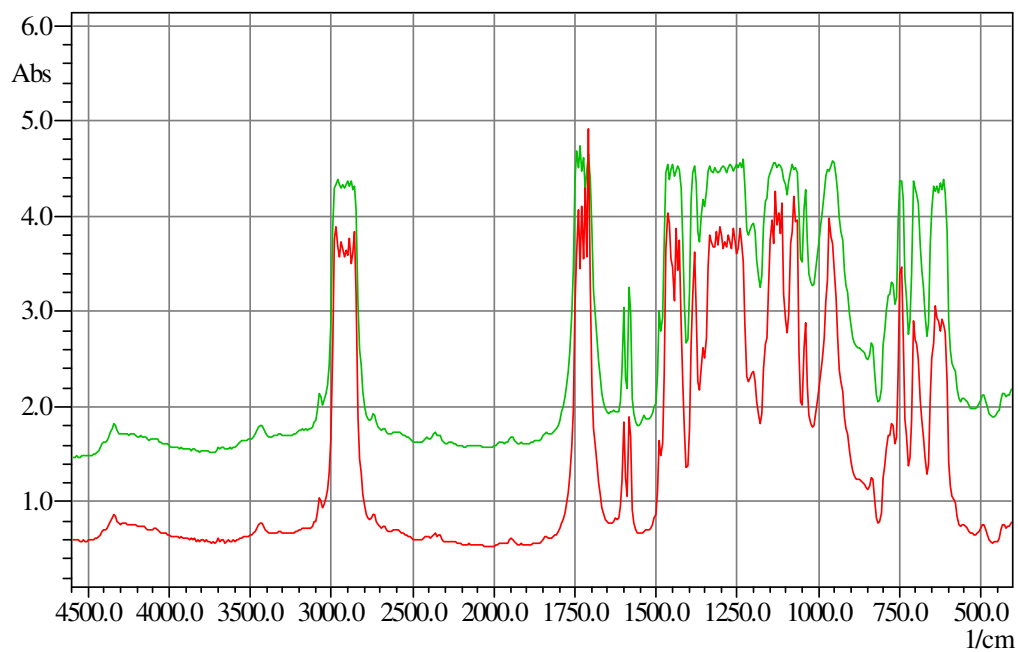


Fig.6.19 FT-IR spectra of sample having 1.36% ZP at 140°C and 160°C. ( — 140°C at 15 min., — 160°C at 90 min).

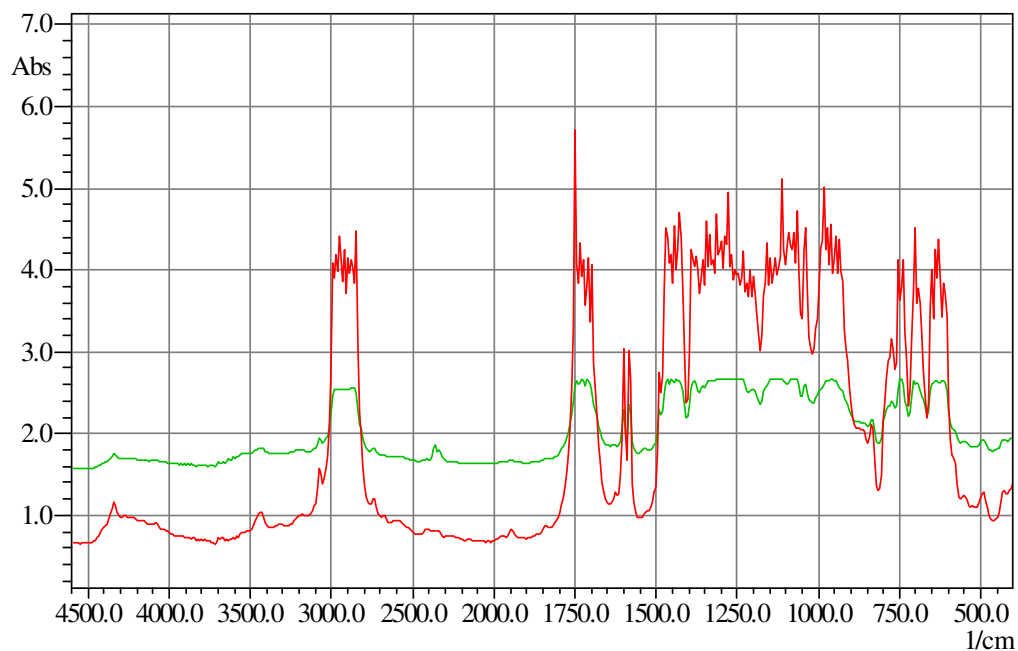


Fig.6.20 FT-IR spectra of sample having 0.27% ZB and 1.29% ZP at 140°C and 160°C. ( — 140°C at 15 min., — 160°C at 90 min.).

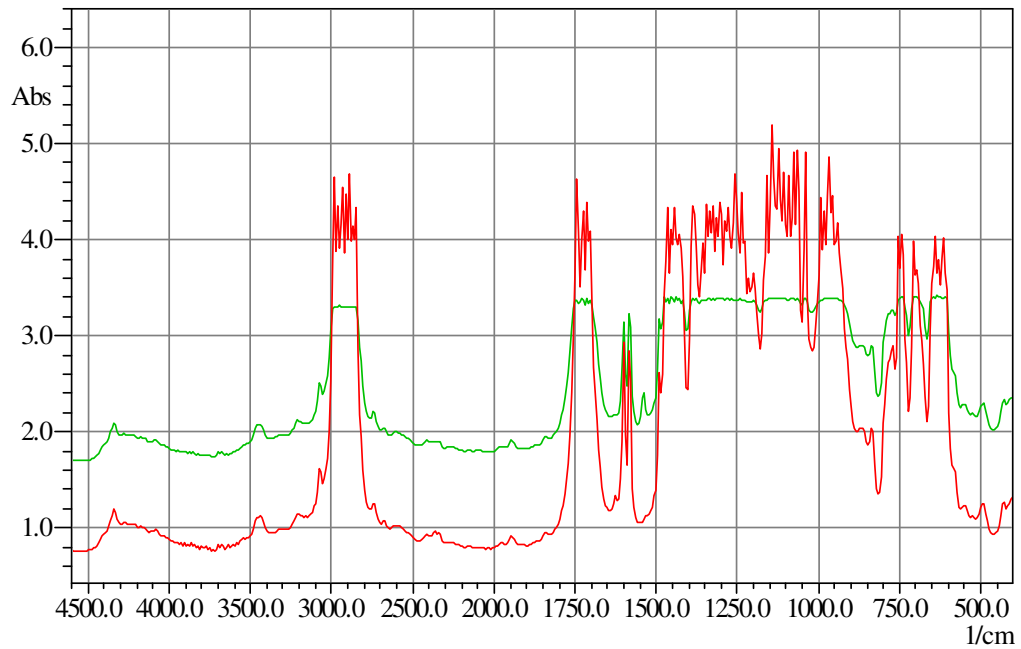


Fig.6.21 FT-IR spectra of sample having 0.54% ZB and 0.81% ZP at 140°C and 160°C. ( — 140°C at 15 min., — 160°C at 90 min.).

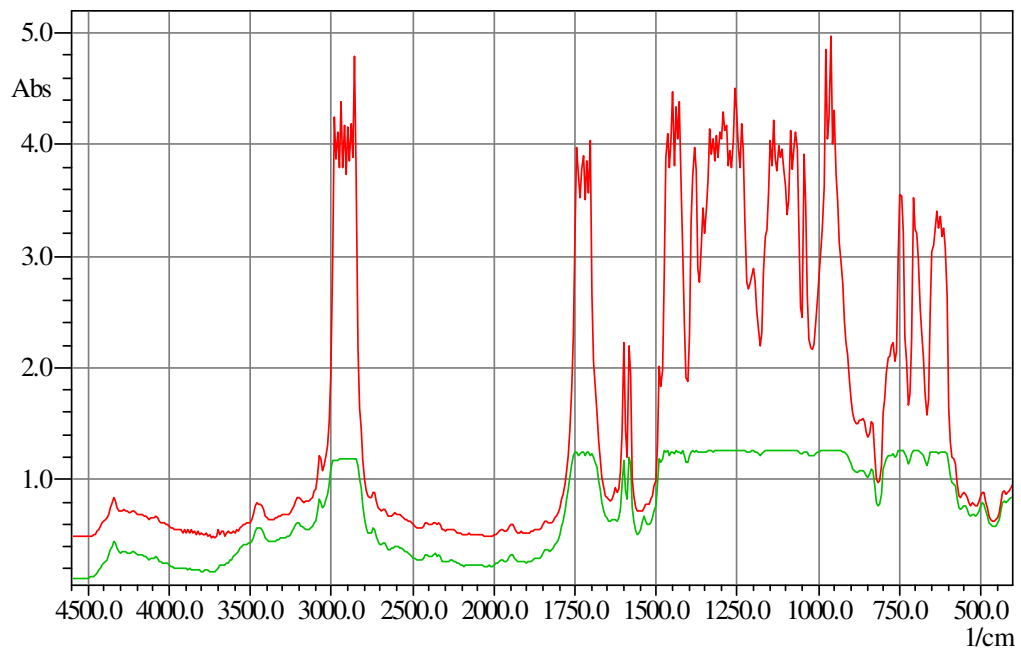


Fig.6.22 FT-IR spectra of sample having 0.68% ZB and 0.68% ZP at 140°C and 160°C. ( — 140°C at 15 min., — 160°C at 90 min.).

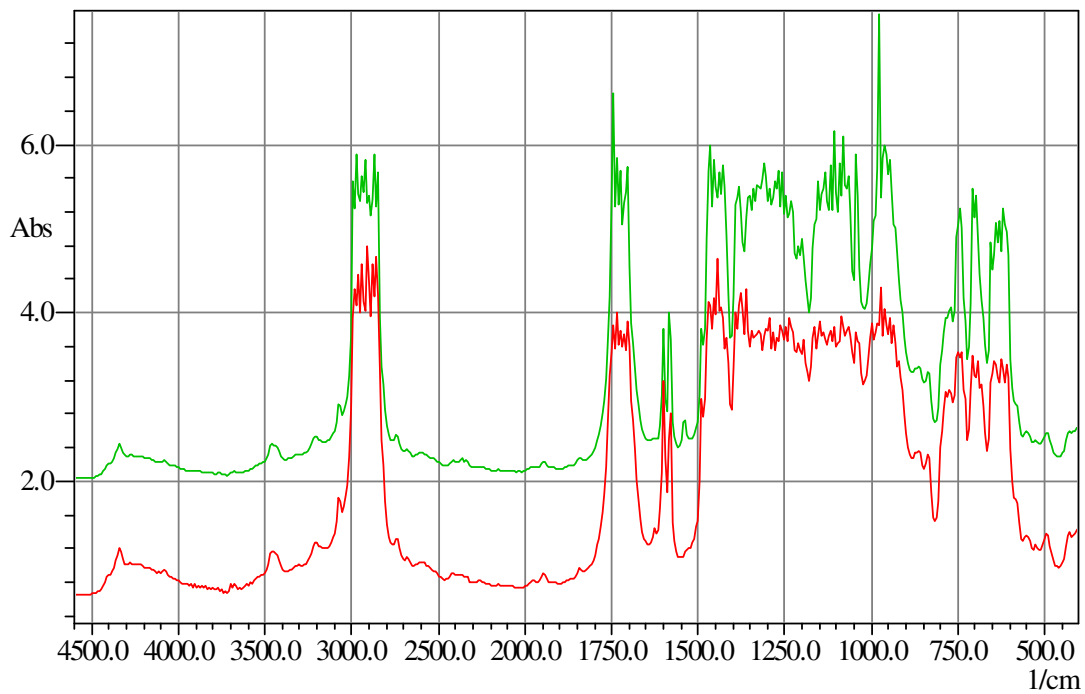


Fig.6.23 FT-IR spectra of sample having 0.81% ZB and 0.54% ZP at 140°C and 160°C. ( — 140°C at 15 min., — 160°C at 90 min.).

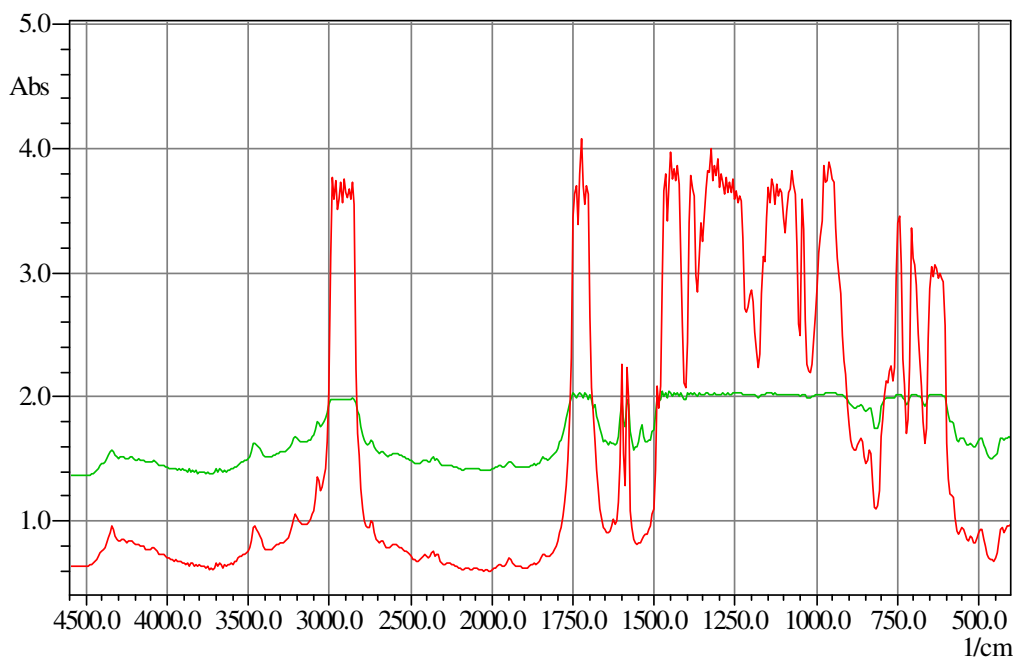


Fig.6.24 FT-IR spectra of sample having 1.29% ZB and 0.27% ZP at 140°C and 160°C. ( — 140°C at 15 min., — 160°C at 90 min.).

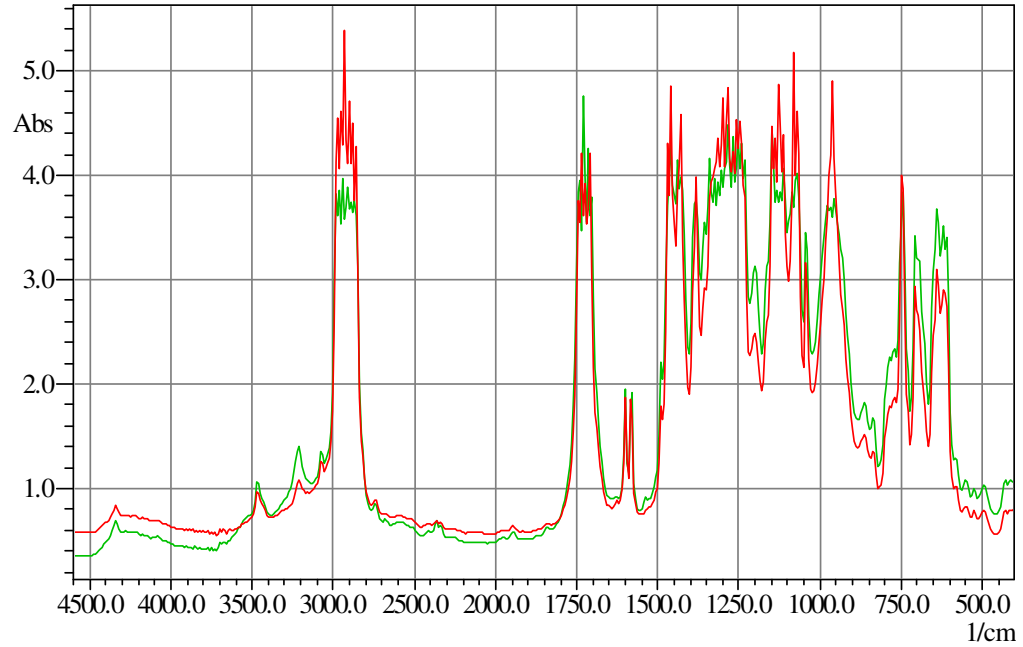


Fig.6.25 FT-IR spectra of sample having 1.36% ZB at 140°C and 160°C. ( — 140°C at 15 min., — 160°C at 90 min.).

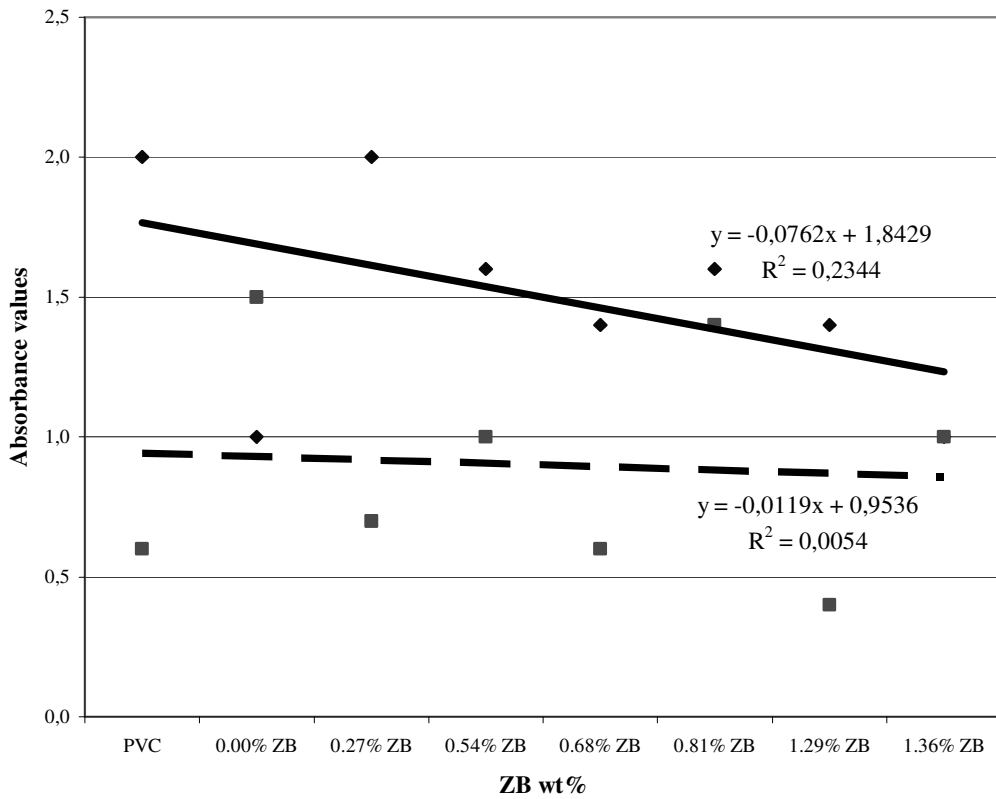


Figure 6.26 Absorbance versus ZB wt% at 1580cm<sup>-1</sup> at 140 and 160°C.

— 140°C, - - - 160°C.

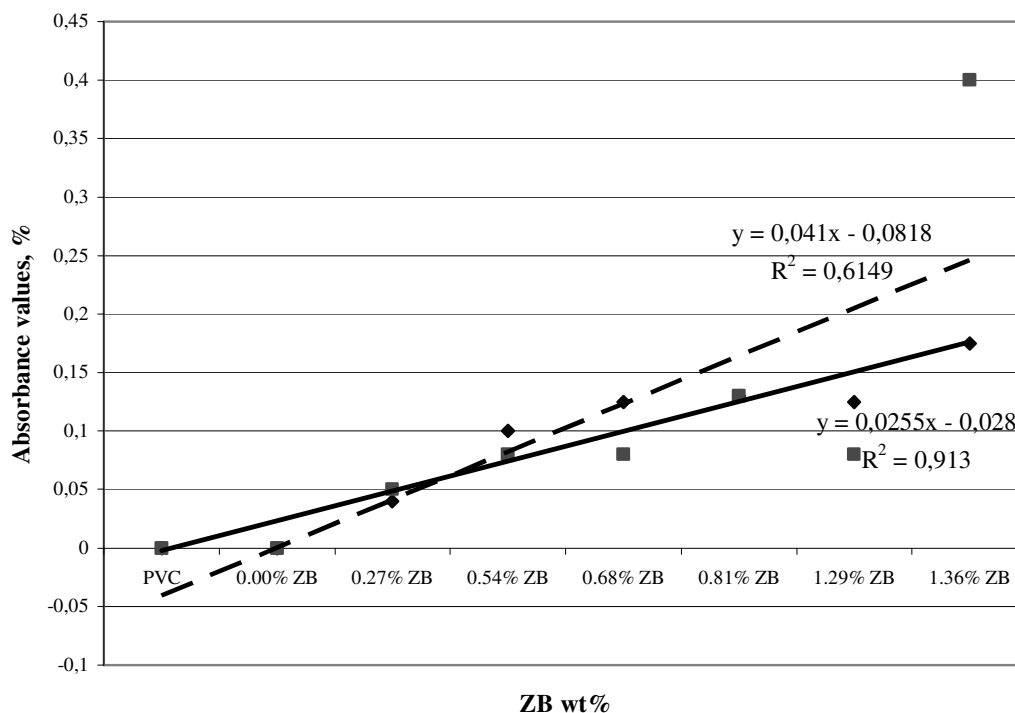


Figure 6.27 Absorbance versus ZB wt% at  $3227\text{cm}^{-1}$  at 140 and  $160^{\circ}\text{C}$ .

—  $140^{\circ}\text{C}$ , - - -  $160^{\circ}\text{C}$ .

### 6.6.2 Attenuated Total Reflection (ATR) Spectra Tests

Transmission IR spectrum of films gives ideas about bulk of the PVC films, but ATR spectrum gives information about the surface of the films. As the temperature of the films increases, DOP is transferred to the surface of the films. Therefore with the help of the results achieved from ATR spectra, the change in surface characteristics of the films due to heating can be evaluated.

ATR IR spectra are given through Figures 6.28 and 6.35. The peak at  $1540\text{cm}^{-1}$  is a characteristic band of  $\text{COO}^-$  belonging to the emulsifier present in emulsion PVC. In general, the absorbance value of this peak is observed to be increasing when films were heated. This can be explained again due to the fact that the migration of the carboxylate groups from the interior of the film to the surface is increasing.

Another point to be discussed is the presence of ZB peak at  $3227\text{cm}^{-1}$  in the figures both at  $140$  and  $160^{\circ}\text{C}$  which show that ZB does not decompose by the effect of heating. The presence of this peak is valid for all of the samples having ZB but its absorbance value changes by the ZB mass added according to the composition. The

peaks for ZP previously mentioned are also overlapped in these figures.

The absorbance values of the samples versus ZB percentage values in the films were graphed in Figures 6.36 and 6.37. These figures were given to have a general idea on the tendency of the absorbance values. The first figure is evaluated on the  $1540\text{cm}^{-1}$  which is the characteristic peak of emulsifier present in PVC, and the second figure is evaluated on the  $3227\text{cm}^{-1}$  which is the characteristic peak of ZB. These two figures again consist of the values both at  $140^\circ\text{C}$  and  $160^\circ\text{C}$  to be able to make a comparison on the effects of heating. The values of  $1540\text{ cm}^{-1}$  both at  $140^\circ\text{C}$  and  $160^\circ\text{C}$  show a small decreasing trend with ZB weight percentage in absorbance. The higher absorbance values at  $160^\circ\text{C}$  indicated emulsifier migrated to the surface of the film from the bulk of the films. The values of  $3227\text{cm}^{-1}$  both at  $140$  and  $160^\circ\text{C}$  show a random change with ZB wt% indicating the surface of the film did not have the same composition with bulk. As seen in Fig.6.27 the transmission spectra showing the state of bulk had an increasing absorbance at  $3227\text{ cm}^{-1}$  with ZB wt%.

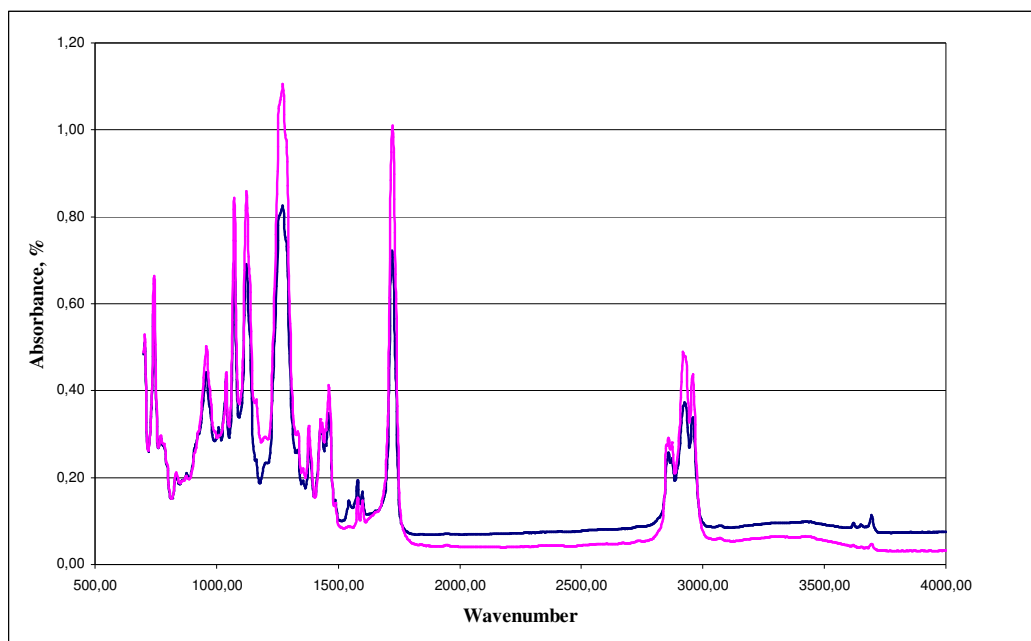


Fig.6.28 FT-IR spectra of PVC Control sample at  $140^\circ\text{C}$  and  $160^\circ\text{C}$ . ( —  $140^\circ\text{C}$  at 15 min., —  $160^\circ\text{C}$  at 90 min.).

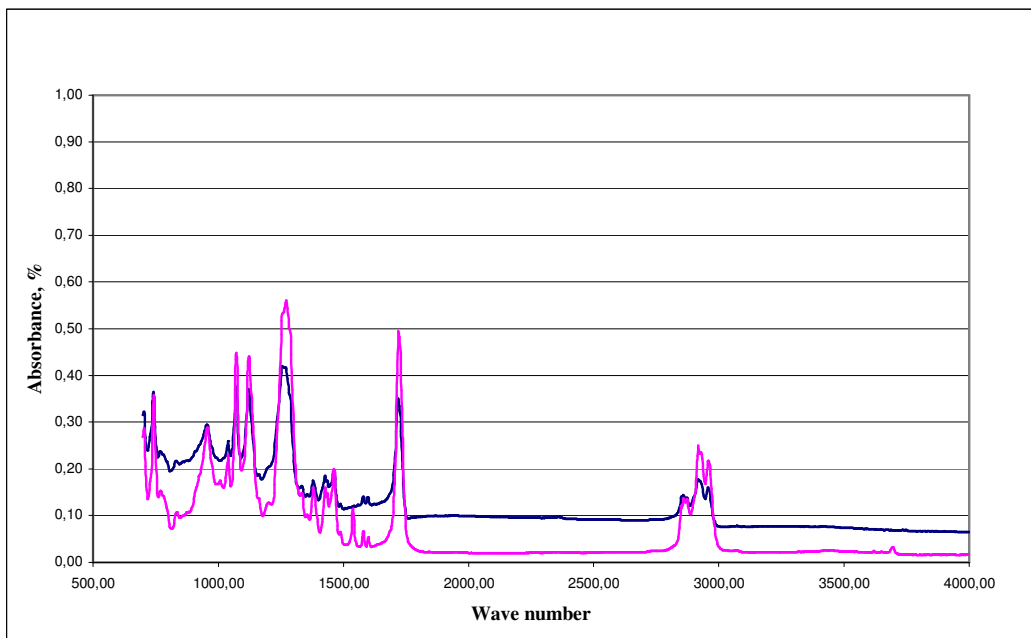


Fig.6.29 FT-IR spectra of sample having 0.00% ZB and 1.36% ZP at 140°C and 160°C. ( — 140°C at 15 min., — 160°C at 90 min.).

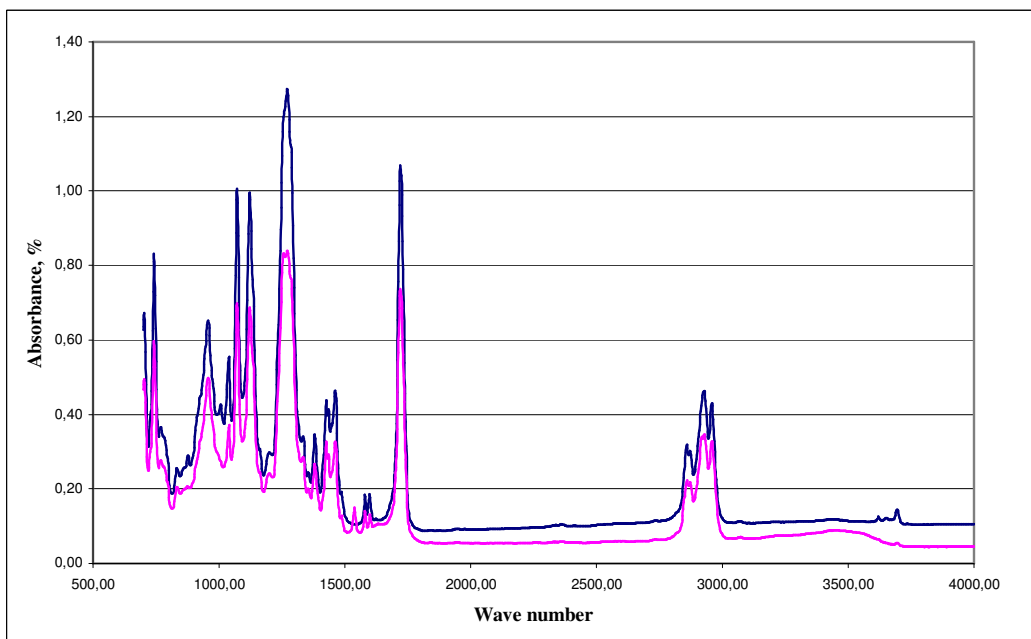


Fig.6.30 FT-IR spectra of sample having 0.27% ZB and 1.29% ZP at 140°C and 160°C. ( — 140°C at 15 min., — 160°C at 90 min.).

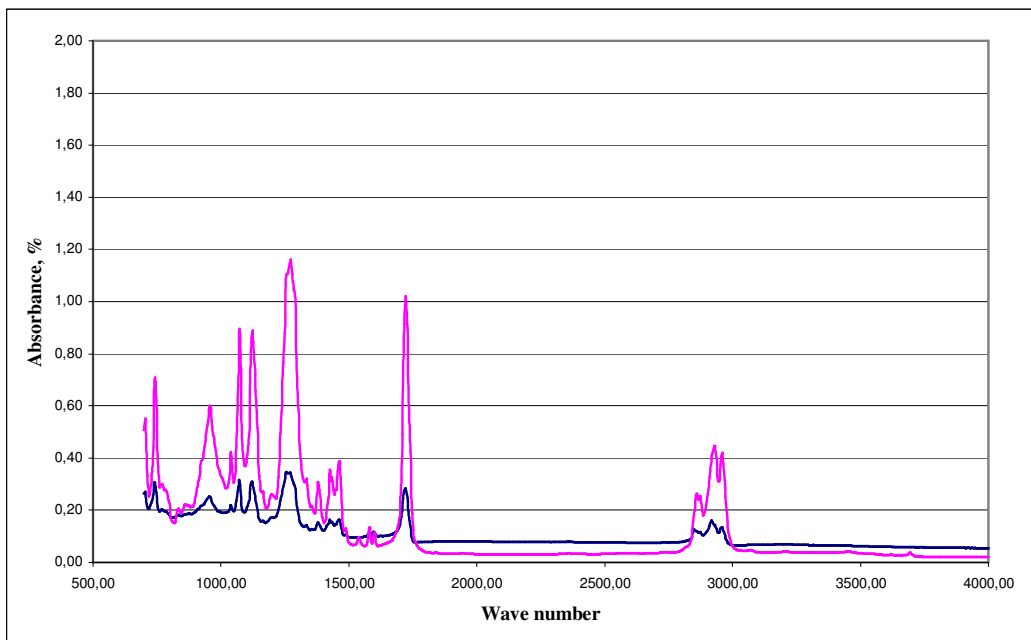


Fig.6.31 FT-IR spectra of sample having 0.54% ZB and 0.81% ZP at 140°C and 160°C. ( — 140°C at 15 min., — 160°C at 90 min.).

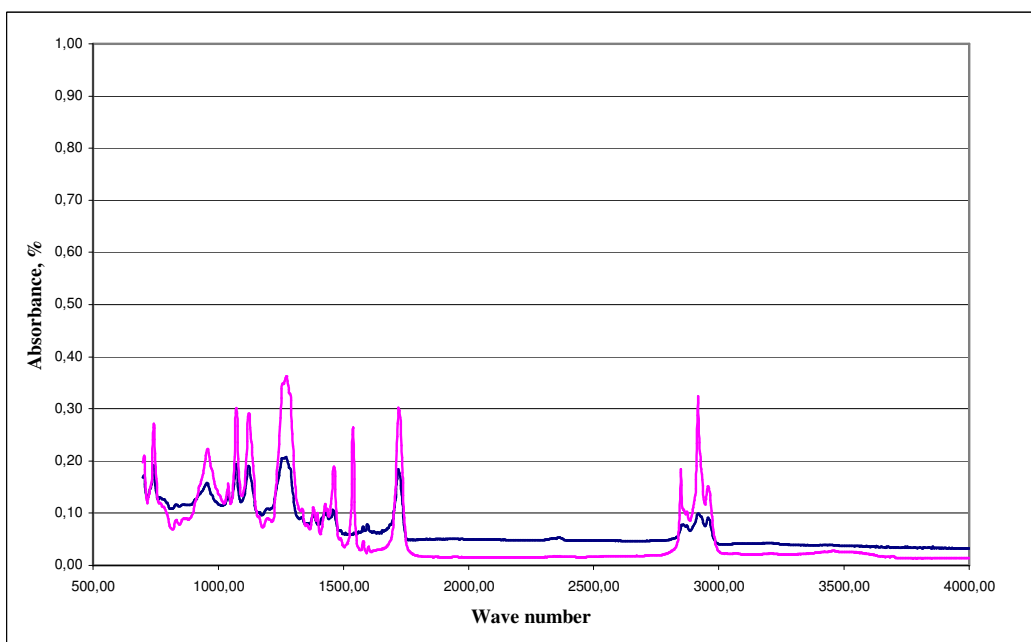


Fig.6.32 FT-IR spectra of sample having 0.68% ZB and 0.68% ZP at 140°C and 160°C. ( — 140°C at 15 min., — 160°C at 90 min.).



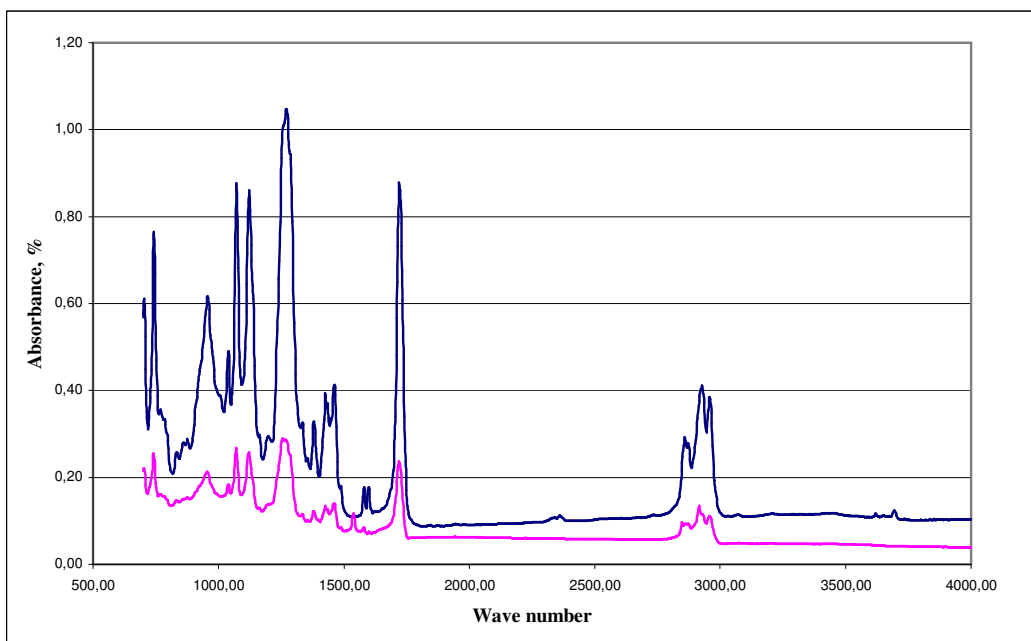


Fig.6.33 FT-IR spectra of sample having 0.81% ZB and 0.54% ZP at 140°C and 160°C. ( — 140°C at 15 min., — 160°C at 90 min.).

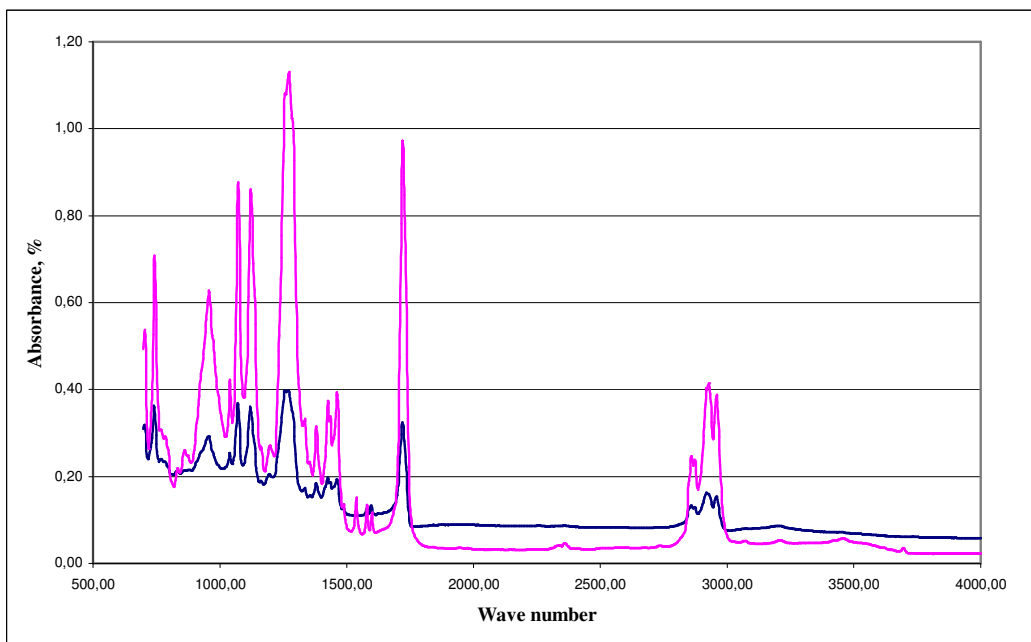


Fig.6.34 FT-IR spectra of sample having 1.29% ZB and 0.27% ZP at 140°C and 160°C. ( — 140°C at 15 min., — 160°C at 90 min.).

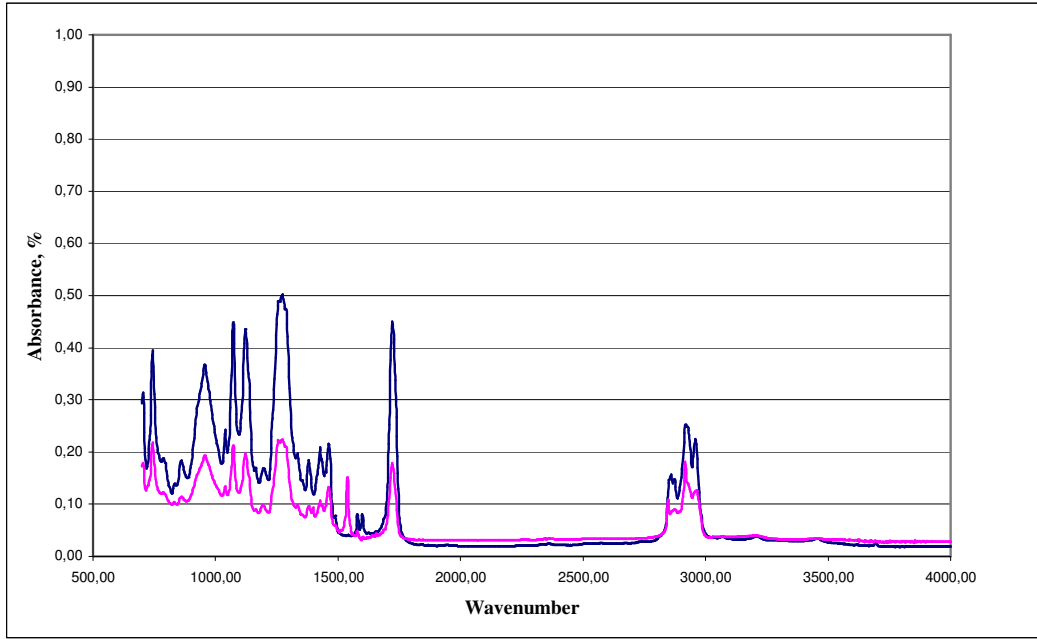


Fig.6.35 FT-IR spectra of sample having 1.36% ZB and 0.00% ZP at 140°C and 160°C. ( — 140°C at 15 min., — 160°C at 90 min.).

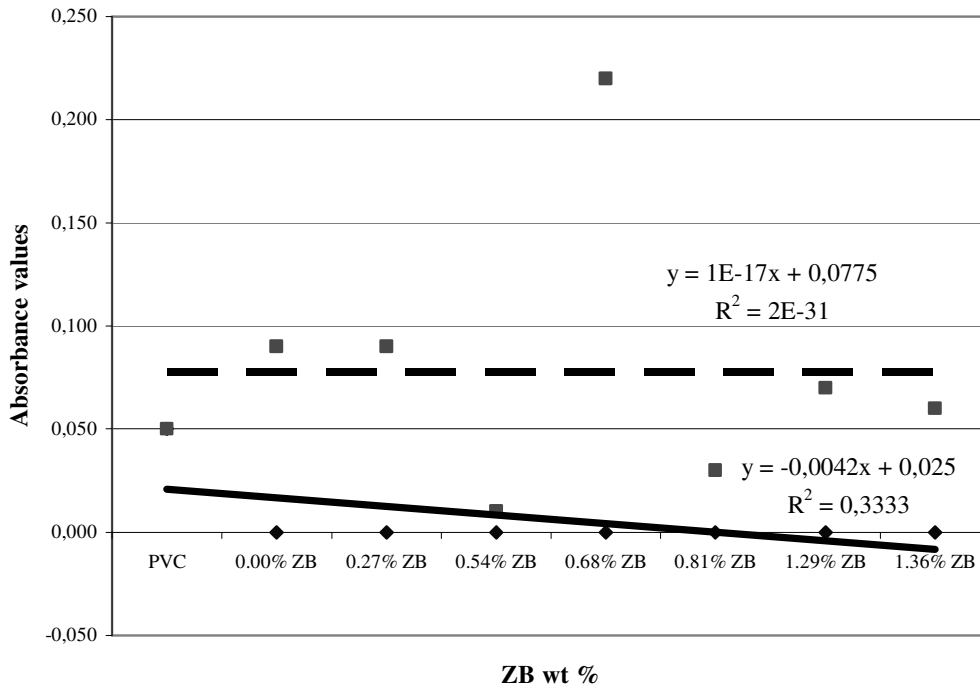


Figure 6.36 Absorbance versus ZB wt% at 1540cm<sup>-1</sup> at 140 and 160°C.  
 — 140°C, - - - 160°C.

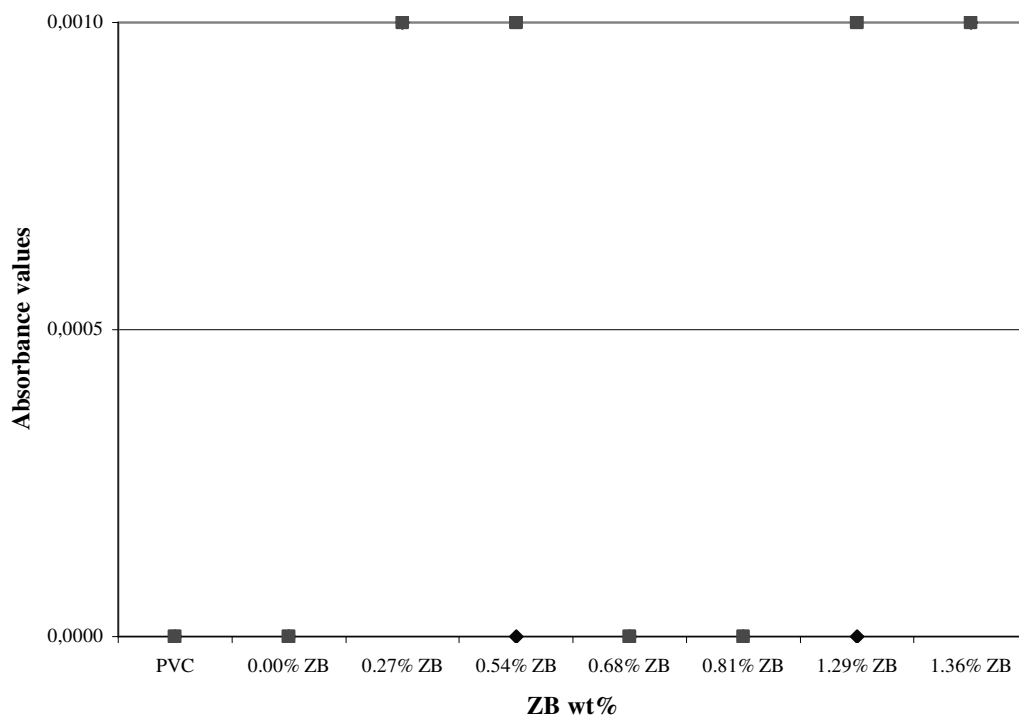


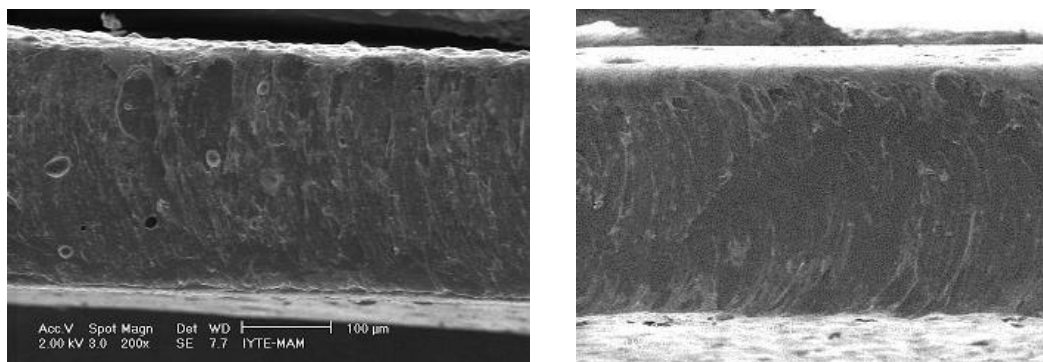
Figure 6.37 Absorbance versus ZB wt% at  $3227\text{cm}^{-1}$  at 140 and 160°C.

■ 140°C, ◇ 160°C.

### 6.7 Morphology of PVC Plastigels

SEM micrographs of PVC plastigels with different compositions were taken to investigate the heat effects on the micro scale. Although there are pores in the micrographs, it is obvious that when the temperature is increased up to 160°C, the number of air bubbles and particles appearing decrease and a more homogeneous plastigel is achieved.

In all of the micrographs it can be concluded that the mixing is done thoroughly and the sedimentation of the particles is not observed. The plasticizer DOP has solvated the PVC and additive particles thoroughly and with the functionality of wetting agent, the particles has been wetted well sticking the particles to each other (Fig.6.38a, Fig.6.40a, Fig.6.41a since the white parts represent both PVC and the plasticizer).



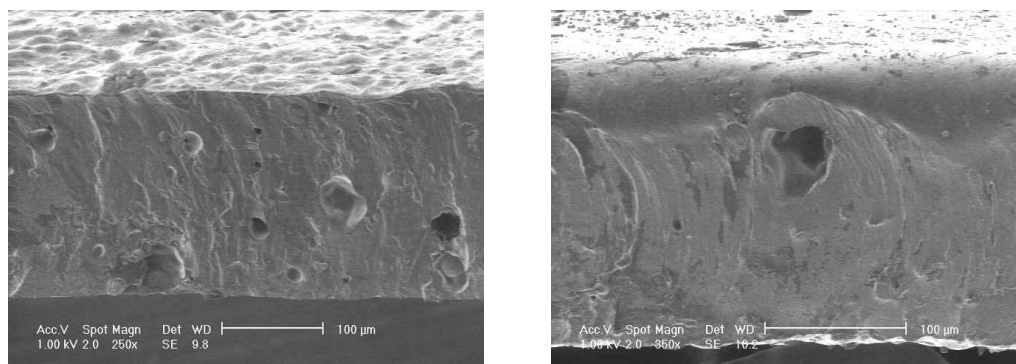
(a)

(b)

Figure 6.38. SEM microphotographs of PVC control samples  
 a) Heated at 140°C for 15 min. b) Heated at 160°C for 90 min.

In general, the microphotographs of the PVC plastigel films heated at 160°C for 90 minutes have got less air bubbles entrapped in their structures and the number of observed additive particles decreased due to better gel formation (Fig.6.40a and 6.40b, Fig.6.42a and 6.42b and Fig.6.45a and 6.45b are some examples).

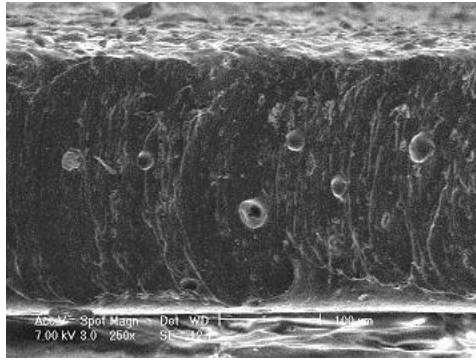
SEM microphotographs with different compositions of ZB and ZP are given between Figures 6.38 and Figure 6.45.



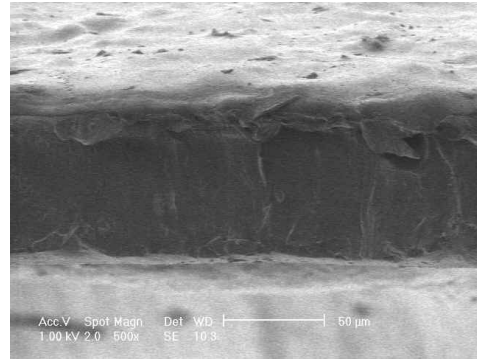
(a)

(b)

Figure 6.39. SEM microphotographs of sample having 1.36% ZP only.  
 a) Heated at 140°C for 15 min. b) Heated at 160°C for 90 min.

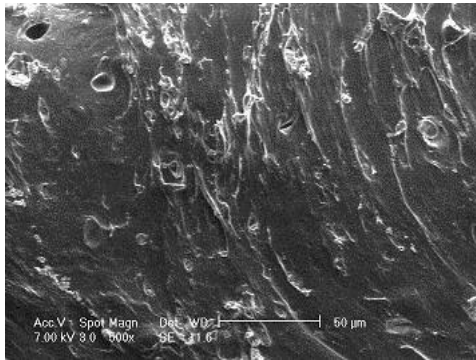


(a)

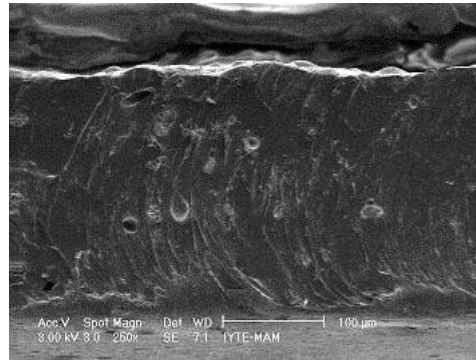


(b)

Figure 6.40. SEM microphotographs of sample having 0.27% ZB and 1.29% ZP.  
a) Heated at 140°C for 15 min. b) Heated at 160°C for 90 min.

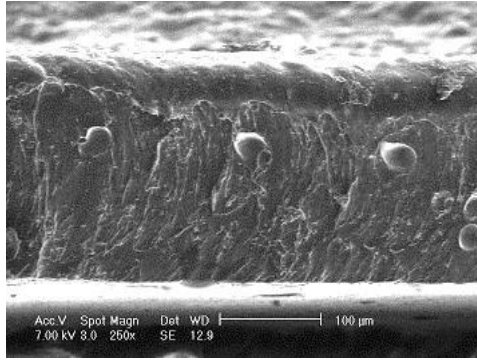


(a)

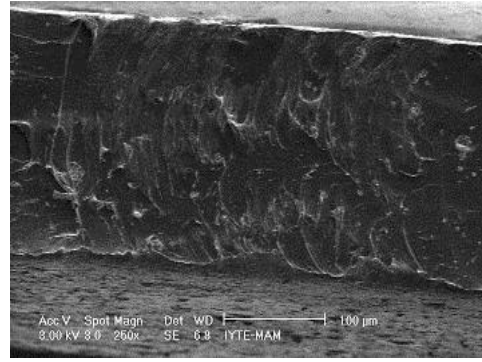


(b)

Figure 6.41. SEM microphotographs of sample having 0.54% ZB and 0.81% ZP.  
a) Heated at 140°C for 15 min. b) Heated at 160°C for 90 min.

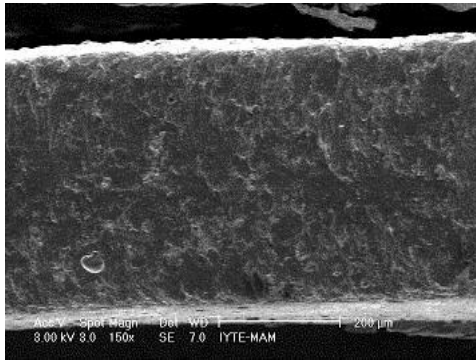


(a)

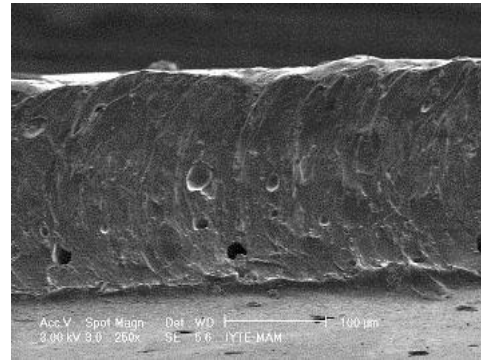


(b)

Figure 6.42. SEM microphotographs of sample having 0.68% ZB and 0.68% ZP.  
a) Heated at 140°C for 15 min. b) Heated at 160°C for 90 min.

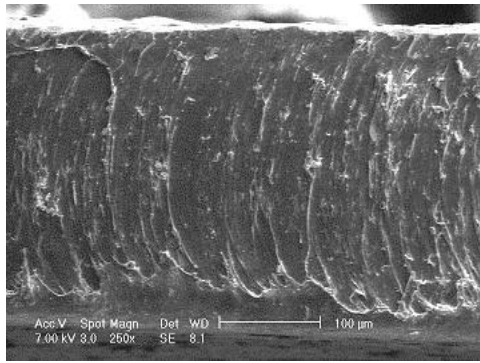


(a)

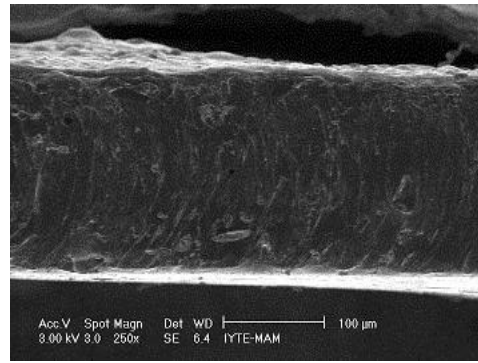


(b)

Figure 6.43. SEM microphotographs of sample having 0.81% ZB and 0.54% ZP.  
a) Heated at 140°C for 15 min. b) Heated at 160°C for 90 min.

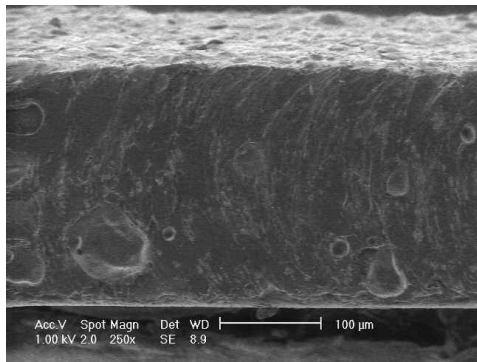


(a)

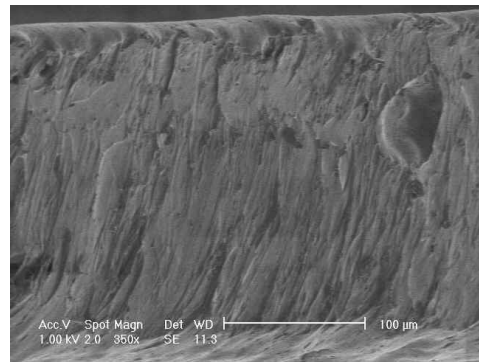


(b)

Figure 6.44. SEM microphotographs of sample having 1.29% ZB and 0.27% ZP.  
a) Heated at 140°C for 15 min. b) Heated at 160°C for 90 min.



(a)



(b)

Figure 6.45 SEM microphotographs of sample having 1.36% ZB only.  
a) Heated at 140°C for 15 min. b) Heated at 160°C for 90 min.

## 6.8 Elemental Analyses of PVC Plastigels

PVC plastigels were analyzed by EDX coupled with a scanning electron microscope (SEM) to have an idea on the elemental compositions of the films composed so far. Both PVC polymer and particle phases were investigated by using this instrument. Two or three different points on the polymer and particles were chosen and evaluated. The weight percentage of each element in the compositions was calculated with average values. Standard deviations were also calculated. A sample EDX photograph is also given in Figure 6.46 as an example. All of the values are given between Tables A.1 and A.16 in Appendix.

The theoretical values were calculated and reported in Table 6.14 (Atakul, 2004). Elemental analyses of the polymer phase and particles at 140°C and 160°C are reported in Tables 6.15 through 6.18. Carbon (C) content for all analyses except polymer phase at 140°C is reported between 57% and 75% which is lower than but close to the theoretical weight percentage of carbon in DOP (73.81%) (Atakul, 2004). The carbon content in the particles at 140°C is reported to be low. This shows that the particles were coated with the polymer phase. The chlorine (Cl) content of the films at 140°C is reported between 11.2% and 27.6% which is lower than the value in PVC plastigel (31.52%). These values decrease to 3.8% - 16.5% when heated at 160°C which indicates that the dehydrochlorination occurred. The oxygen content (O) in the films is reported to be nearly same with the value of PVC plastigel films; between 7 and 9%, which is nearly same as theoretical value of 9% (Atakul, 2004). This value decreased down to 6 to 8 % when heated at 160°C. There is not any phosphate content in the composition with no ZP and there is not any borate content in the composition with no ZB.

For the particles, it may be concluded that the chlorine content was increased at 160°C. This can be because of the increased rate of release of  $ZnCl_2$  formed by the reaction between HCl released as a result of dehydrochlorination and ZB and ZP in the system. The chlorine content is between 0.7% – 5.2% at 140°C while it is between 1.3% – 7.9% at 160°C.



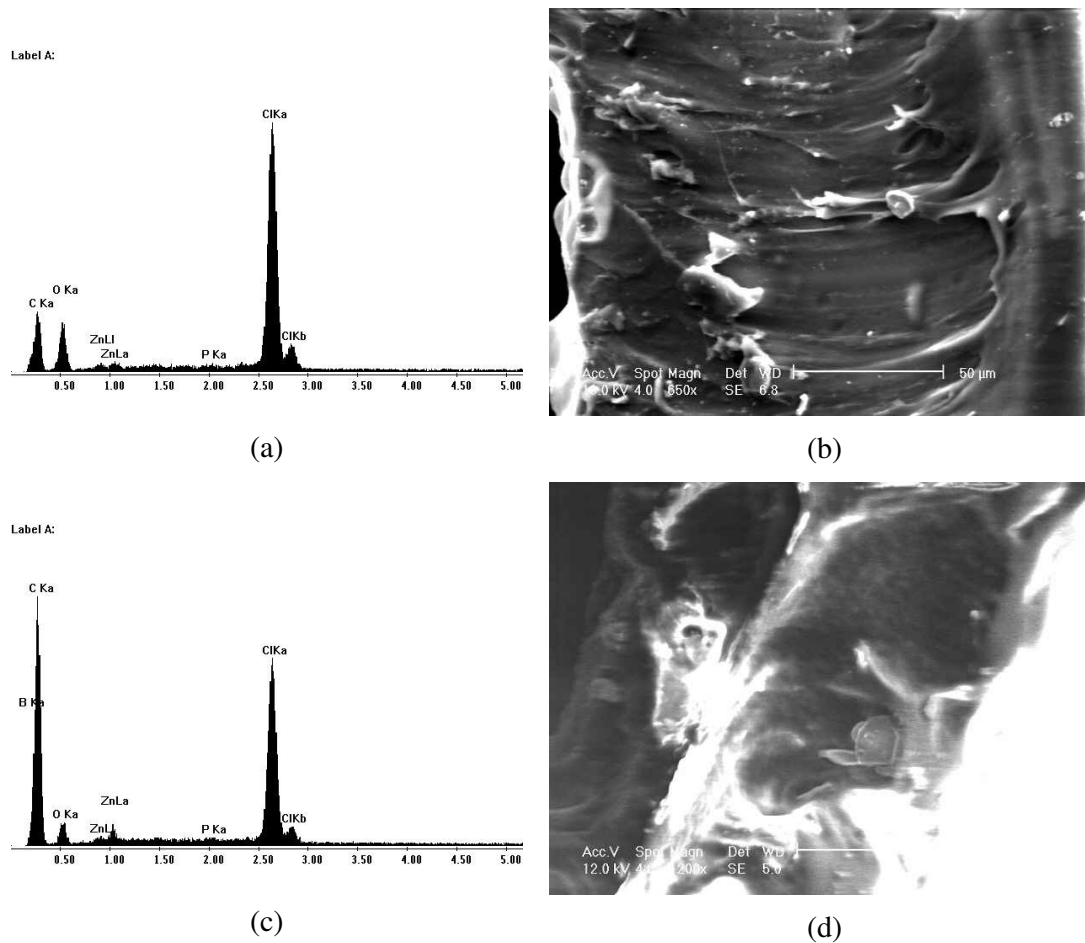


Figure 6.46 a) EDX analysis of elements of PVC plastigel having 1.36% ZP only.  
 b) SEM micrograph of PVC plastigel having 1.36% ZP only.  
 c) EDX analysis of elements of PVC plastigel having 0.27% ZB + 1.29% ZP.  
 d) SEM micrograph of PVC plastigel having 0.27% ZB + 1.29% ZP.

Table 6.14 The theoretical compositions of components(Atakul, 2004).

Elements	PVC	DOP	PVC plastigel
C	38.44	73.81	60.36
O	-	16.40	9.11
Cl	56.74	-	31.52

Table 6.15 Elemental analyses of particles at 140°C for 15 minutes (Average values).

	PVC	1.36% ZP	0.27% ZB + 1.29% ZP	0.54% ZB + 0.81% ZP	0.68% ZB + 0.68% ZP	0.81% ZB + 0.54% ZP	1.29% ZB + 0.27% ZP	1.36% ZB + 0.00% ZP
C	-	19.2	18.0	24.9	63.3	40.5	22.4	51.7
O	-	26.3	18.8	25.3	12.7	17.3	27.4	21.8
Cl	-	0.7	2.0	2.8	3.0	5.2	2.6	4.7
Zn	-	42.7	38.3	34.7	10.6	26.2	36.6	11.5
P	-	11.2	14.5	9.2	3.4	7.3	8.5	-
B	-	-	8.4	3.1	7.0	3.4	2.5	10.3

Table 6.16 Elemental analyses of polymer phase at 140°C for 15 minutes (Average values).

	PVC	1.36% ZP	0.27% ZB + 1.29% ZP	0.54% ZB + 0.81% ZP	0.68% ZB + 0.68% ZP	0.81% ZB + 0.54% ZP	1.29% ZB + 0.27% ZP	1.36% ZB + 0.00% ZP
C	69.1	75.0	57.0	66.0	73.1	67.5	72.5	70.9
O	2.9	7.8	5.4	8.9	9.0	6.6	7.5	7.7
Cl	13.0	15.5	27.6	18.8	12.3	18.4	11.2	12.4
Zn	-	1.4	1.8	1.0	0.5	0.7	0.5	0.7
P	-	0.2	0.4	0.0	0.0	0.1	0.0	-
B	-	-	7.8	5.3	5.1	6.9	8.2	8.3

Table 6.17 Elemental analyses of particles at 160°C for 90 minutes (Average values).

	PVC	1.36% ZP	0.27% ZB + 1.29% ZP	0.54% ZB + 0.81% ZP	0.68% ZB + 0.68% ZP	0.81% ZB + 0.54% ZP	1.29% ZB + 0.27% ZP	1.36% ZB + 0.00% ZP
C	-	64.0	54.8	33.0	56.9	23.6	39.6	67.4
O	-	13.7	11.4	21.8	14.2	23.9	23.8	9.7
Cl	-	4.1	3.8	2.4	1.8	1.3	2.3	7.9
Zn	-	14.4	14.7	29.3	16.2	39.9	25.4	3.4
P	-	3.8	4.9	9.5	3.8	6.2	5.6	-
B	-	-	10.5	4.0	7.1	5.0	3.3	11.6

Table 6.18 Elemental analyses of polymer phase at 160°C for 90 minutes (Average values).

	PVC	1.36% ZP	0.27% ZB + 1.29% ZP	0.54% ZB + 0.81% ZP	0.68% ZB + 0.68% ZP	0.81% ZB + 0.54% ZP	1.29% ZB + 0.27% ZP	1.36% ZB + 0.00% ZP
C	38.8	77.8	69.1	82.1	84.6	88.9	79.9	77.6
O	3.7	5.1	2.9	6.0	10.2	7.5	8.6	7.9
Cl	7.5	16.5	13.0	6.6	5.1	3.7	11.5	3.8
Zn	-	0.5	0.2	0.0	0.0	0.0	0.0	0.5
P	-	0.1	0.2	0.0	0.0	0.0	0.0	-
B	-	-	14.7	5.3	0.0	0.0	0.0	10.2

## CHAPTER 7

### CONCLUSIONS

In this study the development of heat stabilizers for PVC from zinc borate and zinc phosphate was investigated.

Thermogravimetric analyses were done to investigate the mass loss due to the release of HCl and evaporation of plasticizer DOP. The sample having only 1.36% ZB and the sample having 0.81% ZB and 0.54% ZP had the highest onset temperatures of 214 and 200°C which are higher than the onset temperature of 180°C of PVC control sample. The maximum residual mass value of the composition having 1.29% ZB and 0.27% ZP was 26.3% but it is clear that all of the compositions were higher than the value of the PVC control sample (12.5%).

The thermal stability of the prepared PVC plastigels by means of colour was determined by static oven test and colour spectrophotometer. It has been observed that more than one composition has been approved to be synergistic composition according to the results of static oven test. These colours of the final state of these compositions were lighter in colour which means a retarded degradation of PVC. Because when PVC is heated, its colour changes due to the formation of polyene structures. To show this quantitatively, a spectrophotometer was also used leading to the same result. The yellowness index is a measure of this concept. The higher or positive numbers indicate that the sample is going away from whiteness.

The morphology and composition of PVC plastigel films were analyzed in a scanning electron microscope and energy dispersive X-ray instruments, respectively. Although there are pores in the micrographs, it is obvious that when the temperature is increased up to 160°C, the holes disappear and a more homogeneous plastigel is achieved. It has been observed that the mixing was done thoroughly and the sedimentation of the particles was not observed. Both PVC polymer and particle phases were investigated by using EDX. Carbon (C) is reported between 57% and 75% which is lower than but close to the theoretical weight percentage of carbon in DOP (73.81%) due to incomplete gelation. A low C content observed for particle phase at 140°C showed that the particles were coated with the polymer phase. The chlorine (Cl) content

of the particle phase of films at 140°C was reported between 11.2% and 27.6% which was lower than the value in PVC (56.74%). These values become lower down to 3.7% - 16.5% when heated at 160°C which indicated dehydrochlorination occurs.

FTIR spectra of the PVC plastigel films were analyzed both at the surface and bulk phase by transmission and ATR spectroscopy. In all of the spectra it is clear that neither unheated samples at 140°C for 15 minutes nor heated samples at 160°C for 90 minutes have lost the peak at 3227  $\text{cm}^{-1}$  which belongs to  $\text{ZnO}\cdot\text{B}_2\text{O}_3$  meaning that the zinc borate in the composition has not been changed. The peaks belonging to zinc phosphate were overlapped by the peaks of PVC.

The PVC plastigel films containing zinc borate and zinc phosphate were studied in PVC Thermomat instrument to calculate the reaction rates and reaction rate constants at 140°C and at 160°C to evaluate the kinetics of this reaction. The induction time and stability time values were measured by the help of this instrument. The sample having 0.54% ZB and 0.81% ZP had the highest value of 1.87 h, while the induction time value of PVC control sample is 1.49 h at 160°C. However the stability time values of PVC control sample at 140 and 160°C have got higher values when compared with the compositions which mean that the additives can retard the degradation of PVC in the beginning but they cannot be able to do so when it begins to degrade. In fact, they accelerate this reaction. The initial and linear rate constants of the PVC control sample have got lower values indicating that the reaction is slower in the control sample. The activation energies of the initial regions have higher values than the activation energies of the linear region which can be explained by the rapid dehydrochlorination reactions occurring in the linear region. Due to the presence of zinc borate and zinc phosphate in the initial region, the activation energies are higher which means that there must be more energy applied to the system to initiate the reaction when compared with the linear region.

As a future study, the limiting oxygen index (LOI), mechanical tests and analyses of gaseous products of degradation by TGA – MS may be carried out to investigate the fire retardancy of these compositions.

## APPENDIX

Table A.1 The EDX results of PVC control sample at 140°C for 15 minutes.

	No.1	No.2	No.3	Average	Standart Deviation
C	70.4	82.39	81.26	78.02	6.62
O	6.85	13.60	11.28	10.58	3.43
Cl	15	12.00	7.46	11.49	3.80
Zn	0	0.00	0.00	0.00	0.00
P	0	0.00	0.00	0.00	0.00
B	0	0.00	0.00	0.00	0.00

Table A.2 The EDX results of sample 1.36% ZP only at 140°C for 15 minutes.

	Particle Phase				Polymer Phase			
	No.1	No.2	Average	Standart Deviation	Matrix. 1	Matrix. 2	Average	Standart Deviation
C	26.26	12.10	19.18	10.01	75.86	74.18	75.02	1.2
O	24.26	28.24	26.25	2.81	7.91	7.72	7.82	0.1
Cl	0.85	0.52	0.69	0.23	14.12	16.86	15.49	1.9
Zn	37.65	47.79	42.72	7.17	1.76	1.11	1.44	0.5
P	10.98	11.35	11.17	0.26	0.35	0.13	0.24	0.2
B	0.00	0.00	0.00	0.00	0.00	0.00	0.00	0.0

Table A.3 The EDX results of sample 0.27% ZB + 1.29% ZP at 140°C for 15 minutes.

	Particle Phase				Polymer Phase			
	No.1	No.2	Average	Standart Deviation	Matrix. 1	Matrix. 2	Average	Standart Deviation
C	15.14	20.90	18.02	4.07	51.81	62.26	57.04	7.4
O	28.83	8.69	18.76	14.24	5.60	5.14	5.37	0.3
Cl	1.00	3.06	2.03	1.46	33.32	21.86	27.59	8.1
Zn	39.99	36.53	38.26	2.45	1.86	1.66	1.76	0.1
P	9.18	19.90	14.54	7.58	0.44	0.36	0.40	0.1
B	5.86	10.92	8.39	3.58	6.97	8.72	7.85	1.2

Table A.4 The EDX results of sample 0.54% ZB + 0.81% ZP at 140°C for 15 minutes.

	Particle Phase				Polymer Phase			
	No.1	No.2	Average	Standart Deviation	Matrix. 1	Matrix. 2	Average	Standart Deviation
C	11.85	37.89	24.87	18.41	65.67	66.35	66.01	0.5
O	28.27	22.26	25.27	4.25	7.48	10.32	8.90	2.0
Cl	1.17	4.49	2.83	2.35	20.08	17.45	18.77	1.9
Zn	44.03	25.44	34.74	13.15	0.99	0.91	0.95	0.1
P	12.61	5.79	9.20	4.82	0.00	0.09	0.05	0.1
B	2.07	4.16	3.12	1.48	5.78	4.88	5.33	0.6

Table A.5 The EDX results of sample 0.68% ZB + 0.68% ZP at 140°C for 15 minutes.

	Particle Phase				Polymer Phase			
	No.1	No.2	Average	Standart Deviation	Matrix. 1	Matrix. 2	Average	Standart Deviation
C	53.54	73.01	63.28	13.77	73.93	72.33	73.13	1.1
O	19.33	6.10	12.72	9.36	8.70	9.25	8.98	0.4
Cl	1.50	4.58	3.04	2.18	12.17	12.48	12.33	0.2
Zn	18.36	2.88	10.62	10.95	0.47	0.49	0.48	0.0
P	3.65	3.06	3.36	0.42	0.00	0.00	0.00	0.0
B	3.62	10.37	7.00	4.77	4.74	5.45	5.10	0.5

Table A.6 The EDX results of sample 0.81% ZB + 0.54% ZP at 140°C for 15 minutes.

	Particle Phase				Polymer Phase			
	No.1	No.2	Average	Standart Deviation	Matrix. 1	Matrix. 2	Average	Standart Deviation
C	63.95	17.10	40.53	33.13	69.47	65.43	67.45	2.9
O	6.57	28.07	17.32	15.20	6.81	6.29	6.55	0.4
Cl	7.44	2.97	5.21	3.16	15.80	20.99	18.40	3.7
Zn	12.34	40.10	26.22	19.63	0.82	0.51	0.67	0.2
P	5.01	9.61	7.31	3.25	0.09	0.08	0.09	0.0
B	4.68	2.15	3.42	1.79	7.01	6.69	6.85	0.2

Table A.7 The EDX results of sample 1.27% ZB + 0.29% ZP at 140°C for 15 minutes.

	Particle Phase					Polymer Phase			
	No.1	No.2	No.3	Average	Standart Deviation	Matrix. 1	Matrix. 2	Average	Standart Deviation
C	11.44	24.59	31.16	22.40	10.04	72.34	72.67	72.51	0.2
O	30.76	25.86	25.65	27.42	2.89	7.55	7.46	7.51	0.1
Cl	0.64	6.04	1.16	2.61	2.98	11.26	11.14	11.20	0.1
Zn	45.51	31.69	32.54	36.58	7.75	0.47	0.61	0.54	0.1
P	11.65	7.15	6.69	8.50	2.74	0.00	0.04	0.02	0.0
B	0.00	4.70	2.81	2.50	2.36	8.37	8.08	8.23	0.2

Table A.8 The EDX results of sample 1.27% ZB + 0.29% ZP at 140°C for 15 minutes.

	Particle Phase				Polymer Phase			
	No.1	No.2	Average	Standart Deviation	Matrix. 1	Matrix. 2	Average	Standart Deviation
C	45.27	58.07	51.67	9.05	70.06	71.81	70.94	1.2
O	27.09	16.55	21.82	7.45	7.45	8.01	7.73	0.4
Cl	2.13	7.18	4.66	3.57	11.97	12.80	12.39	0.6
Zn	15.96	7.11	11.54	6.26	0.87	0.53	0.70	0.2
P	0.00	0.00	0.00	0.00	0.00	0.00	0.00	0.0
B	9.55	11.10	10.33	1.10	9.66	6.84	8.25	2.0

Table A.9 The EDX results of PVC control sample at 160°C for 90 minutes.

	Particle Phase					Polymer Phase			
	No.1	No.2	No.3	Avg.	Std.Dev.	Matrix. 1	Matrix. 2	Avg.	Std.Dev.
C	79.68	73.11	74.21	45.40	41.5	77.61	0.00	38.81	54.9
O	6.79	5.08	4.74	3.32	3.1	7.37	0.00	3.69	5.2
Cl	13.52	21.81	21.06	11.28	10.8	15.02	0.00	7.51	10.6
Zn	0.00	0.00	0.00	0.00	0.0	0.00	0.00	0.00	0.0
P	0.00	0.00	0.00	0.00	0.0	0.00	0.00	0.00	0.0
B	0.00	0.00	0.00	0.00	0.0	0.00	0.00	0.00	0.0

Table A.10 The EDX results of sample having 1.36% ZP only at 160°C for 90 minutes.

	Particle Phase							Polymer Phase			
	No.1	No.2	No.3	No.4	No.5	Avg.	Std. Dev.	Matrix. 1	Matrix. 2	Avg.	Std.Dev.
C	63.65	41.70	37.69	87.58	89.15	63.95	24.4	77.79	78.9	78.35	0.8
O	15.32	20.78	22.51	8.42	1.51	13.71	8.8	5.11	17.59	11.35	8.8
Cl	1.94	5.17	1.80	3.12	8.60	4.13	2.8	16.51	3.34	9.93	9.3
Zn	15.72	25.06	30.31	0.83	0.26	14.44	13.7	0.46	0.17	0.32	0.2
P	3.37	7.29	7.69	0.06	0.49	3.78	3.6	0.13	0	0.07	0.1
B	0.00	0.00	0.00	0.00	0.00	0.00	0.0	0	0	0.00	0.0

Table A.11 The EDX results of sample having 0.27% ZB + 1.29% ZP at 160°C for 90 minutes.

	Particle Phase							Polymer Phase				
	No.1	No.2	No.3	No.4	No.5	Avg.	Std. Dev.	Matrix. 1	Matrix. 2	Matrix. 3	Avg.	Std.Dev.
C	37.71	78.86	77.12	45.60	34.60	54.78	21.6	69.05	76.69	75.22	73.65	4.1
O	22.81	3.48	6.17	3.67	20.71	11.37	9.6	2.85	6.25	6.34	5.15	2.0
Cl	2.04	8.09	2.63	4.17	1.99	3.78	2.6	13.04	4.93	6.22	8.06	4.4
Zn	25.95	0.34	0.27	17.34	29.36	14.65	13.8	0.19	0.29	1.07	0.52	0.5
P	5.31	0.21	0.00	12.03	7.19	4.95	5.1	0.16	0.07	0.14	0.12	0.0
B	6.19	9.01	13.81	17.19	6.15	10.47	4.9	14.72	11.76	11	12.49	2.0



Table A.12 The EDX results of sample having 0.54% ZB + 0.81% ZP at 160°C for 90 minutes.

	Particle Phase					Polymer Phase			
	No.1	No.2	No.3	Avg.	Std. Dev.	Matrix. 1	Matrix. 2	Avg.	Std.Dev.
C	27.12	47.80	24.00	32.97	12.9	82.18	81.98	82.08	0.1
O	22.78	18.49	24.20	21.82	3.0	6.43	5.66	6.05	0.5
Cl	0.82	4.56	1.79	2.39	1.9	5.96	7.21	6.59	0.9
Zn	33.11	18.73	36.04	29.29	9.3	0.00	0.00	0.00	0.0
P	11.47	5.94	11.10	9.50	3.1	0.00	0.00	0.00	0.0
B	4.71	4.48	2.87	4.02	1.0	5.42	5.15	5.29	0.2

Table A.13 The EDX results of sample having 0.68% ZB + 0.68% ZP at 160°C for 90 minutes.

	Particle Phase						Polymer Phase			
	No.1	No.2	No.3	No.4	Avg.	Std. Dev.	Matrix. 1	Matrix. 2	Avg.	Std.Dev.
C	83.17	82.14	33.47	28.73	56.88	29.8	86.89	82.40	84.65	3.2
O	5.83	6.22	23.11	21.81	14.24	9.5	9.72	10.72	10.22	0.7
Cl	1.29	1.65	1.15	3.09	1.80	0.9	3.40	6.88	5.14	2.5
Zn	0.86	0.58	31.98	31.51	16.23	17.9	0.00	0.00	0.00	0.0
P	0.07	0.06	6.94	8.12	3.80	4.3	0.00	0.00	0.00	0.0
B	8.79	9.36	3.36	6.74	7.06	2.7	0.00	0.00	0.00	0.0

Table A.14 The EDX results of sample having 0.81% ZB + 0.54% ZP at 160°C for 90 minutes.

	Particle Phase					Polymer Phase			
	No.1	No.2	No.3	Avg.	Std. Dev.	Matrix. 1	Matrix. 2	Avg.	Std.Dev.
C	25.92	30.67	14.24	23.61	8.5	88.99	88.72	88.86	0.2
O	22.90	20.42	28.45	23.92	4.1	7.52	7.45	7.49	0.0
Cl	1.42	1.50	0.99	1.30	0.3	3.49	3.83	3.66	0.2
Zn	30.89	39.86	49.09	39.95	9.1	0.00	0.00	0.00	0.0
P	6.45	4.93	7.22	6.20	1.2	0.00	0.00	0.00	0.0
B	12.43	2.62	0.00	5.02	6.6	0.00	0.00	0.00	0.0

Table A.15 The EDX results of sample having 1.29% ZB + 0.27% ZP at 160°C for 90 minutes.

	Particle Phase					Polymer Phase			
	No.1	No.2	No.3	Avg.	Std. Dev.	Matrix. 1	Matrix. 2	Avg.	Std.Dev.
C	25.62	38.71	54.33	39.55	14.4	81.62	78.21	79.92	2.4
O	29.50	25.12	16.89	23.84	6.4	9.03	8.09	8.56	0.7
Cl	3.21	1.11	2.65	2.32	1.1	9.34	13.70	11.52	3.1
Zn	33.83	26.62	15.62	25.36	9.2	0.00	0.00	0.00	0.0
P	7.84	5.94	3.15	5.64	2.4	0.00	0.00	0.00	0.0
B	0.00	2.50	7.36	3.29	3.7	0.00	0.00	0.00	0.0

Table A.16 The EDX results of sample having 1.36% ZB at 160°C for 90 minutes.

	Particle Phase							Polymer Phase				
	No.1	No.2	No.3	No.4	No.5	Avg.	Std. dev.	Matrix. 1	Matrix. 2	Matrix. 3	Avg.	Std.Dev.
C	70.14	69.92	58.87	65.25	72.97	67.43	5.5	82.61	71.25	79.04	77.6	5.8
O	6.72	8.64	14.19	11.63	7.07	9.65	3.2	8.59	8.45	6.7	7.9	1.1
Cl	11.00	1.19	6.34	11.36	9.84	7.95	4.3	1.81	7.4	2.19	3.8	3.1
Zn	0.46	0.22	12.09	3.66	0.42	3.37	5.1	0.38	0.86	0.12	0.5	0.4
P	0.00	0.00	0.00	0.00	0.00	0.00	0.0	0.0	0.0	0.0	0.0	0.0
B	11.67	20.04	8.51	8.08	9.70	11.60	4.9	6.61	12.04	11.96	10.2	3.1

Table A.17 CIE XYZ and Lab\* values of white paper.

XYZ values	Lab* values
74	90.34
77	2.00
95.8	-9.23

Table A.18 CIE XYZ and Lab\* values of the PVC plastigel films heated at 140°C for 15 minutes.

	15'		30'		45'		60'		75'		90'	
	XYZ	Lab	XYZ	Lab	XYZ	Lab	XYZ	Lab	XYZ	Lab	XYZ	Lab
PVC Control	49,2 49,9 56,4	76,0 0,7 2,4	45,6 46,5 49,9	73,9 -0,1 5,0	48,3 49,3 53,4	75,7 -0,1 4,6	51,9 52,7 58,6	77,7 0,4 3,3	47,9 48,8 53,3	75,4 -0,1 4,2	48,3 49,2 54,7	75,6 0,2 3,2
1.36% ZP	62,5 62,6 78,7	83,2 2,5 -3,5	60,4 61,1 74,2	82,5 1,0 -1,5	57,6 58,5 70,2	81,0 0,5 -0,9	63,4 64,6 77,4	84,3 -0,1 -0,7	61,5 62,8 74,2	83,3 -0,2 0,1	62,9 64,2 76,4	84,1 -0,2 -0,3
0.27% ZB+ 1.29% ZP	59,4 59,6 73,7	81,6 2,3 -2,6	54,6 57,7 63,9	80,6 -0,1 -1,8	59,6 62,9 69,4	83,4 -0,1 -1,6	57,8 61,6 65,8	82,5 -0,5 -0,1	56,6 60,0 62,5	81,9 -0,8 1,7	51,7 54,9 56,4	79,0 -1,0 2,4
0.54% ZB+ 0.81% ZP	62,9 63,2 78,6	83,6 2,1 -2,9	59,9 60,9 75,3	82,3 0,4 -2,6	56,8 58,1 66,9	80,8 -0,4 1,5	58,9 60,2 71,4	82,0 -0,3 -0,2	57,2 58,7 67,5	81,1 -0,8 1,5	59,1 60,6 69,3	82,2 -0,8 1,9
0.68% ZB+ 0.68% ZP	58,8 59,2 72,4	81,4 1,8 -1,9	62,2 62,8 77,6	83,4 1,4 -2,6	62,6 63,2 78,5	83,6 1,4 -2,8	61,9 62,6 76,9	83,3 1,2 -2,2	60,7 61,7 73,7	82,7 0,5 -0,6	62,3 63,5 76,8	83,7 0,2 -1,3
0.81% ZB+ 0.54% ZP	58,4 58,6 73,3	81,1 2,3 -3,2	52,9 55,7 63,8	79,5 0,1 -3,6	53,8 56,8 64,6	80,0 -0,1 -3,3	55,0 58,1 62,8	80,8 -0,3 -0,4	55,7 59,0 63,4	81,3 -0,6 0,0	53,2 56,3 61,2	79,8 -0,4 -0,7
1.29% ZB+ 0.27% Zp	65,6 65,5 83,8	84,7 3,2 -4,7	55,9 59,1 64,8	81,3 -0,2 -1,2	58,6 61,7 67,6	82,8 0,1 -1,1	54,6 57,8 61,5	80,6 -0,4 0,5	53,9 57,1 60,4	80,3 -0,7 0,8	55,7 59,3 61,4	81,4 -1,3 2,0
1.36% ZB	67,0 67,0 84,7	85,5 2,8 -3,9	62,3 63,1 80,7	83,5 1,0 -4,5	65,1 66,1 82,3	85,0 0,7 -3,1	61,3 62,3 76,7	83,1 0,4 -2,3	64,4 65,4 81,0	84,7 0,6 -2,7	54,2 57,0 43,3	80,2 -4,1 22,7

Table A.19 CIE XYZ and Lab\* values of the PVC plastigel films heated at 160°C for 90 minutes.

	15'		30'		45'		60'		75'		90'	
	XYZ	Lab	XYZ	Lab	XYZ	Lab	XYZ	Lab	XYZ	Lab	XYZ	Lab
PVC Control	54,8	80,58	59,1	83,02	59,4	83,17	60,2	83,61	52,7	79,46	62,9	83,52
	57,7	0,19	62,2	0,37	62,5	0,4	63,3	0,38	55,7	-0,42	63,2	2,3
	65,9	-3,44	69,7	-2,48	70,8	-3,11	71,7	-3,07	66,3	-5,74	75	-0,23
1.36% ZP	61,2	84,29	59,8	83,47	59,9	83,38	58	82,62	48,8	77,53	59,9	82,3
	64,6	-0,13	63,1	0,02	62,9	0,58	61,4	-0,58	52,4	-2,37	60,8	0,59
	74	-3,8	72,3	-3,83	73,2	-4,71	67,9	-1,66	40,1	17,17	75,3	-2,56
0.27% ZB+ 1.29% ZP	66,9	87,06	65,5	86,35	68,3	87,66	43,6	73,65	60,1	83,96	53,4	79,41
	70,1	0,85	68,7	0,74	71,4	1,4	46,2	-0,34	64	-1,42	55,6	-2,94
	82,7	-5,67	82,1	-6,43	86,7	-7,56	51,5	-2	56,1	11,19	45,2	19,32
0.54% ZB+ 0.81% ZP	58,3	82,57	57,4	82,1	55,9	81,3	57,6	82,22	55,3	80,95	60,5	82,68
	61,4	0,34	60,5	0,14	59	-0,1	60,7	0,04	58,4	-0,19	61,6	0,4
	71,7	-4,85	69,3	-3,7	66,3	-2,6	69,2	-3,47	65,1	-2,13	75,9	-2,37
0.68% ZB+ 0.68 ZP	63,8	85,38	69,7	88,31	45,5	74,89	37,4	67,81	30,4	61,15	28,5	59,38
	66,8	1,27	72,7	1,55	48,1	-0,27	37,7	5,51	29,4	9,86	27,4	6,37
	78,2	-5,2	88,2	-7,52	22,3	38,28	11,4	49,79	6,6	54,25	6,8	52,83
0.81% ZB+ 0.54% ZP	62,9	85,05	61,4	84,21	51,1	78,24	60,9	83,91	61,1	84,09	60,1	82,32
	66,1	0,57	64,5	0,76	53,6	0,78	63,9	0,67	64,2	0,39	60,9	0,87
	78,4	-5,92	76,5	-5,9	64,1	-5,93	75,2	-5,38	74,9	-4,82	76	-3,08
1.29% ZB+ 0.27% Zp	61	83,94	61,5	84,3	57,6	82,15	59,9	83,57	57,4	82,1	59,7	82,23
	64	0,76	64,6	0,48	60,6	0,37	63,2	-0,09	60,5	0,12	60,7	0,42
	75,8	-5,79	75,3	-4,81	70,1	-4,33	70,9	-2,5	68,7	-3,19	74,2	-1,9
1.36% ZB	61,6	84,39	58,5	82,73	61,3	84,08	60,9	84,09	65,8	86,96	37,3	67,92
	64,8	0,28	61,7	0,11	64,2	0,95	64,2	-0,11	69,9	-1,06	37,9	0,56
	75,8	-5,04	70,9	-3,97	76,4	-6	73,5	-3,7	65,8	7,62	15,7	42,7

## REFERENCES

- Atakul S., “Synergistic Effect of Zinc Stearate and Natural Zeolite on PVC Thermal Stability”, 2004.
- Babrauskas V., SFPE Technology Report 84-10, Society of Fire Protection Engineers, Boston, Mass., 1984 in Kirk-Othmer Encyclopedia of Chemical Technology, 1994.
- Baltacıoğlu H., Balköse D., “Effect Of Zinc Stearate And/Or Epoxidized Soybean Oil On Gelation And Thermal Stability of PVC-DOP Plastigels”, Journal of Applied Polymer Science, Vol.74, 2488 – 2498, 1999.
- Basfar, A.A., “Flame Retardancy Of Radiation Cross-Linked Poly(Vinyl Chloride) (PVC) Used As An Insulating Material For Wire And Cable”, Polymer Degradation and Stability, 77, 221 – 226, 2002.
- Beltran M.I., Garcia J.C., Marcilla A., Hidalgo M., Mijangos C., “Thermal Decomposition Behaviour of Crosslinked Plasticized PVC”, Polymer Degradation and Stability, 65, 65 -73, 1999.
- Bowen, 1985; Jenkner et.al., 1985 in Encyclopedia of Industrial Chemistry, 1988.
- Byrne G.A., Gardiner D., Holmes F.H., Journal of Applied Chemistry, 16, p.81 1966 in Kirk-Othmer Encyclopedia of Chemical Technology, 1994.
- Carty S., White S., “Flammability Studies On Plasticized Chlorinated Poly(Vinyl Chloride)”, Polymer Degradation And Stability, 63, 455 – 463, 1999.
- Cella J.A., “Zinc Borate As A Smoke Suppressant”, UK.Patent No.2193216 A, 1986.
- Chaplin D., “Fire-retardant Compositions”, US.Patent No.5338791, 1994.
- Chauffoureaux J.C., Dehennau C, Journal of Rheology, 23(1), 1-24, 1979.
- Dickens E.D., “Smoke Retardant Vinyl Chloride And Vinylidene Chloride Polymer Compositions”, US.Patent No.3965068, 1976.
- Elcik R.G., “Fire Retardant Polyvinyl Chloride Containing Compositions”, US.Patent No.3983290, 1976.

- Ferm D.J., Shen, K.K., “The Effect of Zinc Borate in Combination with Ammonium Octamolybdate or Zinc Stannate on Smoke Suppression in Flexible PVC”, *Journal of Vinyl & Additive Technology*, Vol.3, No.1, 33 – 41, 1997.
- Frost R.L., “An Infrared and Raman Spectroscopic Study of Natural Zinc Phosphates”, *Spectrochimica Acta*, Elsevier, 2003.
- Giudice C.A., Benitez J.C., “Zinc Borates As Flame-retardant Pigments In Chlorine-containing Coatings”, *Progress In Organic Coatings*, 42, 82 – 88, 2001.
- Gökçel H.İ., Balköse D., “Thermal Degradation of Poly(Vinyl Chloride) Plastics”, *Advances In Polymer Technology* Vol.17, No.1, 63 – 71, 1998.
- Hilado C.J., Flammability Handbook for Plastics, 2<sup>nd</sup> ed., Technomic Publications, Lancaster, Pa., 1974 in *Kirk-Othmer Encyclopedia of Chemical Technology*, 1994.
- Jimenez A., Iannoni A., Torre L. and Kenny J.M., “Kinetic Modelling Of The Thermal Degradation of Stabilized PVC Plastics”, *Journal of Thermal analysis and calorimetry*, Vol.61, 483 – 491, 2000.
- Jimenez A., Torre L., Kenny J.M., “Thermal Degradation of Poly(Vinyl Chloride) Plastics Based On Low-migration Polymeric Plasticizers”, *Polymer Degradation And Stability*, 73, 447 – 453, 2001.
- *Kirk-Othmer Encyclopedia of Chemical Technology*, Vol.10 and Vol.4, 4<sup>th</sup> ed., John Wiley and Sons, 910 – 961 and 407 – 408, 1994, N.Y.
- *Kirk-Othmer Encyclopedia of Chemical Technology*, Vol.22, 2<sup>nd</sup> ed., John Wiley and Sons, 606, 1970, N.Y.
- Levine I.N., “Physical Chemistry”, 4<sup>th</sup> ed., McGraw Hill, Singapore, 1995.
- Li B., “An Investigation of The Smoke Suppression and The Thermal Degradation In The Smouldering Mode of Poly(Vinyl Chloride) Containing A Combination of Cuprous Oxide And Molybdenum Trioxide”, *Polymer Degradation And Stability*, 74, 195 – 199, 2001.
- Linsky L.A., “Flame Retardant Compositions”, US.Patent No.5886072, 1999.

- Ning Y., Guo S., "Flame-retardant and smoke suppressant properties of zinc borate and aluminium trihydrate-filled rigid PVC", *Journal of Applied Polymer Science*, Vol.77, 3119 – 3127, 2000.
- Pi H., Guo S., Ning Y., "Mechanochemical improvement of the flame-retardant and mechanical properties of zinc borate and zinc borate-aluminium trihydrate-filled poly(vinyl chloride).", *Journal of Applied Polymer Science*, Vol.89, 753 – 762, 2002.
- Rice P. and Adam H., "Developments in PVC Production and Processing", Applied Science Publishers, London, Ch.5, 1977.
- Sawada H., "Zinc Borate, and Production Method and Use Thereof", European Patent Application No.EP 1 205 439 A1, 2002.
- Schubert D.M., "Zinc Borate", US.Patent No.5472644, 1995.
- Schubert D.M., "Process of Making Zinc Borate and Fire-retardant Compositions Thereof", US.Patent No.5342553, 1994.
- Shen K.K., Griffen T.S., Nelson G.L., Fire and Polymers ACS Symposium Series 245, American Chemical Society, Washington D.C., p.157, 1990 in Kirk-Othmer Encyclopedia of Chemical Technology, 1994.
- Tektaş E., Mergen A., "Çinko Borat", Etibank, 10 – 12, 2003.
- Titow W.V., "PVC Technology", 4<sup>th</sup> Edition, Elsevier Applied Science Publishers, London and New York, 1985.
- Ullmann's Encyclopedia of Industrial Chemistry, Vol.A11, 5<sup>th</sup> ed., VCH Publication, 123 – 139,1988, Weinherm
- Vrandecic N.S., Klaric I., Roje U., "Effect of Ca/Zn Stabiliser On Thermal Degradation of Poly(Vinyl Chloride)/Chlorinated Polyethylene Blends", *Polymer Degradation And Stability*, 74, 203 – 212, 2001.
- Woods W.G., "Halogenated Polymeric Compositions Containing Zinc Borate", US.Patent No.3718615, 1973,
- Xie R., Qu B., Hu K., "Dynamic FTIR Studies of Thermo Oxidation of Expandable Graphite-based Halogen-free Flame Retardant LLDPE Blends", *Polymer Degradation and Stability*, 72, 313 – 321, 2001.